Universidade do Minho
Escola de Ciências

Ana Rita Guimarães Machado Vaz da Silva

Evaluation of the neuroprotective effect of medicinal plants

Outubro de 2020

Evaluation of the neuroprotective effect of medicinal plants
Ana Rita Guimarães Machado Vaz da Silva
Uminho | 2020

Universidade do Minho
Escola de Ciências

Ana Rita Guimarães Machado Vaz da Silva

Evaluation of the neuroprotective effect of medicinal plants

Dissertação de mestrado
Bioquímica Aplicada, especialização em Biomedicina

Trabalho efetuado sob a orientação de:
Professor Doutor Alberto Carlos Pires Dias
E co-orientação de:
Doutora Vanessa Alexandra Fernandes Magalhães

Outubro de 2020

DIREITOS DE AUTOR E CONDIÇÕES DE UTILIZAÇÃO DO TRABALHO POR TERCEIROS

Este é um trabalho académico que pode ser utilizado por terceiros desde que respeitadas as regras e boas práticas internacionalmente aceites, no que concerne aos direitos de autor e direitos conexos.

Assim, o presente trabalho pode ser utilizado nos termos previstos na licença abaixo indicada.

Caso o utilizador necessite de permissão para poder fazer um uso do trabalho em condições não previstas no licenciamento indicado, deverá contactar o autor, através do RepositóriUM da Universidade do Minho.

Licença concedida aos utilizadores deste trabalho:

Atribuição
CC BY

https://creativecommons.org/licenses/by/4.0/

Acknowledgments

> “One of the wonderful things about science is that when scientist don´t know something, they can try out all kinds of theories and conjectures, but in the end they can just admit their ignorance.”
>
> Yuval Noah Harari

All this work was result of so many people who helped me in this challenging year to face my limits and grow as person and student.

To my guiding professor Alberto Dias and Vanessa Magalhães, I would like to thank for their supervision and support showed during my research work, as well as their friendship. I would also like to gratify professor Tarsila Castro from Biological Engineering Center who helped me in docking techniques that contributed to support the work. To my group of investigation, Luís, Bárbara, Marta, Teixeira and Vera, I am so much grateful for their funny company, to bring me music, so many laughs, joint cleanings and scientific advices. Thank you all for taking care of me.

To my friends Anette, Sofia and Eduarda, my older friends who always give me so many advices and share so many experiences. All these conversations and pre-pandemic hugs gave me more peace to my bad moments, thus facing the simple and great things Universe gave to us. To my longtime friend Ricardo, the most ambitious and smart person I met in my life, for pushing me there to high levels. Thank you to be so patient to me, to give me companion, long talks and so many laughs.

Finally, and most importantly, I would like to extremely thank my parents and brother Jorge for their constant support and love. It was a difficult year with so many challenges, but I cannot express how much gratitude I fell to have you in my life, to bring me joyness to my sadness, an open-minded and big heart. Thank you very much. I love you.

Declaration of integrity

I hereby declare having conducted this academic work with integrity. I confirm that I have not used plagiarism or any form of undue use of information or falsification of results along the process leading to its elaboration. I further declare that I have fully acknowledged the Code of Ethical Conduct of the University of Minho.

Resumo

Tendo em conta o seu potencial terapêutico, os produtos naturais têm sido usados na medicinal tradicional oriental ao longo dos tempos. O crescente interesse pela comunidade científica no uso de fitofarmacêuticos tem levado a um aumento significativo de investigação no que concerne a elucidar o seu efeito terapêutico no potencial tratamento das doenças neurodegenerativas. Uma abordagem amplamente abordada e recente para o seu eventual tratamento consiste em confrontar a problemática da neuroinflamação/stress oxidativo no contexto da neurodegeneração. Isso diz respeito a uma condição pré-patológica caraterizada por um stress oxidativo crónico e sistemático associado a um estado de inflamação crónica que causa a perda neuronal. Assim, ao reverter e/ou atenuar este estado, os produtos naturais podem prevenir e tratar as doenças neurodegenerativas através da modulação das células de microglia, as células do sistema imunitário do cérebro, inibindo ou reduzindo o seu caráter inflamatório e pró-oxidante.

Este trabalho tem como principal objetivo avaliar o potencial farmacológico de extratos de plantas usadas na Medicina Tradicional Chinesa: *Hemerocallis citrina* e *Dendrobium nobile*, assim como compostos puros de *Panax ginseng* e alcaloides de *Nelumbo nucifera*, no que diz respeito às suas propriedades anti-inflamatórias e antioxidantes. Para isso, foi avaliada a sua capacidade de capturar radicais DPPH e de óxido nítrico, assim como a sua atividade anti-acetilcolinesterase. Adicionalmente, foram efetuados métodos *in silico* para realizar estudos de relação estrutura/atividade de compostos puros. Em seguida, foi avaliada, na linha celular BV2 (microglia murina): (i) a sua citoxicidade; (ii) o seu potencial antioxidante (avaliado pela capacidade de citoproteção face a insultos oxidativos) e (iii) o seu potencial anti-inflamatório (avaliado pela quantificação de compostos pró-inflamatórios após o estímulo inflamatório

(lipopolissacarídeo bacteriano)). Finalmente, os perfis fitoquímicos dos extratos foram delineados com vista à sua caraterização.

Apesar de o extrato de *Dendrobium nobile* e os alcaloides de *Nelumbo nucifera* terem demonstrado atividade quelante de radicais DPPH e NO, assim como atividade anti-acetilcolinesterase (embora fraca), a sua elevada toxicidade na linha celular BV2 levou-nos a abortar o seu estudo em ensaios posteriores.

Por outro lado, os compostos de *Panax ginseng* revelaram ter capacidade antioxidante e anti-inflamatória na sua maioria através de efeitos indiretos, provavelmente por regulação da maquinaria genética. Os nossos estudos e de outros autores indicaram, na maioria das vezes, que os grupos açúcares poderão não ser de grande relevância para a atividade biológica e farmacológica dos compostos.

Finalmente, todos os ensaios planeados foram efetuados com os extratos de *Hemerocallis citrina*. Estes extratos apresentaram atividade antioxidante e anti-inflamatória. O seu elevado conteúdo em ácidos fenólicos e flavonoides como ácidos cafeoilquínicos e derivados de quercetina e apigenina parecem contribuir para a sua atividade antioxidante, evidenciada pelo efeito protetor na linha celular BV2 após insulto oxidativo. Por outro lado, a atividade anti-inflamatória foi evidenciada, também em células BV2, pelo decréscimo da expressão de citocinas pró-inflamatórias e na enzima produtora de óxido nítrico, iNOS, após indução de inflamação com o lipopolissacarídeo bacteriano. Os resultados obtidos mostram que estes extratos poderão apresentar um potencial terapêutico em organismos vivos no controlo e/ou reversão da neuroinflamação/stress oxidativo e no tratamento das doenças neurodegenerativas.

Abstract

Given their therapeutic activity, natural products have been used in traditional medicines throughout the centuries. The growing interest of the scientific community in phytopharmaceuticals has resulted in a significant number of research efforts towards in understanding their effect in the potential treatment of neurodegenerative disorders. An approach to develop new ways of treatment concerns facing the context of neuroinflammation/oxidative stress on these group of diseases. This regards to a pre-pathological condition characterized by a chronic and systemic oxidative stress associated to a mild-subclinical chronic inflammation which causes neuronal cell loss. Thus, by reverting and/or attenuating this state, natural products can prevent and treat neurodegenerative diseases through modulation of microglia, the cells from brain innate system, inhibiting or reducing its inflammatory or oxidative status.

The main goal of this work is to evaluate the pharmacological potential of plants used in Traditional Chinese Medicine as *Hemerocallis citrina* and *Dendrobium nobile* extracts, as well as *Panax ginseng* compounds and alkaloids from *Nelumbo nucifera*, regarding to its anti-inflammatory and antioxidant properties. For that, the scavenging activities on DPPH and NO radicals as well as the anti-acetylcholinesterase activity were evaluated. *In silico* methods were carried out to perform structure-activity relationships of pure compounds. Moreover, using a BV2 murine microglia cell line, the following parameters were evaluated: i) their citoxicity; ii) their antioxidant potential evaluating their ability in reverting oxidative insults and iii) their anti-inflammatory potential evaluating the capacity in decreasing pro-inflammatory compounds after inflammatory stimulation (bacterial lipopolysaccharide) . Finally, phytochemical analysis was performed for the extracts in order to characterize them.

Although *Dendrobium nobile* extract and *Nelumbo nucifera* alkaloids have DPPH and NO radical-scavenging activity, as well as weak anti-acetylcholinesterase activity, their toxicity in the BV2 cells did not enable their study in subsequent assays. Moreover, *Panax ginseng* compounds have been shown to have antioxidant and anti-inflammatory properties, mostly through indirect effects, probably through regulation of genetic machinery. In addition, our studies and others indicated that, in most cases, the sugar groups may not be necessary for the biological and pharmaceutical activity. In the end, all planned assays were carried out with extracts of *Hemerocallis citrina*. Its high content of phenolic and flavonoid acids such as caffeoylquinic acids, quercetin and apigenin derivatives can contribute to its antioxidant and anti-inflammatory activity. This last activity seems to be related to a decrease in the expression of pro-inflammatory cytokines and in the nitric oxide-producing enzyme, iNOS. Eventually, these extracts may have a therapeutic potential in living organisms in reversing neuroinflammation / oxidative stress and in the treatment of neurodegenerative diseases.

Index

Figure Index

Figure 24. *In silico* image of AChE from *Eletrophorus eletricus* (PDB ID: 1C2B) represented in **a)** cartoon and **b)** surface. Represented structures were obtained by *PyMol* software

Figure 25. EC_{50} values for AchE assay of *Hemerocallis citrina* (ODL) extracts, compared with standard physostigmine. Each bar represents the mean ± SD considering the results obtained at least three independent experiments. All the values are statistically different ($p \leq 0.0001$) vs positive control, physostigmine.

Figure 26. EC_{50} values for AchE assay of *Panax ginseng* compounds, compared with standard physostigmine. Each bar represents the mean ± SD considering the results obtained at least three independent experiments. All the values are statistically different ($p \leq 0.0001$) vs positive control, physostigmine.

Figure 27. Docking mode of AChE from *Eletrophorus eletricus* (PDB ID: 1C2B) (represented by blue sticks) with **a)** RG1, **b)**PPD **c)**PPT and **d)**RB1(represented by green sticks) obtained by *PyMol* software

Figure 28. General structure of *Panax ginseng* compounds. Chemical structures of **a)** RG1 (R1=OH, R2-O-Glc, R3-O-Glc), **b)** PPD(R1=OH, R2-H, R3-OH), **c)** PPT(R1=OH, R2-OH, R3-OH) and **d)** RB1 R1= -O-Glc^{2}-^{1}Glc, R2-H, R3- O-Glc$^{\mathbf{6}}$-^{1}Glc). Adapted from Tawab *et al.*[53]

Figure 29. Chemical structures of N-methylasimilobine (R1=OH, R2-CH_3) and 2-hydroxy 1-methoxyaporphine (R1-OH, R2=H). Chemical structure was drawn in *ChemSpace.*

Figure 30. Docking mode of AChE from *Eletrophorus eletricus* (PDB ID: 1C2B) (represented by blue sticks) with **a)** nuciferine, **b)**N-nornuciferine **c)**

Hydroxy-metylasimiboline and **d)** 2-hydroxy 1-methoxyaporphine (represented by green sticks) obtained by *PyMol* software.

Figure 31 . Effect of ODL treatment on BV2 cell lines. Values represent mean± standard deviation (SD) of three independent experiments. Statistical differences are presented **p<0,01, ***p<0,001, **** p < 0.0001 vs. control (cells subject to medium without treatment).

Figure 32 . Effect of ODL extracts at 50 and 100 µg/mL against t-BHP insult. BV2 cells were treated with extracts for **a)** 3 h and **b)** 20 h, then were co-incubated with t-BHP for 2h30 min. Then, supernatant was removed and cells were incubated for 1 h with MTT, to evaluate cell viability. Data are represented as means ± SD (n = 9) with one-way ANOVA. Statistical differences are presented **** p < 0.0001 vs. control (cells subject with t-BHP treatment).

Figure 33. Effect of DN treatment on BV2 cell lines. Values represent mean ±SD of three independent experiments. Statistical differences are presented **** p < 0.0001 vs. control (cells subject to medium without treatment)

Figure 34. Effect of PG compounds treatment on BV2 cell lines a)mixture of compounds DS1227 and 1226 at concentrations of 0.5,1, 1.5 and 2 µg/mL , **b)** sapogenins PPT and PPD at 0.5,1 and 1.5 µg/mL and **c)** ginsenosides RB1 and RG1 at 0.5,1 and 2.5 µg/mL Values represent mean ±SD of three independent experiments. Statistical differences are presented ***p<0.001,**** p < 0.0001 vs. control (cells subject with medium without treatment).

Figure 35. Effect of PG compounds at 0,5 µg/mL against t-BHP insult. BV2 cells were treated with extracts for **a)** 3 h and **b)** 20 h, then were co-incubated with t-BHP for 2h30 min. Then, supernatant was removed and

cells were incubated for 1 h with MTT, to evaluate cell viability. Data are represented as means ± SD (n = 9) with one-way ANOVA. Statistical differences are presented **** $p < 0.0001$ vs. control (cells subject with t-BHP treatment).

Figure 36. Effect of NC alkaloids treatment on BV2 cell lines at concentrations of 0.25, 2.5 and 10 µg/mL. Values represent mean±SD of three independent experiments. Statistical differences are presented **** $p < 0.0001$ vs. control (cells subject to medium without treatment).

Figure 37. Effects of ODL extracts on NO production induced by LPS in BV2 cells. Microglia were pretreated with ODL50, ODLBu and ODL30 extracts at concentrations of 25,50 and 100 µg/mL, followed by stimulation with LPS (2µg/ml) for 3 hr. Cell-conditioned supernatants were collected, and the production of NO was measured by the presence of nitrite in the supernatants using Griess reaction. Values represent mean ±SD of three independent experiments. Statistical differences are presented **** $p < 0.001$ vs. control (LPS 2µg/mL).

Figure 38. Effects of dammarane sapogenins compounds on NO production induced by LPS in BV2 cells. Microglia were pretreated with DS1227 and 1226 at concentrations of 0.5 and 1.5 µg/mL, followed by stimulation with LPS (2µg/ml) for 3 hr. Cell-conditioned supernatants were collected, and the production of NO was measured by the presence of nitrite in the supernatants using Griess reaction. Values represent mean±SD of three independent experiments. Statistical differences are presented **** $p < 0.001$ vs. control (LPS 2µg/mL).

Figure 39. Effects of ginsenosides and its aglycones on NO production induced by LPS in BV2 cells. Microglia were pretreated with RB1 and RG1 at concentrations of 0.5,1.5 and 3 µg/mL, followed by stimulation with LPS (2µg/ml) for 3 hr. Cell-conditioned supernatants were collected, and the

Table Index

Abbreviations

AchE – Acetylcholinesterase

AD · Alzheimer disease

AS – Anionic Sites

Aβ ·Amyloid·beta

BBB – Brain Blood Barrier

BDNF – Brain Derived Neurotrophic Factor

CAT – Catalase

CCL2 – Chemokine C·C motif ligand 2

CNS · central nervous system

COX-2 – Cyclooxygenase 2

CUMS- Chronic Unpredictable Mild Stress

DAMPs · Damage Associated Molecular Patterns

DN- *Dendrobium nobile*

DNP – *Dendrobium nobile* Polysaccharides

DPPH · 1,1·diphenyl·2·picrylhydrazyl

DS- Dammarane Sapogenins

DTNB – Dithiobis·(2·Nitrobenzoic Acid)

EE – *Electrophorus eletricus*

ES – Estereatic Sites

GABA-A – Gamma·aminobutyric Acid

GAE- Gallic Acid Equivalents

GDNF – Glial Derived Neurotrophic Factor

GSH · Glutathione

H_2O_2 - Hydrogen Peroxide

HMA – 2·hydroxy·1·methoxyaporphine

HOO• · Hydroperoxyl Radical

HPLC · High Performance Liquid Chromatography

HP – Hydrophobic Pocket

HS – *Homo sapiens*

IDO – Indoleamine 2·3 dioxygenase

IL – Interleukins

iNOS – Inducible NO synthase

JNK – Junk Kinase

LPS – lipopolysaccharide

MDA – Malondialdehyde

MRC – Mitochondrial Respiratory Chain

NADPH · Nicotine Adenine Dinucleotide Phosphate Hydrogenated

NC - *Nelumbo nucífera*

ND - Neurodegenerative Disorders

NED · N-(1-naphthyl) ethylenediamine

NF- Nuciferine

NF-kB – Nuclear Factor Kappa B

N-NF – Nornuciferine

NO · Nitric Oxide

NO· · Nitric Oxide Radical

NOX2 – NADPH Oxidase 2

Nrf2 – Nucleus E2-Related Factor

O2•– · Superoxide Anion

ODL- Orange Day-lily

ODL30 – Orange day-lily fraction in 30%ethanol

ODL50 – Orange day-lily fraction in 50%ethanol

ODLBu – Orange day-lily fraction in N-butanol

OH• · Hydroxyl Radical

ONOO– · Peroxynitrite Anion

PAMPs · Pathogen Associated Molecular Patterns

PAS- Peripheral Anionic Sites

PD · Parkinson disease

PG – *Panax ginseng*

PGE2 – Prostaglandin E2

PGH2-Prostaglandin H2

PI3K – Phosphoinositide 3-kinase

PPAR – Peroxisome Proliferator Activated Receptor

PRRs · Pattern Recognition Receptors

QE – Quercetin Equivalents

RNS – Reactive Nitrogen Species

ROS – Reactive Oxygen Species

SNP – Sodium Nitroprusside

SOD- Superoxide Dismutase

t-BHP – tert-butyl hydroperoxide

TF – Total flavonoids

TLR · Toll-like Receptors

TNF – Tumor Necrosis Factor

TP- Total Phenols

TrkB – Tyrosine Receptor Kinase B

XO – Xanthine Oxidase

α-syn · alpha-synuclein

1.INTRODUCTION

1.1Neuroinflammation/oxidative stress on neurodegenerative diseases

Neurodegenerative disorders (ND) are pathologies characterized by gradual motor and sensorial loss, as well as deficits of perceptual functions, knowledge and behavior associated with reduction of neuronal survive and increase of neuronal death in the Central Nervous System (CNS)[1,2,3,4]. ND cover several diseases including Alzheimer (AD), Parkinson (PD), Huntington, Amyotrophic Lateral Sclerosis, spinal cord injury and prion diseases[4]. Due to the complex molecular pathology, most of the current therapeutics are ineffective for the treatment of ND, as these are focusing on a single molecular target and/or on alleviating symptoms without halting neuronal cell loss [5,6].

Neuroinflammation is a protective mechanism aiming to restore damaged glia and nervous cells from CNS. This process is mediated essentially by microglia, the resident macrophages from brain, and astrocytes[3]. In infection, several factors including pathogen associated and danger associated molecular patterns (PAMPs and DAMPs) are recognized by pattern recognition receptors (PRRs), such as toll-like receptors (TLRs) highly expressed in the membrane of these cells. In a similar context from infection, proteins as amyloid beta(Aβ) or alpha-synuclein (α-syn) in AD and PD, can bind and activate TLRs, particularly TLR2, thus promoting the phagocytic activity of these cells and the expression of proinflammatory cytokines, reactive oxygen species (ROS) and chemokines, such as tumor necrosis factor (TNF), interleukins (ILs) and chemokine ligand 2 (CCL2) [7,8,9] (**Figure 1)** The ROS and inflammatory cytokines can activate transcription factors such as nuclear factor kappa-B (NF-κB)[7,10,11]. NFκB is a potent inducer of NADPH oxidase (NOX2) and inducible NO synthase (iNOS), thus contributing to the generation of ROS/reactive nitrogen species (RNS). It also activates the expression of cyclooxygenase-2 (COX-2) which is involved

in the generation of prostaglandins thus further promoting the recruitment of inflammatory cells [3,7].

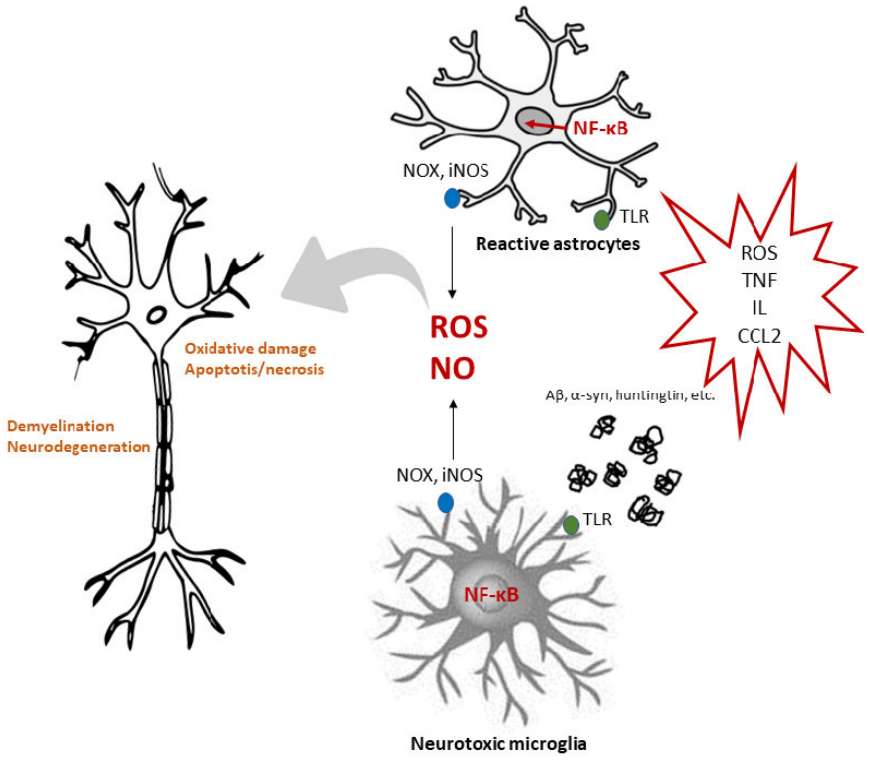

Figure 1. General and simple scheme of the inflammatory process. Proteins, as Aβ, α-syn and huntingtin form aggregates which activate microglia, through TLRs. These receptors activate NF-κB, which induces the production of ROS and inflammatory mediators. It directly acts on neurons and stimulates astrocytes, thus amplifying proinflammatory signals, inducing neurotoxic effects. Also, enzymes as NOX and iNOS generate ROS and NO contributing to neuroinflammation/oxidative stress.

ROS and RNS cause biological damage, causing processes called oxidative and nitrosative stress, respectively [11]. Unfavorable side effects occur when there is an imbalance between prooxidant stress and decrease of antioxidant molecules in body [11,12]. Most ROS, in animals, are produced at mitochondrial respiratory chain (MRC) which represent 20 % of the total energy consumption of the body [7,13,14]. During its endogenous metabolic reactions, superoxide anion ($O_2^{\cdot-}$), hydrogen peroxide (H_2O_2), hydroxyl radical (OH·) and organic peroxides are produced as normal products. Under hypoxic conditions, the MRC also produces nitric oxide (NO) which generate RNS (as NO· and nonradical species as peroxynitrite, ONOO·), that can further generate other reactive species such as malondialdehyde

(MDA) through lipid peroxidation [12,15]. This changes the membrane fluidity and elasticity which can lead to cell rupture [7,11]. To face oxidative stress process, cells contain mechanisms of antioxidizing molecules, as ascorbic acid (vitamin C), α-tocopherol (vitamin E), carotenoids and flavonoids, and enzymes to prevent the accumulation of ROS [7,11](**Figure 2)**. Beyond inactivating protein with iron-sulfur clusters in the mitochondrion, superoxide anion (O_2·), rapidly reacts with NO· to produce ONOO− or can be catalyzed by superoxide dismutase (SOD) to produce H_2O_2 [7,11]. Conversely, H_2O_2 can be neutralized by catalase (CAT) or glutathione peroxidase [7,11]. H_2O_2 can also act as an antioxidant and, in the presence of transition metal ions (Fe^{2+} and Cu^{+}), produce highly reactive OH· radicals via the Fenton reaction [7,11]. Along with ROS, RNS also contribute to oxidative stress due to the formation of ONOO [7,12]. NO itself is produced by NO synthases, which has three isoforms in the CNS, endothelial (eNOS), neuronal (nNOS) and iNOS, being the last one highly expressed in glial cells under inflammatory conditions[7,16].

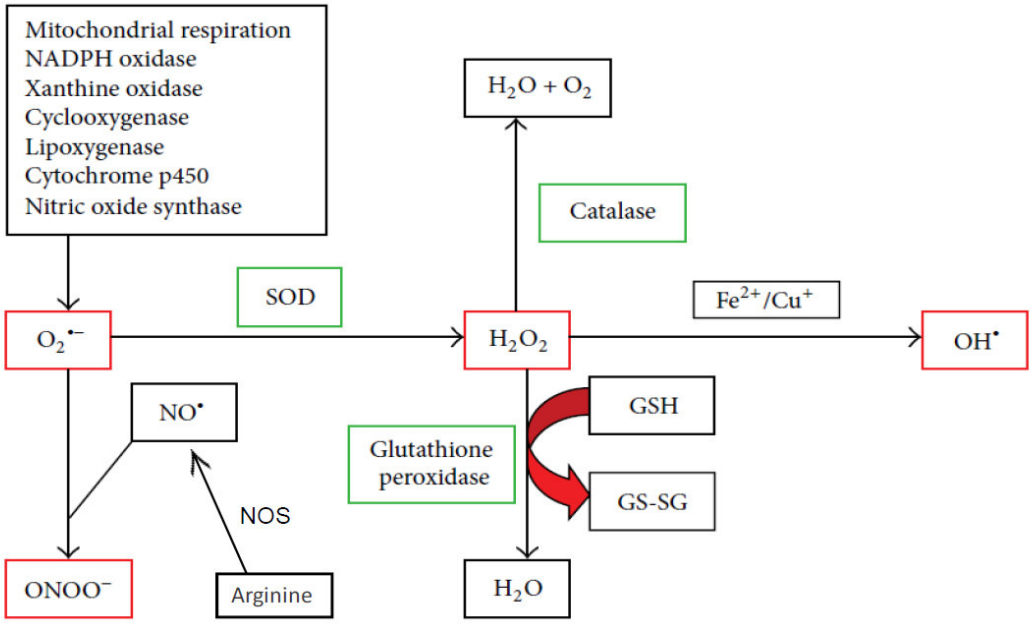

Figure 2. Major prooxidant/antioxidant reactions relevant in biological system. Reactive species are shown in red and antioxidant enzymes are represented in green boxes. SOS: superoxide dismutase; GSH: reduced glutathione; GS-SG: oxidized glutathione; NOS: nitric oxide synthase (adapted from Biswas *et al*,2016)[11].

Neuroinflammation and oxidative stress are interrelated processes. On the one hand, inflammatory mediators such as cytokine can induce the production of ROS through activation of NOX and iNOS. On the other, ROS can themselves modulate inflammation through the activation of NF-κB[7,17] and p38 or Junk-kinase(JNK), promoting apoptosis. In this process, the destabilization of the mitochondrial membrane has been described to lead to ROS generation and the other associated process (**Figure 3**). Furthermore, there are other receptors involved as peroxisome proliferator activated receptor (PPAR-ϒ), cannabinoid receptor CB2R and factors mainly expressed in microglia, neurons and astrocytes, as nucleus E2-related factor 2 (Nrf2)[1]. Recently, the term "oxinflammation" was proposed to describe a pre-pathological condition characterized by a chronic and systemic oxidative stress associated to a mild-subclinical chronic inflammation. This mean that, against to an initial stimulus, an inflammatory response was triggered but, if it is not properly quenched and

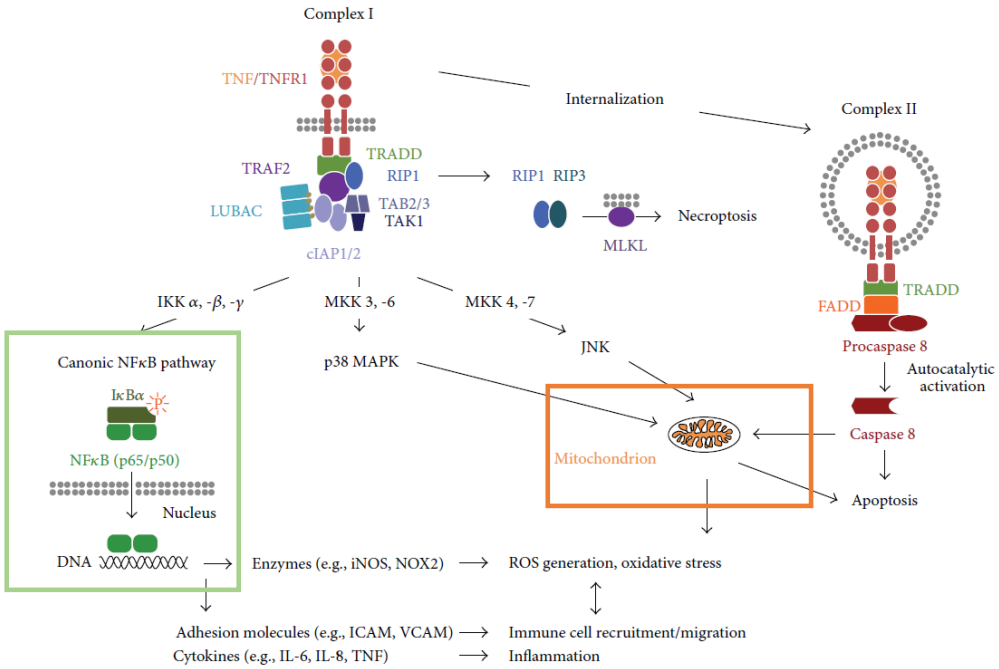

Figure 3. General scheme of pathways mediated by tumor necrosis factor receptors (TNFRs). The binding of TNF to TNFR leads to activation of NF-κB pathway (green box), via phosphorylation and degradation of IκB and translocation of NF-κB to nucleus where it promotes the expression of cytokines and ROS generating enzymes. Also, the complex TNF/TNFR promotes, via MAP kinase kinases (MKKs), the activation of stress-activated kinases p38 MAPK and JNK, which in cytosol induces apoptosis and cell death. After TNFR internalization, a complex II is formed and, after autoproteolytic activation, caspase 8 induces apoptosis directly or by targeting the mitochondria (orange box). The generation of ROS is triggered, as well as inflammation processes (adapted from Fischer and Maier,2015)[6].

terminated by appropriate negative feedback signals, it may result in the stabilization of a low-grade chronic activation of a vicious circle, characterized by a constant generation of a pro-oxidant environment [17]. Several studies have shown that many of the primary metabolites (e.g. carbohydrates, lipids and amino acids), as well as secondary metabolites (e.g. flavonoids, alkaloids, terpenoids and fatty acids) of plants, marine organisms and others, have several biological activities, thus playing a crucial role in the treatment of diseases affecting the CNS in mammalians[18]. Particularly, numerous studies have indicated that natural products prevent and treat NDs through modulation of microglia, inhibiting or reducing its inflammatory toxicity, as well as oxidative stress [1,19].

1.2.Plants and compounds studied

1.2.1. *Dendrobium nobile*

Dendrobium nobile (DN) is one of the most famous *Dendrobium* plants used in Traditional Chinese Medicine, belonging to Orchidaceae family and it is one of the five species specified in the Chinese Phamacopeia [20,21]. *Dendrobium* extracts have been reported to possess immunostimulant activity and antioxidative effects [22]. The pharmacological effects of DN are associated with its chemical constituents and bioactive ingredients, such as alkaloids, stilbenoids, glicosides and polysaccharides, among others [21, 22, 23, 24].

Modern pharmacological studies revealed that alkaloids are the main active ingredients of DN, related with its anti-tumor and anti-aging herbal medicine. Other pharmacological properties include:(i) the improvement of memory; (ii) the enhancement of immunity[25]; (iii) regulatory effects on hepatic lipid homeostasis and in glucose and lipid metabolism, probably through the activation of the Nrf2 signaling pathway [26,27,28]. The relative

percentage of alkaloids was determined by gas chromatography analysis, demonstrating the presence of dendrobine (90,7 %), as the main alkaloid, being accompanied by nobilonine (4,47%), dendrobime (2,31%) and 3-hydroxy-2-oxodendrobine (1,29%)[24](**Figure 4).**

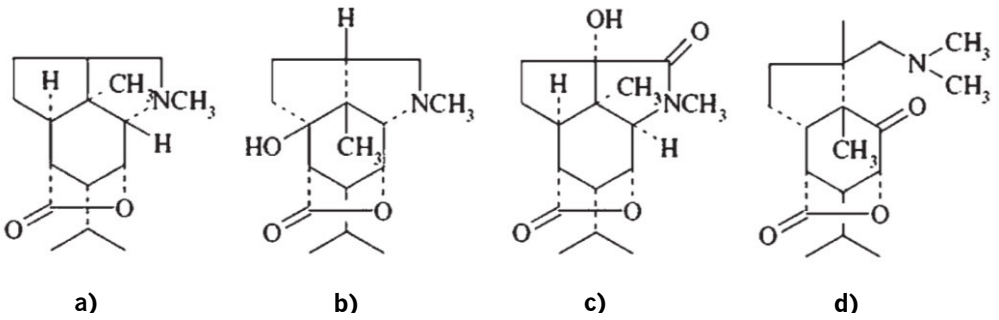

Figure 4. Chemical structures of *Dendrobium* alkaloids **a)** dendrobine, **b)**dendromine, **c)**3-hydroxy-2-oxodendrobine and **c)**nobilonine((adapted from Li *et al,* 2010)[24].

Regarding to its effects in CNS, alkaloids have high solubility in lipid and a potential ability to permeate the brain blood barrier (BBB) [22,24]. These compounds demonstrated having protective effects against neuronal damages (LPS-induced), oxygen-glucose deprivation and reperfusion, decreasing neuron apoptosis and Aβ deposition in rat hippocampus[21,24]. Nie *et al* showed that this antiapoptotic effect is mediated, at least in part, by an increase of brain derived neurotrophic factor (BDNF), glial cell line neurotrophic factor (GDNF) and ciliary neurotrophic factor (CNTF) in the hippocampus and cortex of mice, thus improving Aβ- induced spatial learning and memory impairment [29]. Also, DNLA is effective in protecting against LPS-induced brain impairment in mice. This effect is believed to be associated with a prevention of TNFR1 overexpression via inhibition of the NF-kB pathway and to an inhibition of LPS-induced p-p38 activation, thus inducing anti-inflammatory effects in the rat hippocampus [24]. Another study performed by Yang *et al* showed that DNLA attenuated τ protein hyperphosphorylation and apoptosis induced by LPS in rat brain [30].

Several bioactivities such as immuno-modulatory, anti-tumor, anti-diabetic and antioxidant have been attributed to polysaccharides from *Dendrobium* species[31]. Luo *et al.* performed structural studies for the DN polysaccharides (DNP), verifying the dominance of mannose, glucose, galactose, and smaller amounts of rhamnose, arabinose and xylose. Also, DNP has been shown to have a valuable high scavenging activity on ABTS radicals, and appreciable scavenging effect on OH· radicals [32,33]. Furthermore, i*n vitro* tests showed that the DNP significantly improve the phagocytosis ability of macrophage cell line RAW264.7 and promote the secretion of cytokines TNF-α, IL-6 and IL-1[34].

Phenanthrenes isolated from a methanolic extract of the stems of DN were also reported to inhibit LPS-induced production of NO in RAW 264.7 cells [21]. Additionally, bibenzyl derivatives, namely nobilin D and nobilin E, and a fluorenone (nobilone) (**Figure 5)** from DN exhibited significant inhibitory effects of NO production in macrophages [35]. Furthermore, phenanthrene derivatives such as phenanthraquinone and a phenanthrene derivative with a spirolactone ring from other species of *Dendrobium* have been reported to inhibit the NO production [36].Sesquiterpenoids isolated from a n-butanol soluble fraction of a 95% EtOH extract of the stems of DN

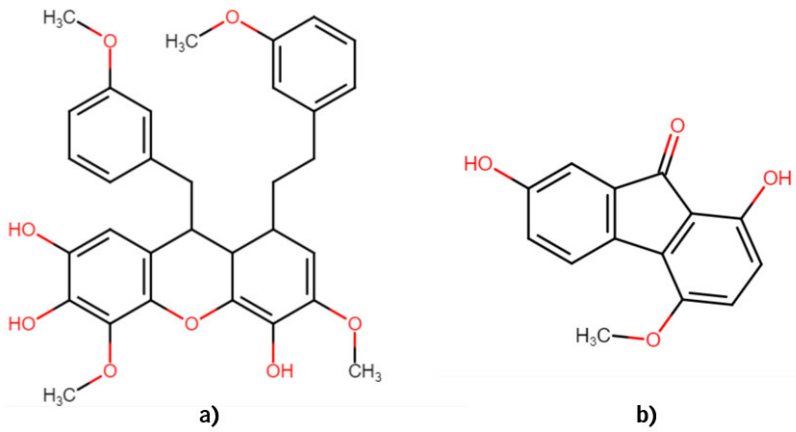

Figure 5. Structure of a bibenzyl derivative **a)** nobilin E and a fluorenone **b)**nobilone. Chemical structures were drawn in *ChemSpace*.

also showed significant neuroprotective activity against H_2O_2-induced oxidative damage in rat adrenal medulla PC12 cells, even better than the positive control, vitamin E [37].

1.2.2. *Hemerocallis citrina* (Orange day-lily, ODL)

Day-lily, a plant widely grown in East Asia which, has been used for thousands of years as adjuvant in antidepressant treatment. Its high content in flavonoids and polyphenols has attracted a growing interest in food, pharmaceutical and cosmetic industries[38]. Also, its bioactive substances have been reported as having antibacterial, antioxidant and nitrite-eliminating-activities [38,39]. This plant is largely known as being clinically efficient in relieving depression in patients with a broad age range[39]. The antidepressant like effect of ODL ethanol extracts is believed to be correlated with an improvement in monoaminergic, neurotrophic and inflammatory systems[38].

Regarding to monoaminergic system, there are evidences showing that the ODL75 extract (in 75% ethanol) promotes an enhancement of neurotransmitters serotonin (5-HT) and noradrenaline (NA) in frontal cortex and hippocampus of mice[40]. Also, dopamine levels increased in cortex after ODL75 treatment. The investigators showed that the anti-depressive effects of ODL75 are dependent of its interaction with serotonergic 5-HT1A, 5-HT2 receptors, noradrenergic α_1-, α_2 and β -adrenoreceptors and dopaminergic D2 receptors[40]. In neurotrophic system, ODL75 also shows an increase in BDNF/tyrosine receptor kinase B (TrkB) signaling in depressed mice [40].

Concerning the inflammatory system, ODL75 also showed to normalize the activation of NF-kB, iNOS and COX-2 (induced by LPS) in prefrontal cortex of mice[38]. Also, ODL75 displayed an inhibition of IL-1β, IL-6 and TNF-α expression in chronic-unpredictable mild stress (CUMS) models. The increased activity of the tryptophan degrading enzyme

ODL75 treatment, thus decreasing tryptophan metabolism and improving serotonergic neurotransmission[41].

Furthermore, acetate fraction (ODLAce) of ODL ethanolic extract also showed a strong antioxidant capacity and effectively protected BRL-3A cells against tert-butyl hydroperoxide (t-BHP)-induced oxidative stress[42]. It reduced ROS accumulation by enhancing cellular antiapoptotic events, namely enhancement of anti-apoptotic protein BCL-2 expression and repression of caspase-3 and 9 expression. Its high antioxidant capacity has been reported to be due to an increase in the expression of genes codifying for antioxidant enzymes such as SOD and CAT. In addition, ODLAce treatment has been shown to increase the activation of antioxidant pathways related with AMPK, ERK, p38 and *Nrf2*[42].

Du *et al* [39] verified that the increase in ethanol concentration normally decreased the carbohydrate and protein content, while increased the flavonoid content in ODL. ODL100 displayed an increase in crude fat content due to the extraction in pure ethanol but, despite of that, had a slightly higher content in flavonoids comparing to ODL75[39].Also, regarding to antidepressant effects on mice , ODL75 had proved be the most effective extract. It has been shown to be a toxically safe percentage for oral administration, therefore being the value used in mostly of the studies reviewed so far [39]. HPLC analyses of flavonoid profiles of ODL75 showed the main presence of rutin, hesperidin, quercitrin and quercetin [39,41,43] (**Figure 6)**. Besides that, it has been reported that the phenolic derivatives and flavonoids were likely the active constituents of ODL, conferring a neuroprotective effect on PC12 cells from rat adrenal medulla[44]. The phenolic acid derivatives were proposed to represent the active constituents responsible for the mediation of dopaminergic system, being the flavonoids likely responsible for the modulation of serotonergic and noradrenergic systems[44].

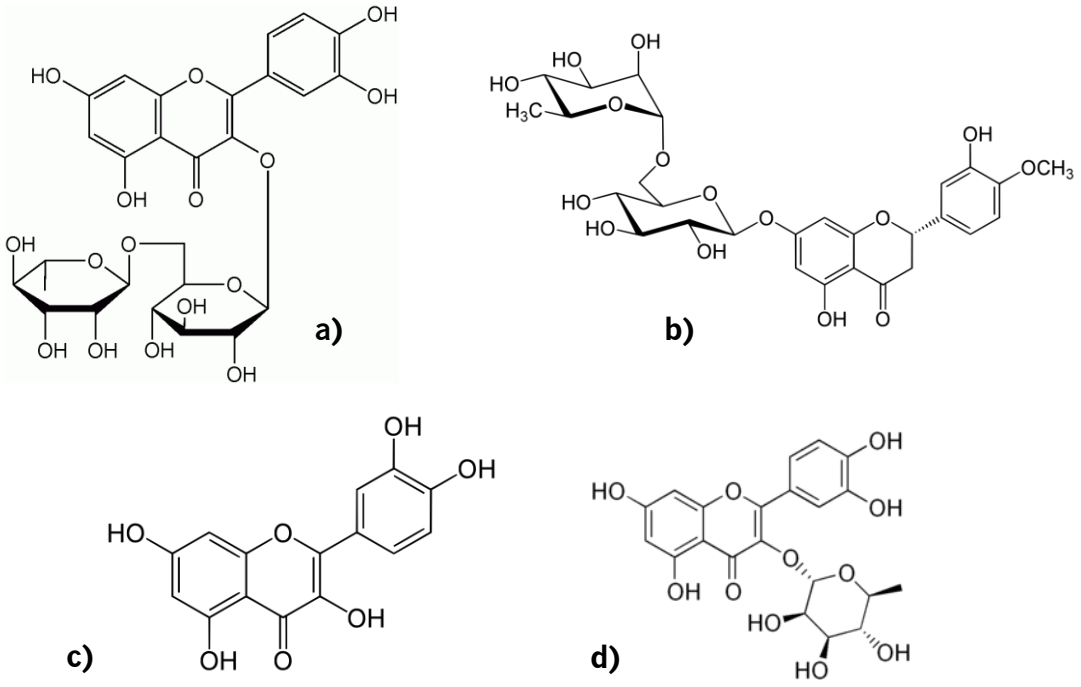

Figure 6. Structure of flavonoids **a)** rutin, **b)** hesperidin**, c)** quercetin and **c)** quercetrin. Chemical structures adapted from Nidjvelt et *al.* ,2001[49].

In order to understand the mechanism underlying the antidepressant effect of ODL, Xu *et al.* performed metabolic studies in a simulated microgravity-induced rat model of depression. They found that ODL80 (in 80% ethanol) might be associated with the regulation of several metabolic pathways, including phenylalanine, glutamic acid, and tryptophan metabolism and changes in energy metabolism in rats. Thus, essential neurotransmitters can be produced, as dopamine and serotonin, increasing its levels in rats treated with ODL [45].

1.2.3. *Panax ginseng* and derivatives

Saponins (ginsenosides) and sapogenins (the respective aglycones) of ginseng types are the major bioactive constituents in three *Panax* sp, namely *Panax ginseng, Panax quinquefolium* and *Panax notoginseng*. Ginsenosides have dammarane-type triterpenoidal structure with sugar moiety binding at C-3, C-6, and C-20 positions[46,47]. Based on their chemical structures, they are divided into three groups: protopanaxatriol (PPT, $C_{30}H_{52}O_4$,33%), protopanaxadiol (PPD, $C_{30}H_{52}O_3$,16%) and oleanane types[46,48]. The ginsenosides Rb1($C_{54}H_{92}O_{23}$, 1109.3 g/mol) and Rg1 ($C_{42}H_{72}O_{14}$, 801,01g/mol), containing sugar groups, are derived from the structure of PPD and PPT-type, respectively (**Figure 7, Table 1)**. Dammarane sapogenins (DS) are the deglycosylated product of ginsenosides formed naturally in the gut lumen by bacterial metabolism[49]. Compared with their precursor ginsenosides, DS are more easily absorbed by the body, exhibiting robust pharmacological activity, and may therefore have a more potent clinical effect [49]. Indeed, several studies have proved that the bioactivity of *Panax* compounds are dependent from aglycone-structure, suggesting that the role of the sugar moieties in biological and pharmaceutical activity is not necessary [50,51].

Table 1. Chemical structure of ginsenosides and some of their main degradation products (adapted from Tawab *et al* 2003)[53]

General structure		R1	R2	R3
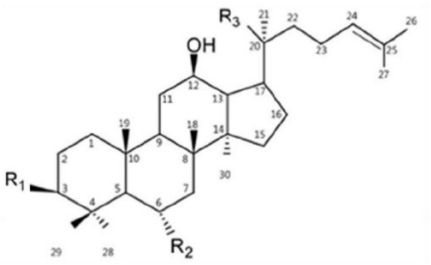	Protopanaxadiol (PPD)type			
	Rb1	-O-Glc$^{2\text{-}1}$Glc	-H	-O-Glc$^{6\text{-}1}$Glc
	Rh2	-O-Glc	-H	-OH
	Rg3	-O-Glc$^{2\text{-}1}$Glc	-H	-OH
	20-(S)-aglycone PPD	-OH	-H	-OH
	Protopanaxatriol(PPT) type			
	Rg1	-OH	-O-Glc	-O-Glc
	Rh1	-OH	-O-Glc	-OH
	20-(S)-aglycone PPT	-OH	-OH	-OH

Glc, β-D-glucopyranosyl

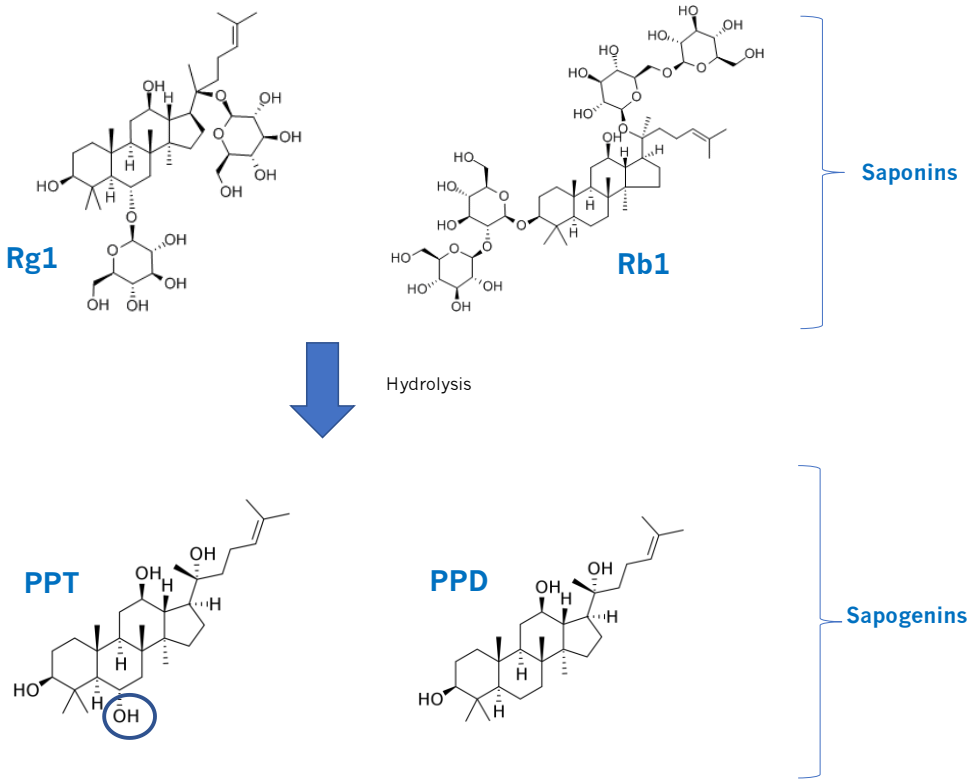

Figure 7. Structure of two types of ginsenosides and its aglycones. The designation of the various types of *Panax* compounds is represented on **Table 1**.

Ginsenosides had been proved as presenting several biological activities, including neuroprotective effects, antioxidant and anti-inflammatory effects [54,52]. RB1 has been shown to decrease the expression of inflammatory mediators such as IL-1β, iNOS, COX-2 and TNF-α, in mice models, decreasing the activation of microglia cells [46,53,54]. It also downregulated caspase-3 expression, as well as NO production and $O_2^{\cdot-}$ in PC12 cells [53] and reduced oxidative stress induced by t-BHP, activating Nrf2 pathway in neuronal progenitor cells [55]. Pretreatment with several doses of RB1 also attenuated hyperphosphorylation and expression of JNK/p38 MAPK [46,56].

Ginsenoside RG1 inhibited expression of several mediators in BV2 LPS-activated microglial and RAW-264.7 cells, as well as in mice models [52,54]. Pretreatment with RG1 significantly reduces ROS production, iNOS

levels and NO production. RG1 helped to remove H_2O_2 damage by downregulation of NF-kB signaling pathways [46,57]. Both ginsenosides have been shown to improve the function of neurotransmitters and exert neuroprotective and neurite outgrowth[58]. It is believed that RB1 (but not RG1) promotes a modulation of neurotransmission by increasing phosphorylation of synapsins via PKA pathway[59,60] .

The aglycones, PPT and PPD, have also shown its several biological effects, especially anti-tumor activities[61]. PPT and PPD have very similar chemical structure, differing in C-6 position, however, their chemical reactivity in body is found to be quite different. PPT has one more hydroxyl group at C- position and is more quickly absorbed and eliminated from the body than PPD[48]. Regarding to its neuroprotective effects, 20-(S)-PPT had significantly inhibited acetylcholinesterase (AchE) activity, increasing Ach levels, SOD activity and decreasing MDA levels in the mice hippocampus[62]. PPT has also been shown to block the increase in LPS-induced iNOS and COX-2 expressions through inactivation of NF-kB in RAW-264.7 cells[63]. 20-(S)-PPD has been shown to inhibit the glutamate-induced morphological changes in PC12 cells, showing antioxidant activity [58, 61,64]. Important roles in redox equilibrium and neuroprotection through modulating of ROS levels or influencing mitochondrial function has been also shown for 20-(S)-PPD. Besides that, it inhibited the degradation of inhibitory factor-kBα, thus inactivating NF-kB and suppressing iNOS expression[61].

Commercial DS were obtained from alkaline hydrolysis of total ginsenosides of *Panax ginseng*, containing mostly 20(S)-aglycone protopanaxadiol (a PPD) ($C_{30}H_{54}O_3$) and 20(S)-aglycone protopanaxatriol (a PPT) ($C_{30}H_{54}O_4$) and in minor quantities sapogenins and saponins as Rh1 ($C_{36}H_{64}O_9$), Rg3 ($C_{42}H_{72}O_{13}$) and Rh2 ($C_{36}H_{64}O_8$)[65,66] (**Table 1)**. Focusing on neuroprotective effects, this mixture of compounds showed an improving in the learning and memory impairment induced by scopolamine in mice[67].

In addition, it has been shown to enhance cognition function by regulating brain neurotransmitter levels, as ACh, 5-HT, NA, glutamate, dopamine and GABA [49,51,68]. It inhibits SLSE-induced neuronal injury [68] and decrease sucrose consumption in CUMS models[51]. Also, it increases the levels of proteins as BDNF, phosphoinositide 3-kinase (PI3K)/kinase B AKT/ mTOR, associated with regulation of learning and memory, and decrease p-JNK, p-p38, involved in apoptosis[49,68]. Additionally, DS attenuated the oxidative damage in liver of exhaustive exercised rats [69]. Curiously, DS displayed an hormetic effect on antioxidant status against exercise challenge in rat skeletal muscle. It means that DS, at low and medium doses, exerts a beneficial effect at multiple levels, as decrease of lipid peroxidation, increase of xanthine oxidase (XO), CAT and SOD activity. However, at high doses, the effect is opposite [65].

1.2.4. *Nelumbo nucifera*

The *Nelumbo nucifera* (NC) belongs to the Nymphaeaceae family and is an aquatic perennial plant that is widely cultivated throughout Eastern Asia, Australia and India. This plant was used for centuries for food, beverages, ornamental, and therapeutic purposes [70]. Almost all parts of lotus as the flowers, leaves, leaf stalks, seeds, and rhizomes, are utilized [71]. Also, its health-promoting effects in diabetes, cancer, hepatoxicity, obesity [70] and in CNS[71] have been reported. For example, the seeds of NC protect the mouse embryonic fibroblast cells by inhibition of H_2O_2-induced cytotoxicity[72] and its rhizome enhances neurogenesis in rat hippocampus[73,74]. NC semen extract and procyanidins (condensed tannis) from the seed have been reported to ameliorate scopolamine-induced dementia by inhibition of AchE activity[75,76]. The embryo extract from this

plant also showed a protective effect in Aβ protein induced apoptosis in PC12 cells [77].

The leaves' extract of *Nelumbo nucifera* reduces pro-inflammatory mediators and cytokines expression through suppression of NF-kB activity in LPS-activated macrophages RAW 264.7 [70]. This effect has been reported to be mediated by phenolic compounds such as catechin, quercetin and proanthocyanidins. The *N. nucifera* aqueous extract has been also shown to decrease more iNOS, Il-6 and TNF-α production than its ethanolic counterpart, due to the presence of taxifolin [70].

Phytochemical studies have shown that the NC is also rich in alkaloids, which are considered the major bioactive compounds of the herb[78,79]. It includes aporphine and benzylisoquinoline-type alkaloids[80]. These compounds were reported as easily crossing the BBB and being quickly distributed into the liver, kidney, lung, and heart of rats [78]. Regarding to alkaloids from leaves, aporphine-like alkaloids nuciferine (NF) and N-nornuciferine(N-NF) are the most important refereed in the literature [80,81] (**Figure 8)**. Its shows neuroprotective effects, such as a significant hypnotic and anxiolytic effects by allosteric binding to $GABA_A$ receptor and activation of monoaminergic system[78,80]. Furthermore, the alkaloids from NC leaves were found to exert a strong inhibitory effect on the cytochrome P450 CYP2D6 isoenzyme, related with its aporphine like-alkaloids, thus affecting the metabolism of drugs in the body[82].

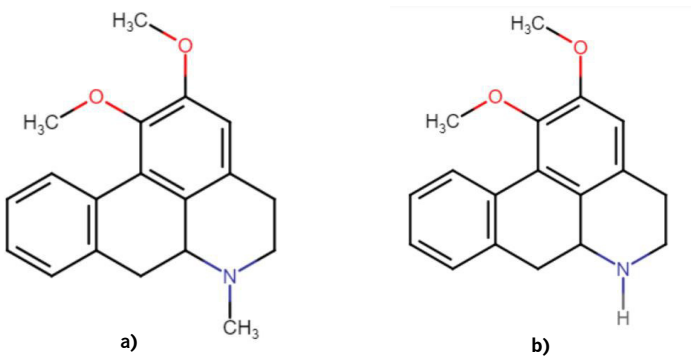

Figure 8. Structure of aporphine-like alkaloids **a)** nuciferine and **b)** N-nurciferine. Chemical structures were drawn in *ChemSpace*.

On the other hand, bisbenzylisoquinoline alkaloids liensinine, neferine and isoliensinine (**Figure 9**) isolated from the seeds of NC suppressed the release of NO and cytokines (TNF-a, IL-1β, and IL-6) by LPS-activated microglial cells, thus exerting neuroinflammatory effects[83,84]. Further studies revealed that they blocked IkBα phosphorylation and degradation, as well as ROS production. In addition, they direct scavenge DPPH, OH, and $ONOO^{-}$ radicals [83,84].

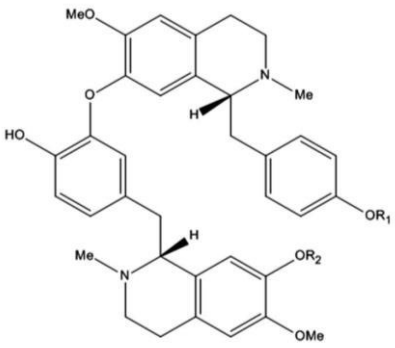

a)R1-H, R2-Me

b)R1=R2-Me

c)R1-Me,R2-H

Figure 9. Structure of bisbenzylisoquinoline alkaloids **a)** liensinine**, b)** neferine and **c)** isoliensinine (adapted from Meng *et al.,* 2007[89].

1.3. Objetives

The goal of this work was to evaluate the pharmacological potential of *Hemerocallis citrina* and *Dendrobium nobile* extracts, as well as *Panax ginseng* compounds and alkaloids from *Nelumbo nucifera*, regarding to its anti-inflammatory and antioxidant properties. For that, the main tasks of this work were i)evaluate the scavenging activity on DPPH and NO radicals, and anti-acetylcholinesterase activity, (ii) *in silico* methods to perform structure-activity relationships of pure compounds; iii)evaluate their citoxicity on BV2 cell line of murine microglia; iv) evaluate its antioxidant potential effect, regarding to its ability in protecting cells from oxidative insults; v) evaluate its anti-inflammatory potential, assessing the level of pro-inflammatory compounds and of pro-inflammatory genes expression and vi) perform a phytochemical analysis of the extracts.

2.MATERIAL AND METHODS

2.1. Material

2.1.1.Reagents

The reagents used in this work are listed in the **Table 2.**

Table 2. List of reagents used for this study, its specifications and company

Name	Company	Molecular weight (Mw)	Reference
1, 1-diphenyl-2-picrylhydrazyl (α-α-diphenyl-β-picrylhydrazyl (DPPH)	Aldrich	394,32g/mol	1898-66-4
Acetylcholinesterase (AchE) from *Electrophorus electricus* (electric eel) (500U)	Sigma	280kDa	9000-81-1
Acetylcholine iodide (AtCl)	Honeywell Fluka	289,18g/mol	101185301
Aluminum chloride ($AlCl_3.6H_2O$)	Sigma-Aldrich	241,45g/mol	231-208-1
Antibiotic (10.000 Units of penicillin, 10 mg of streptomycin and 25µg amphotericin)	Sigma		A5955
L-Ascorbic acid	Sigma-Aldrich	176,12g/mol	100143694
Bovine serum albumin (BSA)	Sigma	66,5KDa	9048-46-8
Dimethyl sulfoxide (DMSO)	Sigma	78,13g/mol	102057602
Dipotassium hydrogen phosphate	M&B	174,2g/mol	256 LGT 35990
Dulbecco's Modified Eagle Medium (DMEM)	Sigma-Aldrich		1002415614
Ellman's Reagent, 5,5'-Dithiobis-(2-Nitrobenzoic Acid) (DTNB)	Aldrich	396,35g/mol	101241619
Ethanol	Carlos Erba	46,07g/mol	4146052
Fetal bovine serum (FBS)	Sigma-Aldrich		025M3361

Folin-Ciocalteu's phenol reagent	Panreac AppliChem		251567.1609
Gallic acid, 3,4,5-Trihydroxybenzoic acid (GA)	Sigma	170,12g/mol	205-749-9
Hydrochloric acid (HCl)	Carlos Erba	36,46g/mol	524525
Lipopolysaccharide (LPS) from *Escherichia coli* purified by phenol extraction (lyophilized powder)	Sigma		019M4009V
Magnesium chloride hexahydrate ($MgCl_2$)	Merck	203,30g/mol	948A450933
Methanol	Carlo Erba	32,04 g/mol	414816
N-1-napthylethylenediamine dihydrochloride (NED)	Aldrich	259,17 g/mol	1002375582
Phosphoric acid	Ridel-de Haën	97,994 g/mol	51600
Physostigmine salicylate	Sigma-Aldrich	413.5 g/mol	3900576
Potassium chloride	Panreac	74,5513 g/mol	131494.1211
Potassium phosphate monobasic	Ridel-de Haën	342.30g/mol	27480.294
Quercetin (QE)	Sigma	302,236 g/mol	1001970327
Sodium bicarbonate (Na_2CO_3)	Sigma	84,01g/mol	101492860
Sodium chloride (NaCl)	VWR Prolabo BDH	58,44 g/mol	27788.297
Sodium hydroxide (NaOH)	Merck	39,997g/mol	1.06498.1000
Sodium nitroprusside dihydrate(SNP)	Merck	297,95g/mol	13755-38-9
Sulfanilamide	Merck	172,21 g/mol	1.11799
Thiazolyl Blue Tetrazolium Blue (MTT)	Sigma	414,32 g/mol	1002753350

Tert-butyl hydroperoxide (t-BHP)	Aldrich	90,12 g/mol	101780848
Tris	Sigma	121,14 g/mol	101209135
Trolox	Aldrich	250,29 g/mol	53188-07-01
Trypsin-EDTA solution	Sigma	23,3 kDa	SLBZ9297

2.1.2. Equipment

The list of equipment used for this work is listed on **Table 3:**

Table 3. List of equipment required for this study and its description

Name	Company
Agitator	IbX instruments
Centrifuge 5418R Eppendorf	Fischer Scientific
ChemiDoc Imaging System	VWR. Geno-Smart
Centrifuge falcons	Sigma 2-16K
Deep freezer	Sanyo and Panasonic
Docking software	PyMOL, AutoDockTools, AutoVina
HPLC apparatus	HITACHI, LabChrom Elite
Humidified CO_2 incubator	Sanyo
Inverted microscope	Olympus CK2
Laminar flow chamber	Telstar Bio II A and Holten HBB2448
Micro analytic balance	VWR
Microplate reader	Spectramax Plus384 and BioRadiMark
Nanodrop spectrophotometer	ND-100, Thermo Fischer
pH calibrator	Hanna instruments
Real-Time Detection System	CFX96, Bio-Rad
Thermal cycler	C1000, Bio-Rad
Vacuum pump	Uniweld and Fischer Scientific
Vortex	VWR
Water bath	Gran

2.1.3. Extracts under study:

The extracts studied in this work (**Table 4)** were provided by professor Qiong Wang, from School of Pharmacy, Southwest Medical University, Sichuan province, China. This work is included in the project Sino -Portugal TCM International Cooperation Center.

Table 4. Extracts under study, its composition and features

Specie	
Dendrobium nobile (DN, stems)	Extract in 80% ethanol
Hemerocallis citrina (Orange day-lily, ODL, flowers)	ODL fraction in 30% ethanol (ODL30)
	ODL fraction in 50% ethanol (ODL50)
	ODL fraction in N-butanol (ODLBu)

The stems of *Dendrobium nobile* were collected in Luzhou, Sichuan province, China. The air-dried stems were crushed and soaked in 80% acidic ethanol during night. The extract was re-extracted for three times using boiling 80% acidic ethanol (80℃). After filtrate, the extracting solution was concentrated by vacuum-rotary evaporation at 60℃ and then freeze-drying 12 h. The extraction rate was of 14% [85].

The flowers part of *H. citrina* (Orange day-lily, ODL) were collected in Hunan province, China and its crude materials were extracted for three times with 20 volumes of 80% ethanol for 1 h for each extraction. Combined extracts were evaporated under reduced pressure in a rotary vacuum evaporator and then smashed after drying. Then the extracts were suspended in water and extracted three times with petroleum ether, ethyl acetate and n-butanol, respectively. These parts were then obtained by decompression and concentration. The n-butanol part (ODLBu) was eluted by HP-20 macroporous resin with water, 30% ethanol (ODL30), 50% ethanol (ODL50), 70% ethanol and 95% ethanol. The ODL30 eluting part and the ODL50 eluting part are rich with flavonoids.

2.1.4. Compounds under study:

The compounds studied in this work (**Table 5)** were provided by professor Qiong Wang, from School of Pharmacy, Southwest Medical University, Sichuan province, China. This work is included in the project Sino -Portugal TCM International Cooperation Center.

Table 5. Compounds under study, its composition and features

Specie	Compound/mixture of compounds	Chemical formula	Molecular weight (g/mol)	Reference
Panax ginseng (PG) and derivatives	PPT	$C_{30}H_{52}O_4$	476,73	
	PPD	$C_{30}H_{52}O_3$	460,73	
	RB1	$C_{54}H_{92}O_{23}$	1109.3	
	RG1	$C_{42}H_{72}O_{14}$	801,01	
	Dammarane sapogenins 1227 (DS1227) (Rh1,17.19%, Rg3,3.96%, Rh2, 9.56%, 20(S)-aglycone protopanaxadiol (aPPD) ,7.02%) and 20(S)-aglycone protopanaxatriol (aPPT),20.51%)	_____	_____	[65,69]
	Dammarane sapogenins 1226 (DS1226) (aPPD,16%,aPPT,33%)	_____ __	_____ _	[51]
Nelumbo nucifera (NC)	Alkaloids from leaves (nuciferin (NF, 27.76%), N-nornuciferine (N-NF, 13.23%), and 2-hydroxy-1-methoxyaporphine (HMA, 4.23%)	_____		[80,78]

Ginsenosides RG1 and RB1, as well as its sapogenins, PPT and PPD were obtained commercially by HPLC with a purity > 98%.

DS is a powdered Asian ginseng extract available at Pegasus Pharmaceuticals Group Inc (Richmond, Canada, U.S.A.). DS was prepared by alkaline hydrolysis of total ginsenosides derived from the stems and leaves of *Panax ginseng*[51,69]*.* Briefly, and accordingly to Jiang *et al.* and Wang *et al.* the total ginsenoside powder was processed with a sodium hydroxide/water solution at elevated temperature (150–300°C) and pressure (2.5–8.4 MPa) for approximately 1.5 h in a 50 L tank [51,65]. The liquid content was separated from the solid content that contains a hydrolyzed ginsenoside and neutralized with hydrochloric acid prior to disposal. Then, it was neutralized and purified by filtration and ethanol extraction/water precipitation repeatedly. Subsequently, the spin-dried solid, the refined DS, was placed into an oven for drying under vacuum[65].

The alkaloids extracts were obtained from the air-dried lotus leaves (*Nelumbo nucifera).* They were ground into small pieces and exhaustively extracted with 0.1% HCl (10 L, three times). The filtered extract solution was inserted in a D001 resin column, which was packed with 95% ethanol and equilibrated with water. After intense washing, the absorbed alkaloid compounds were eluted from the resin column by 95% ethanol containing 1% ammonia. The eluent was concentrated to dryness under reduced pressure to yield an alkaloid extract [80,78].

2.2. Methods

2.2.1.Phytochemical characterization

2.2.1.1.Total phenols and flavonoids quantification

To determine total phenols (TP) quantity, the assay was based on Folin-Ciocalteu (FC) method originally postulated by Singleton *et al.* [86] In this reaction there is a transfer of electrons in alkaline medium from phenolic compounds to form a blue chromophore with phosphosmolybdic/phosphotungstic acid complexes from FC reagent. The maximum absorption of these complexes depends on the concentration of the refereed compounds[87,88,89,90] (**Figure 10)**.

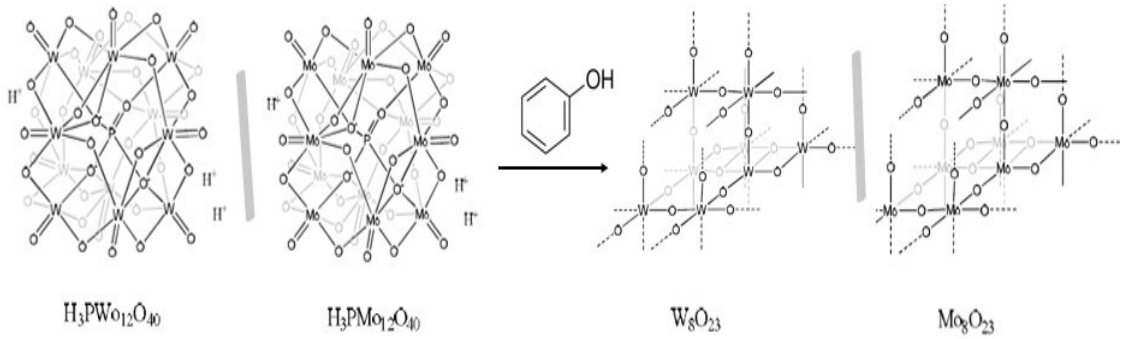

Figure 10. Specific reactions of Folin-Ciocalteu reagent with phenolic compounds. Reaction between phosphotungstic acid ($H_3PW_{12}O_4$) or between phosphomolybdic acid ($H_3PMo_{12}O_40$) (adapted from Chilina 2016)[106].

Briefly, 100µL of FC reagent and 80µL of an alkaline solution (Na_2CO_3 (20% w/v) were added to 20 µL of DN and ODL extracts (stock concentration 100 x 10^3 µg/mL), diluted in water. On its turn, the blank contains 180 µL of water and 20 µL of the sample. The mixture was left for 60 min of incubation in the dark and the D.O. was measured at 765 nm. TP were expressed as mg Gallic Acid Equivalent (GAE) per g of extract (GAE/g) using a standard curve of gallic acid mass (0,005-0,025 mg/mL).

The total flavonoid (TF) content was measured using a modified aluminum chloride ($AlCl_3$) colorimetric method by Chang *et al*(**Figure 11)**

[91,92,93]. For that, 5 µL of each extract were added to deionized water up to 750 µL and 100 µL of 0.05 g/mL $NaNO_2$. After 6 minutes, 150 µL $AlCl_3 \cdot 6H_2O$ 0.1 g/mL solution was supplemented. After the same period of incubation, 750 µL of NaHO 1 M was added. The mixture was vortexed and 15 min later the absorbance at 510 nm was measured. TF were calculated according to the standard curve of quercetin(0,010-0,5 mg/mL) and

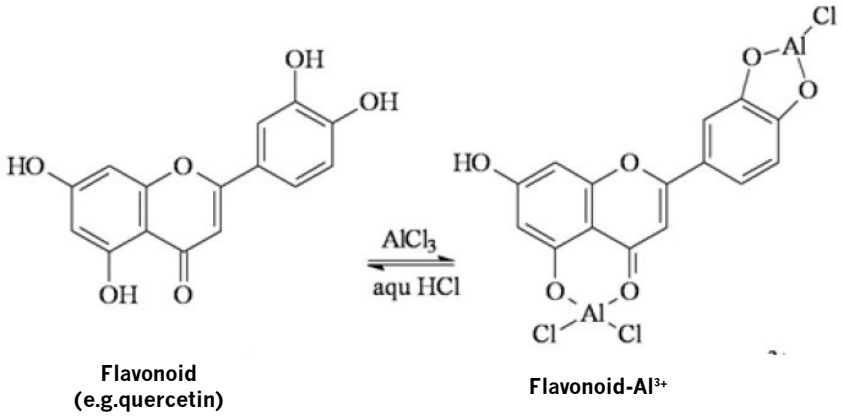

Figure 11. Illustrated scheme for the reaction between flavonoid and $AlCl_3$, forming a stable flavonoid-$AlCl^{3+}$complex (adapted from Amorim 2008)[109].

expressed as quercetin equivalents (mg quercetin equivalents/ g extract).

2.2.1.2.High Performance Liquid Chromatography (HPLC)

Hemerocallis citrina and *Dendrobium nobile* extracts were used for HPLC analysis of phenolics content. Extracts were dissolved in pure methanol at concentrations of 10 mg/mL. 1 ml of each extract was filtered using a hydrophobic polytetrafluoroethylene (PTFE) filter (Branchia, 0.45 µm, Spain) and stored in dark at 4°C till further analysis for HPLC. A pure standard of quercetin at concentration of 0,0625mg/mL was also run in order to perform its quantification on biomass.

Samples were run in a HPLC-DAD apparatus controlled by the computer software EZChrome elite. The detection was performed in a 230-550 nm range, and chromatograms were recorded at 260, 280 and 350

nm. The samples were injected at a 1mL/min flow rate. The separation was executed on a L300 Column Oven. The used solvents were acetonitrile (solvent A) and ultra-pure water containing formic acid (0.1%) (solvent B). Elution was executed using the gradient described on the **Table 6.**

Table 6. Elution specifications for HPLC analysis

Time	%solvent A	%solvent B
0	5	95
2	5	95
5	12	88
25	20	80
30	60	40
35	60	40
40	70	30
45	70	30
50	5	95
65	5	95

2.2.2. Biochemical assays and *in silico* methods

2.2.2.1.Antiradical activity

a)DPPH

The scavenging activity of the DPPH stable free radical was measured according to the method described by Brand-Williams et *al.*[94] with slight modifications. DPPH is a generated by the delocalization of the spare electron over the molecule, so that the molecule does not dimerize. This delocalization gives a substance characterized by a deep violet color in an absorption band in ethanol solution at 517 nm. When a solution of DPPH is

mixed with a substrate (AH) containing a hydrogen atom, the reduced form is produced, thus leading to the loss of color [95] (**Figure 12).**

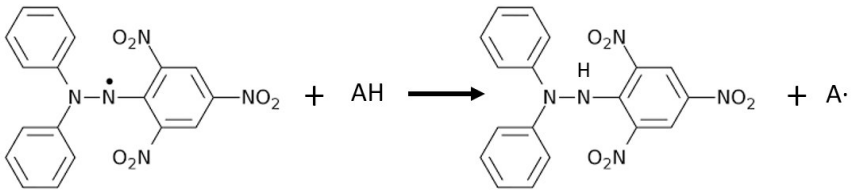

F**igure 12.** DPPH-scavenging reaction scheme (adapted from Alam *et al* 2013)[93].

Before starting the assay, the absorbance of work solution (400μM) was corrected within 0.9 and 1. Then, in a 96 well plate, 10μL of extract in different concentrations, as well as ethanol 100%(w/v) (negative control) were added to 140 μL of DPPH work solution. The absorbance at 517 nm was read at 10 minutes and the percentage of inhibition was calculated using the following formula:

$$\% \text{ inhibition} = \frac{Abs\ EtOH - \text{Abs(sample} - \text{blank)}}{Abs\ EtOH} * 100\%$$

EC50 was determined in GraphPad software, from the graphs inhibition percentage of free radical activity vs concentration of extracts and compared to a positive control, Trolox.

b)Nitric oxide

To determine NO presence a measurement of stable decomposition product NO_2^- was performed by the Griess reaction. This reaction is a two-step diazotization in which the NO-derived nitrosating agent (sodium nitroprusside, SNP), at physiological pH, reacts with sulfanilamide. It produces a diazonium ion that couples to N-(1-napthyl) ethylenediamine

(NED) to form a chromophoric azo product that absorbs strongly at 546 nm [96,97] (**Figure 13)**. If the extract/compound has the property to

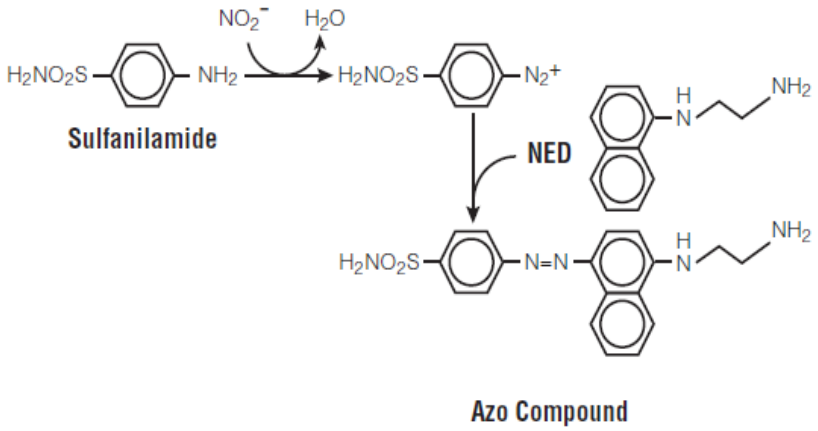

Figure 13. Griess reaction scheme. Figure from Promega Manual [95].

counteract the effect of NO formation, its directly competes with O in the reaction, leading to the inhibition of the NO_2– formation [98,99,100].

In this assay, 50µL of sample at different concentrations or ultrapure water (in the case of negative control) was added in triplicate to 50 µL of SNP (10mM in phosphate buffer, pH 7,4). After that, the plate was incubated at light for 120 minutes. Then, it was added to the control and samples 50 µL of Griess reagent, containing 50:50 of sulfanilamide and NED, both dissolved in 2% phosphoric acid (H_3P0_4) buffer. On its turn, 50 µL of H_3P0_4 buffer was added to the blanks. The plate was incubated in the dark 10 minutes and the absorbance was read at 546 nm. The percentage of $NO^{\cdot}$ scavenging was determined according to the following formula:

$$\% \text{ inhibition} = \frac{Abs\ (control - blank\ control) - \text{Abs(sample} - \text{blank sample)}}{Abs\ EtOAbs\ (control - blankcontrol)H} * 100\%$$

As previously mentioned, EC_{50} was obtained in GraphPad software, being the samples compared to a positive control, ascorbic acid.

2.2.2.3. Acetylcholinesterase activity

a) Ellman assay

AChE activity in the different extracts/compounds was measured indirectly using a modified 96-microplate assay based on Ellman´s reagent [101]. The substrate acetylthiocholine (AtCl) is hydrolyzed by AChE and the generated thiocholine reacts with the chromogen 5,5'-dithiobis-2-nitrobenzoic acid (DTNB) under formation of 5-thio-2-nitrobenzoic acid (TNB) which is monitored at 412 nm. Hereby, the formation of TNB- is directly proportional to the hydrolysis of AchE [102](**Figure 14).**

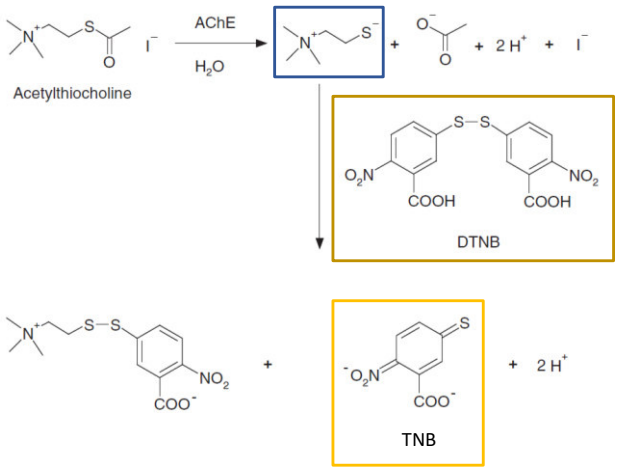

Figure 14. Principal reactions of the Ellman assay for the determination of AChE activity (adapted from Worek 2011)[97].

Briefly, 20µL of the sample at different concentrations were added to 40µL of Tris-HCl buffer pH=8 and 20µL of 0,26 U/mL AchE from electric eel (diluted in BSA 0,1%). To the blanks, it was added 20µL of buffer instead of enzyme. The negative control contains, instead of sample, buffer, while the positive control contains physostigmine ($500x10^{-8}$-$500x10^{-3}$ µg/mL). To all the wells it was added 100 µL of 3mM DTNB (in buffer containing 0.1 M NaCl and 0.02 M $MgCl_2$). The plate was incubated for 15 minutes at room temperature. Then, the enzymatic reaction was initiated by the addition of 20µL of 15mM ATCl and the hydrolysis reaction was monitored every 5

minutes for 20 minutes. The percentage inhibition was calculated accordingly to the next formula[101]:

$$\% \text{ inhibition} = \frac{Abs(control - blank\ control) - \text{Abs(sample} - \text{blank sample)}}{Abs(\ control - blank\ control)} * 100\%$$

, and EC_{50} was determined from the graphs inhibition percentage of free radical activity vs concentration of extracts and compared with a positive control, physostigmine.

b) Molecular docking

Molecular docking is a computational procedure that attempts to predict the interaction mode and binding affinity within macromolecules or, more frequently, of a macromolecule (receptor) and a small molecule (ligand) [103].Potential docking between the AchE enzyme and *Panax ginseng* and *Nelumbo nucifera* compounds was analyzed using the *AutoVina* software (The Scripts Research Institute, Version 4.2., San Diego, California, USA) , a new generation of docking software from the Molecular Graphics Lab [103].

AutoDock Vina performs a structure-based docking, generating different ligands conformers towards a target macromolecule, using a Broyden-Fletcher-Goldfarb-Shanno (BFGS) algorithm. The energy-based scoring function includes terms accounting for short range van der Waals and electrostatic interactions, loss of entropy upon ligand binding, hydrogen bonding and solvation[103,104].

3D structures of the ginsenosides, sapogenins and alkaloids compounds were generated by changing similar molecules obtained in *The Cambridge Crystallographic Data Centre* (CCDC) and using *PyMol.* Then, the designed structures were optimized on *Automated Topology Builder* (ATB)[105]

which performs a refinement of crystal structures using semi-empirical and quantum calculations.

From crystal structures of AchE enzyme (PDB ID: 1C2B for *Electrophorus eletricus* and 4EY7 for *Homo sapiens*) it was possible to understand the complex structure and ligands interactions, as well as the binding site participating residues. The binding site of target protein and the ligand was selected as the active site, using *AutoDock Tools* by drawing of the GridBox (**Figure 15)**.

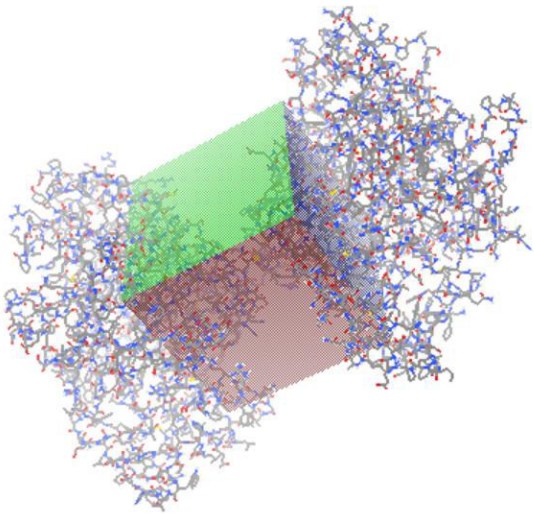

Figure 15. Grid box selection for the active site of AchE enzyme (PDB ID: 1C2B for *Electrophorus eletricus).* The configuration files were made according to the size of this box (x=36, y=36, z=36; center_x=32.747, center_y=65.719, center_z=-52.49; exhaustiveness=20).

Configuration files were prepared for each one of the ligands. The docking and scoring of the compounds with the target molecules were carried out, and the molecular conformation of the docking was obtained according to the score. Docking poses generated by the docking program were directly loaded into PyMOL through the plugin, allowing the visualization of its interactions. Each result from multiple docking runs is summarized in a small text viewer, thus allowing to collect binding energy conformations(kcal/mol)[106].

2.2.3.Culture of BV2 cells and use

2.2.3.1.Principle

BV2-cells were derived from rat/mice-immortalized murine neonatal microglia and it was used as *in vitro* model, reducing the necessity of continuous cell preparations and animal experimentation[107] .

2.2.3.2.Preparation of solutions

a)Medium

BV2 cells were cultured in DMEM containing 10% antibiotic [108]. For that, DMEM powder was dissolved in 3,7 g of sodium bicarbonate and 990 mL of ultrapure water under continuous agitation. pH was adjusted between 7,1-7,3. The medium was filtered into an autoclaved flask using a 0,2 μm Filtropur unit in a laminar flow chamber, under strict aseptic conditions. 10 mL of the referred antibiotic was supplemented and the flask was kept at 4°C [109].

2.2.3.3.Basic cellular protocols

a)Subculturing cells

In this procedure, the culture medium was removed and discarded and the cell layer was washed twice with warm sterile PBS. 1 mL of 0,05% trypsin was added in order to disengage the cells. The flask was incubated at 37°C a few minutes and then the cells were observed at inverted microscope to see rounded cells and dispersed cell layer. 6 mL of DMEM medium with 10% FBS were added to the flask and cells were dissociated by resuspension. This cell resuspension was transferred to a falcon. 20 μL were used in a Neubauer chamber in order to count the number of cells presented (mean of quadrantsx10^4 cells). According to this number, a certain volume of cell resuspension was transferred to the T25 flask, as well

as DMEM medium with 10%FBS up to 6 mL. The cells were incubated at 37°C in a humified incubator gassed with 5% CO_2 [109].

b) Plating cells

According to the number of cells presented in the flask, a certain volume of cell resuspension was added to DMEM medium in 10% FBS. 200 µL, 1mL or 2mL of this resuspension is transferred to each well on 96, 12 or 6-well plate, respectively, to obtain 1,5x10^5cells/mL for subsequent assays[109].

c) Cell extraction

BV2 cells inserted in a plate were washed with warm sterile PBS (37°C) and trypsinized (0,05%). The cells were recovered in DMEM medium with 10%FBS and transferred to marked (for each condition) eppendorfs on ice. A centrifugation at 1000 rpm, 5 minutes yield a pellet which was washed with PBS ice-cold. The final pellet was placed at -80°C for the subsequent steps[110].

2.2.3.4.Cellular assays

a) Cytoprotective/toxicity assay

In order to determine the antioxidant capacity of the extracts/compounds, BV2 cells were co-incubated with an toxic insult ,t-BHP, that induce significantly cell death [111,112]. After pre-incubation with extract/compounds for 3 or 20 hours, half of 96-well plate was co-supplemented with 50 µL of DMEM medium without FBS, while the other half is co-incubated with 50 µL of 0,5 mM t-BHP solution. After 2h30minutes of incubation, cell viability was determined by MTT assay.

b) Nitric oxide determination in culture medium/LPS insult

In order to determine the amount of NO released from BV2 cells which was converted to nitrite, it was performed a determination using Griess reaction[113]. Firstly, the cells were incubated with extracts/compounds of study and incubated for 3 hours until supplementation with LPS (2 µg/mL final concentration). After 20 hours of treatment, supernatants (100 µL) of culture medium were transferred, in triplicate, to the 96-well plate. Then, it was incubated 10 minutes at room temperature in the dark with 100 µL of 1% (w/v) sulfanilamide in phosphoric acid buffer 2%. After that, samples were incubated with 100 µL of 0.1%, w/v NED under the same conditions. Finally, the absorbance at 543 nm was read. Also, the cells incubated with the extracts and LPS were extracted for RNA extraction.

2.2.3.5.MTT assay/Cell viability test

MTT assay is one of the most used colorimetric assay to assess cytotoxicity or cell viability [114]. The principle based on the purpose that the soluble yellow tetrazolium MTT (light sensible) is reduced to an insoluble purple formazan by dehydrogenases occurring in the mitochondria [115,116]. This product can posteriorly be solubilized and quantified spectrophotometrically at 570 nm, being proportional to viable cells [116] (**Figure 16).**

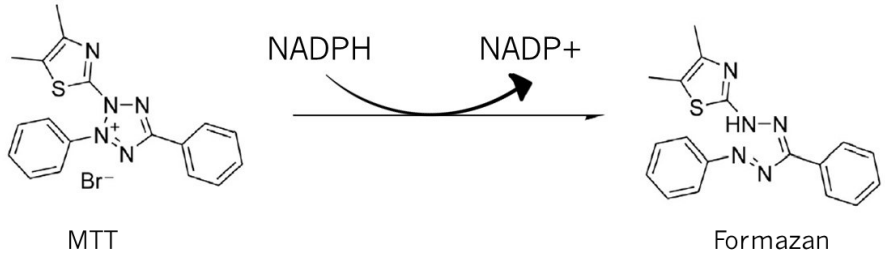

Figure 16. Enzymatic reduction of MTT to formazan (adapted from Kuete 2017)[119].

In this protocol, after cell incubation with the extracts/compounds under of study, the medium was removed and 100µL of MTT (final concentration of 0,5 mg/mL) was added to all the wells. After that, the plate was incubated at 37°C 1h-1h30. The medium presented in the plate was discarded and then 150 µL of a 50:50 mixture of DMSO and methanol was added in order to solubilize the purple formazan dye. The plate was shaken, and the absorbance was read at 570 nm. The percentage of cell viability was calculated as followed:

$$\%\text{cell viability}=\frac{Abs(negative\ control)-\text{Abs(sample)}}{Abs(negative\ control)}*100\%$$

2.2.3.6. Gene expression protocol

a) RNA extraction protocol

Total RNA was extracted from the isolated cells, using the GRS Total RNA Kit – Blood & Cultured Cells (GrisP)[117] with the supplied protocol. The RNA purity and concentration were checked through the ratios 260/280 and 260/230 in a Nanodrop spectrophotometer. To control the integrity of RNA, the samples were run in a 1% agarose gel (agarose in TAE 0.5x buffer). *Cybersafe* dye was used for the samples and a specific marker GRisp Ladder 1kB was used to control the visualization of RNA bands. Electrophoresis was performed at 100 V voltage and the gel was visualized in ChemiDoc.

b) cDNA protocol

The reverse transcription /first-strand cDNA synthesis was performed using 1 µg of each sample RNA with the Xpert cDNA Synthesis Mastermix (GrisP)[118] and the supplied protocol. Using the thermocycler,

the samples were run at the following conditions: 5minutes at 65ºC, 2 minutes on ice, 10 minutes at 25ºC, 15 minutes at 50ºC and finally, to inactive RTase enzyme, 5 minutes at 85ºC. cDNA samples were kept on ice to the posterior step.

c) Real Time Polymerase Chain Reaction (RT-PCR)

Quantitative real-time PCR was carried out with Xpert Fast SYBR Green Master Mix (GrisP) and performed in 96-well plates using a CFX96 Real-Time Detection System (Bio-Rad). For each cDNA sample, qPCR reactions were undertaken in triplicate using 5 μL Master Mix, 300 nmol/L of each primer, 1 μL of diluted cDNA (1:10) and nuclease-free water to a final volume of 10 μL. The conditions used in the cycler were 15 min at 95°C and 45 cycles of 15 s at 95°C, 30 s at 55°C and 30 s at 72°C. Experiments were analyzed with the software Bio-Rad CFX Manager (Bio-Rad), using glyceraldehyde-3-phosphate dehydrogenase (GAPDH) as internal control [119]. For each well, melting curves were analyzed and the results were optimized. IL-6, iNOS, COX-2 and TNF-α were the genes under evaluation.

3.RESULTS AND DISCUSSION

3.1.Phytochemical characterization

3.1.1. Total phenols and flavonoids quantification

Phenolic compounds are very important plant constituents which exhibit antioxidant activity by inactivating free radicals or preventing decomposition of hydroperoxides into free radicals[120]. The total phenols (TP) content of ODL and DN extracts were determined using the Folin-Ciocalteu phenol reagent, being expressed in mg gallic acid equivalents (GAE) per gram dry extract weight. Phenolic compounds undergo a complex redox reaction with phosphotungstic and phosphomolybdic acid present in the reagent[121] and the maximum absorption of these complexes depends on the concentration of these compounds [87,88,89]. However, this assay is not so reliable since ,as reported in the literature, Folin reagent is poorly specific, also reacting with aromatic amines of amino acids and other purines [86, 121, 122, 123]. On its turn, flavonoid content was determined using aluminum chloride in a colorimetric method being results expressed in mg quercetin equivalents (QE) per gram dry extract weight (**Table 7**). This method is specific for flavones and flavonols, some types of polyphenols [122].

Regarding to TP and TF content of the extracts (ODL30, ODLBu. ODL50,DN), it is possible to visualize that ODL50 contains the highest amount (51,957±0,898 GAE/g and 47,615±0,982 QE/g), while DN extract have the lower content of all the extracts (30,296±0,206 GAE/g and 28,581±0,252 QE/g).

Focusing on TP quantities, within the ODL fractions, ODL50 contains the highest content of all the fractions (51,957±0,898 GAE/g), being followed by ODLBu (41,245±0,794 GAE/g). On its turn, ODL30 contains the lowest content in phenols (36,164±0,878 GAE/g). Additionally, TF follows the same trend with ODL50 containing the highest content

(47,615±0,982 QE/g), followed by ODLBu and ODL30 (39,614±0,624 QE/g and 29,300±0,258 QE/g, respectively).

Table 7. Quantities of total phenols and flavonoids of the extracts of study, determined by Folin-Ciocalteau and aluminium chloride methods

Extract	Total phenols (GAE/g)	Total flavonoids (QE/g)
DN	30,296±0,206	28,810±0,252
ODL30	36,164±0,878	29,230±0,258
ODL50	51,957±0,898	47,615±0,982
ODLBu	41,245±0,794	39,614±0,624

GAE-gallic acid equivalents; QE-quercetin equivalents, in mg/g extract

The extractability of the phenolic compounds depends on the type of the solvent, nature and preparation of material to be extracted, chemical structure of phenolic compounds, temperature, extraction time, solid-liquid ratio, extraction method employed and possible presence of interfering substances[124].

Concerning to ODL fractions and its precursor N-butanol fraction, one obtained from an ODL extract in 70%ethanol had previously demonstrated a content of TP of 63,310 GAE/g and TF of 56,690 QE/g [42], higher quantities than those presented for an extract in 80% ethanol. As observed, ODLBu contains a higher amount of TF and TP than ODL30 and lower content than ODL50. This might be to a better affinity of some compounds to this solvent. To a better approach of this theory, HPLC method was performed in order to understand this relation.

Regarding to DN extracts, Bhattacharrya *et al.* showed that methanolic extract of DN stem have a TP of 41,39 ± 0,100 GAE/g [125], higher than the one presented in this work (30,296±0.206 GAE/g).

3.1.2.High Performance Liquid Chromatography (HPLC)

In order to understand the relation of the biochemical and biological activities with their chemical profile, HPLC was performed for the ODL extracts. Its chromatograms are represented in the **Figure 17.** However, it was only preformed the identification of ODL30 and ODLBu compounds as indicated in the **Table 8.** The chromatogram of ODL50 was not well succeeded. The detection of the compounds was unstable, not enabling the individualization of peaks. Instead, it is represented its total content quantification. For future approaches, the running must be repeated, with other conditions. The phenolics quantification, in mg QE/g extract was performed using the chromatograms at 280 nm: the retention time, area and UV spectrum of a standard solution of QE at 0,0625 mg/mL.

Table 8. Distribution and content of identified compounds in HPLC at 280 nm of ODL extracts, expressed in mg QE/g

		Extracts		
Number	Compound	**ODL30**	**ODLBu**	**ODL50**
1	Derivatives of apigenin	_____	24,397	?
2	Derivatives of quercetin	_____	132,482	?
3	Derivatives of caffeoylquinic acid	32,762	96,595	?
4	Catechin	4,810	_____	?
5	Glycosylated quercetin	6,443	_____	?
6	Glycosylated caffeoylquinic acid	1,357	_____	?
	Total	89,498	371,343	439,605

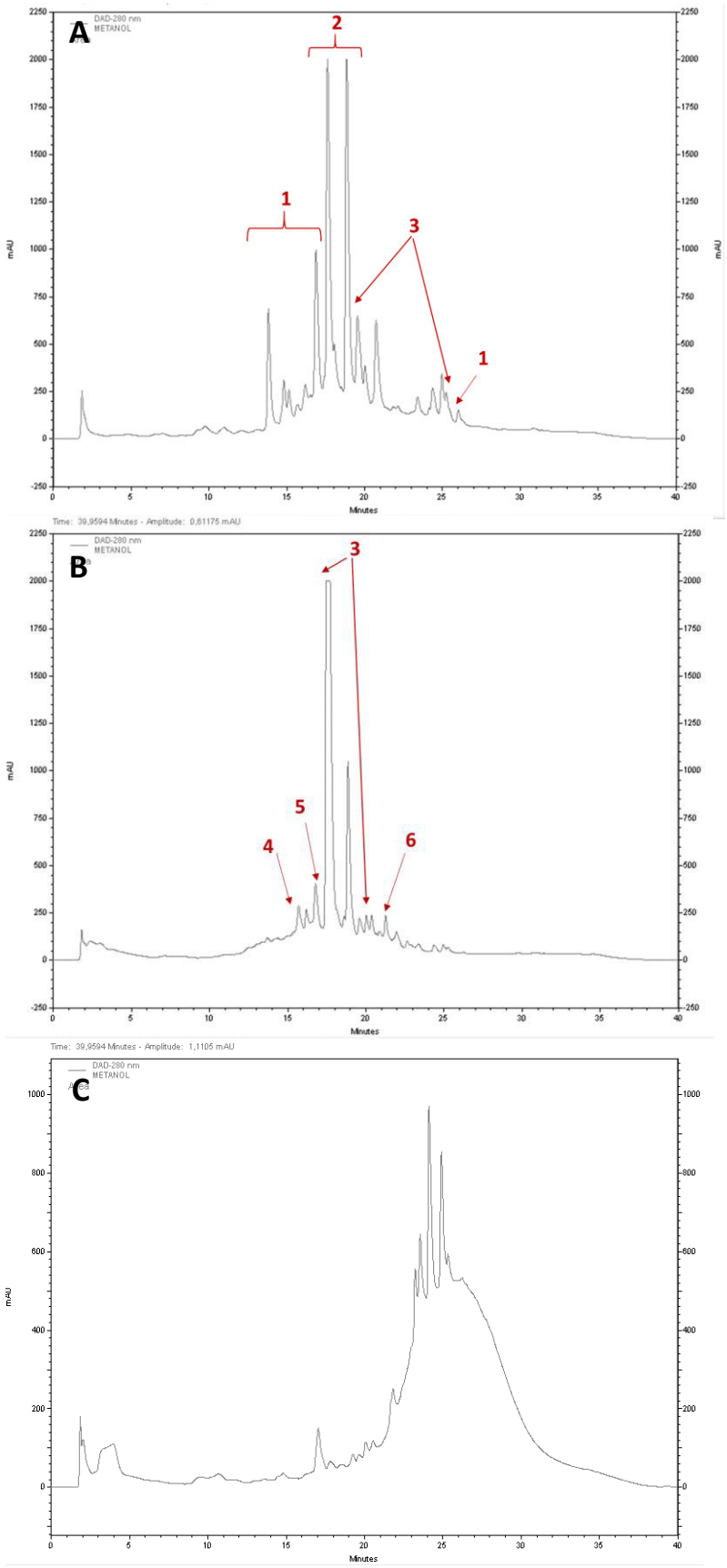

Figure 17. HPLC chromatograms of **a)** ODLBu, **b)** ODL30 and **c)** ODL50, recorded at 280 nm. The identification of the compounds in the figure are listed in the **Table 13.**

The tendency of total QE content of HPLC chromatograms for ODL extracts seems to be in accordance with the TF content determined by aluminum chloride method (29,723 ±0,258 QE/g for ODL 30; 39,614 ±0,624 QE/g for ODL Bu and 47,615±0,982 QE/g for ODL50). However, the values obtained in the assay are much lower than those quantified in the chromatograms (89,498 QE/g; 371,343 QE/g and 439,605 QE/g, respectively).Despite of the fact that aluminum chloride being a sensitive and widely used method, flavanols and flavones exist in plants as glycosides and the presence of sugar moieties may interfere in the chelation with $AlCl_3$. Thus, any blockage of the hydroxyl groups prevents the bathochromic shift towards another wavelength. Also, even methoxylation of some carbons can reduce the bathochromic shifts[126]. On its turn, HPLC is an analytical technique that couples high-resolution chromatographic separation with sensitive spectrometric detection, thus comprising a larger range of compounds detected[127].

Regarding to the ODL composition, ODL30 and ODLBu are both rich in flavonoids as quercetin derivatives, as well as in phenolic acids (caffeoylquinic acids). In addition, ODLBu has apigenin derivatives (24,397 QE/g) which are not presented in its posterior fraction ODL30. Conversely, the last shows the existence of catechins (4,810 QE/g). According to the method described by the collaborator professor Qiong, the ODL flower extract in 80 % ethanol was extracted in a n-butanol part (ODLBu). This precursor fraction was eluted by HP-20 macroporous resin with 30% and 50% ethanol, obtaining the ODL30 and ODL50 parts. This resin has as purposes the enrichment of phenolic compounds[128]. It is noted that apigenin is practically insoluble in highly polar solvents such as water[129] . Thus, it might explain its absence in ODL30 (30%ethanol:70%water) with a higher polarity. The compounds identification was not possible to perform for ODL50 but it is predicable that ODL50 will contain a higher content in apigenin derivatives since there was a decrease in solvent polarity of the extract (50%ethanol:50% water). Also, its total quantification (439,605

QE/g) follows the prediction of Du *et al.* who said that an increase of ethanol concentration in the extracting solvent increase flavonoid contents in the ODL extracts[39].

Previously, *Hemerocallis fulva* flowers demonstrated containing high levels of caffeoylquinic acids and a potent ROS scavenging activity[130,131]. Caffeoylquinic acids, especially chlorogenic acid in *H. fulva* flowers may, at least partially, contribute to their ROS scavenging effect[130,131]. More than 40 ingredients, including anthraquinones, flavonols, amides, polyphenols, and other compounds were purified from *Hemerocallis citrina* for 30 years. Liu *et al* [132] obtained HPLC-MS chromatograms of fresh flowers of ODL, among other parts of the plant. In the fresh flowers of ODL, there was a high amount of phenols as chlorogenic acid derivatives (e.g. dihydroxy-chlorogenic acid IV and methyl-clorogenic acid) and cinnamic acid. Also, flavonoids as derivatives of rutin, kaempferol and quercetin were found.

The identification/quantification of the compounds of *Dendrobium nobile* extract was not also possible. The chemical composition of various part of the plant is well reviewed[133]. The isolated compounds are mainly alkaloids, polysaccharides, sesquiterpenoids, phenanthrenes, bibenzyls, and other compounds, among which alkaloids are high in content and widely used in research and application[133]. Zhang *et al* used the 60% EtOH extract of the stems of *D. nobile* which was suspended in H_2O and partitioned with EtOAc fraction[35]. In HPLC, this fraction accused the presence of 12 phenolic compounds, including hydoxycinnamic and hydroxybenzoic acids[35]. Since alkaloids may absorb at lower wavelengths[134] (not included in this HPLC assay), the major alkaloidal composition in DN extract can be the cause to obtain an adequate profile in HPLC chromatogram.

The presence of alkaloids as dendrobine and dendramine might explain its better activity on AChE activity (EC_{50}=740±28 µg/mL) than ODL30(EC_{50}=1203±16 µg/mL). Also, its toxicity on BV2 cells may derivate from its major alkaloidal composition which is reported as having toxic effects on animal cells. Indeed, dendrobine induced cytotoxicity and apoptosis at 2.5 µg/mL on A549 NSCLC lung cancer cells[135].

3.2. Antioxidant assays

3.2.1. DPPH assay

In this study, DN and ODL extracts, as well as PG compounds and alkaloids from NC were evaluated for their ability to scavenge DPPH radicals. Some of the tested plant extracts/compounds inhibited, to different extents, the DPPH radical. This result proved that the extracts/compounds can donate an electron or hydrogen which could react with DPPH radical. Their activities were compared with standard Trolox (6-hydroxy-2,5,7,8-tetramethylchroman-2-carboxylic acid), a potent antiradical, water-soluble derivative of vitamin E[136]. The values of EC_{50}(50 % effectiveness value), i.e,, the concentration where 50% of its maximal effect is observed, from DN, ODL extracts and alkaloids from NC ranged from 109-1004 µg/mL. On its turn, all the compounds of PG demonstrated non-detectable activity in scavenge DPPH radicals, even at maximum tested concentration(1500µg/mL) (**Table 8**).

Concerning the results of EC_{50}, as reported in the literature, a significant antioxidant activity for plant extracts comprises EC_{50}<50µg/mL, while moderate activities includes 50<EC_{50}<100µg/mL and low activities are higher than 100 µg/mL[137,138]. Therefore, for the ODL and DN extracts, all of them present low antioxidant activity since their EC_{50} are higher than 100 µg/mL On its turn, to the pure compounds elevated activities are correlated with EC_{50} <10 µg/mL, moderate activities within 10-20 µg/mL, while low activities are >20 µg/mL[137]. Thus, for alkaloids from NC, its activity is also low since its EC_{50} value is higher than 20 µg/mL.

Table 9. Effectiveness values (EC_{50}) obtained on DPPH assay of the extracts and compounds/mixture of compounds of study, compared with standard Trolox

		EC_{50} (µg/mL)
Extracts	DN	1004±45
	ODL30	1002±30
	ODL50	244±32
	ODLBu	658±43
Compounds	Alkaloids from NC	109±12
	DS1227	N.D.
	DS1226	N.D.
	PPT	N.D.
	PPD	N.D.

N.D.-non detectable even at maximum tested concentration (1500 µg/mL)
EC_{50} (Trolox):19±03 µg/mL
The results are expressed as mean±SD (n=6).

3.2.1.1 *Hemerocallis citrina* and *Dendrobium nobile* extracts

Focusing on ODL extracts, it was verified that the ODL50 reveals the strongest DPPH scavenging effect since its EC_{50} is of 244±32 µg/mL, being that effect lower to the standard Trolox (EC_{50} = 19±03 µg/mL). Then, the ODLBu contained a weaker effect (EC_{50} = 658±43 µg/mL), being followed by ODL30 with EC_{50} = 1002±30 µg/mL (**Figure 18)**. An inverse correlation is observed between the EC_{50} values of the ODL extracts

(ODL50>ODLBu>ODL30) and the amount of TP and TF, stresses the solvent used for its extraction. Chao *et al.* had tested extracts of *Hemerocallis fulva* in acidified methanol and found an anti-DPPH activity of 206 ±05 µg/mL, similar of those obtained for ODL50 eluted fraction[139]. A n-butanol fraction of *Hemerocallis citrina* in 70% ethanol demonstrated an EC_{50} value of 115 µg/mL for scavenging of DPPH radicals, being this value lower than any of the fractions tested [42].

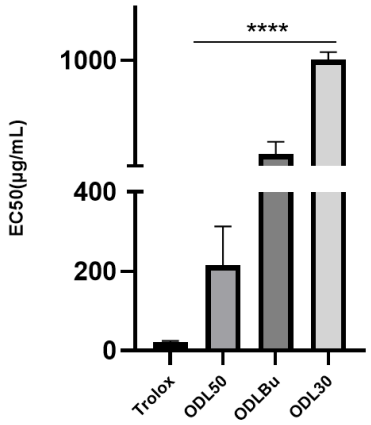

Figure 18. EC_{50} values for DPPH assay of *Hemerocallis citrina* (ODL) extracts, compared with standard Trolox. Each bar represents the mean ± standard deviation (SD) considering the results obtained at least three independent experiments. All the values are statistically different ($p \leq 0.0001$).

Previously, the DPPH radical scavenging activities of *Dendrobium signatumium* leaves extracted with 95% ethanol showed an activity of 112 µg/mL [140], and ethanolic extract of *Dendrobium crepidatum* showed an EC_{50} of 99 µg/mL [141], values lower than those obtained for ethanolic DN extract (1004±45 µg/mL). Besides that, Bhattacharyya *et al.* tested DN methanolic extracts of leaves and stems at final concentrations of 33 µg/mL, with an activity of 89,8±2,9% and 65±5%, respectively[125]. The ethanolic extract of DN stem of this study showed an activity of 51,35± 4,20% at concentrations of 1000 µg/mL (not shown), which means that possess lower capacity on capture DPPH radicals than methanolic extracts. This

might be in accordance with their TP content (41.39 ± 0.1 GAE/g and 30.296±0.206 GAE/g for methanolic and ethanolic extracts, respectively).

It is well reported that there is generally a direct correlation between TF/TP content and radical scavenging activity [38,42,142,143]. Phenols contributing to reduce the rate of oxidation by transferring a H atom from their ·OH groups to DPPH radicals or by-concerted transfer of H as proton and one electron from the radical (proton-coupled electron transfer mechanism) [143,144,145,146]. Therefore, its number and position of ·OH groups, and the twisting angle of rings influence its antioxidant proprieties[146]. Finally, it is important to note that divalent N from DPPH radicals is strongly hindered by an ortho H atom on each of the phenyl rings and by the o-NO_2 groups of the picryl ring, which leads to a sterical shielding and to a entropic reaction in DPPH·phenols reaction[145,147,148]. Therefore, the results for the AA of ODL and DN extracts cannot be conclusive for its antiradical properties and must be performed other antioxidant assays, as ABTS radical scavenging activity and ferric reducing antioxidant power (FRAP) assays.

3.2.1.2. *Panax ginseng* compounds

Regarding to PG compounds, as previously mentioned, their scavenging activity on DPPH radicals is poor, even at the maximum tested concentration (1500 µg/mL). Still, there is a tendency according to the compound/mixture of compounds tested (**Figure 19)**. Indeed, at the

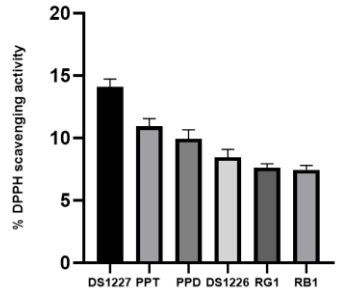

Figure 19. DPPH scavenging· activity of *Panax ginseng* compounds at concentrations of 1500 µg/mL. Values are represented in mean ±SD.

concentration of 1500 µg/mL, DS1227 presented the strongest activity (14,09%), being accompanied to the compounds PPT, PPD (10,94 and 9,94%) and DS1226(8,46%). Then, RG1 (7,63%) and RB1 (7,42%) displays the weakest activity.

According to the literature, compared with their precursor ginsenosides(RG1 and RB1), sapogenins or aglycones (PPT and PPD, respectively) showed better biological activity, suggesting that the bioactivity of *Panax* compounds are dependent from aglycone-structure, and that the role of the sugar moieties in its activity is not necessary [50,51], in accordance with these results(**Figure 18)**. As concerning there, the slightly activity of sapogenins on scavenge DPPH radicals is probable due to the presence of hydroxyl (-OH) groups which gives H that reacts with its radical. Also, the effect is stronger in PPT than PPD since the first compound contains one more -OH group at position C-6(**Figure 7)**, effect also showed in other studies[149].

Concerning to the mixture of compounds DS1227, containing mostly 7.02 % PPD and 20.51% PPT, it displays better activity than DS1226, comprising 16% PPD and 33% PPT. The main difference within both mixture of compounds is that DS1226 presents a higher percentage of sapogenins PPT and PPD. Despite the fact sapogenins elicit a little stronger effect in scavenging DPPH radicals, DS1227, with less content in aglycones, presents better activity. Both mixtures seem to do not have potential DPPH scavenging activity as seen in the **Figure 18**. Also, Chae *et al.*[150], Xie *et al.*[151] and Kang *et al*[149] have been demonstrated the weak degree of electron donating ability of both ginsenosides and sapogenins.

3.2.1.3. *Nelumbo nucifera* alkaloids

Alkaloids from NC were evaluated regarding to its DPPH scavenging effect, showing, among the compounds/extracts tested, it exhibited the

strongest anti-DPPH radical activity (109±12 µg/mL), p=0.001, regarding to Trolox control. Alkaloids are well reported as having beneficial effects on neurodegenerative disorders, concerning to its antioxidant activities [152,153]. They are also recognized as the main active compounds in lotus leaves, including aporphine- and benzylisoquinoline-type alkaloids [80].

The effect of isolated alkaloids from embryo seeds has been studied, demonstrating its strong anti-DPPH activity, from values of 12.07 to 25.68 µM [84] It was verified that, at 100µM, the compound nuciferin (NF) exhibited 9,1% of activity, while nornuciferin(N-NF) displayed 16,9%, being that values compared to vitamin C. Also, it revealed the presence of other aporphine-alkaloids as lysicamine and cepharadione B [154]. The air-dried NC leaves used in our study had revealed the presence of aporphine-type alkaloids as NF (27.76%), N-NF (13.23%), and 2-hydroxy-1-methoxyaporphine (HMA, 4.23%)[80,81]. As visualized in the graph of **Figure 20**, at maximum tested concentration (500 µg/mL), alkaloids display in mean 92,29% of activity, demonstrating its good antioxidant activity, even it is not considered strong as predicted in literature (EC_{50}>20 µg/mL) [137].

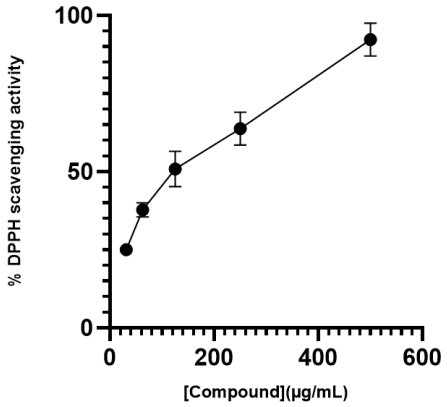

Figure 20. DPPH scavenging- activity (%) of *Nelumbo nucifera* alkaloids. Values are represented in mean ±SD.

Most aporphine and benzytetrahydroisoquinoline alkaloids have multiple -OH groups on the benzene rings, being expected to have the ability to scavenge free radicals, at least by generating thermodynamically and kinetically stable phenoxy radicals[155,156]. Generally, aporphine alkaloids displays higher antioxidant activity than benzytetrahydroisoquinoline-type alkaloids [155,156]. This is due to an increase of spin delocalization of phenoxy radicals in the plane of biphenyl configuration leading to a more stable configuration in aporhine-type alkaloids[155].

3.2.2.Nitric oxide assay

It is well known that NO· has an important role in various inflammatory processes but an increased level is directly toxic to tissues causing serious damages[157].This is because NO· can react with $O_2^{\cdot}$ to form the OONO· anion, a potential oxidant that can decompose to produce OH and NO [158,159]. Therefore, the inhibitory activities against NO· and $O_2^{\cdot}$ have the potential to blocking the accumulation of these radicals and may help to arrest its chain of reactions, which partly cause continued oxidative stress and chronic inflammation[159, 100].

In this assay, plant extracts/compounds were tested for NO·scavenging activity and compared with a known positive control, ascorbic acid (EC_{50}: 2±1 µg/mL). The extracts and compounds inhibited the accumulation of NO radical, to different extents, with EC_{50} values for DN and ODL extracts ranged from 84-464 µg/mL, while for NC alkaloids and PG compounds comprises values from 100 to 863 µg/mL. On its turn, RB1 and RG1 compounds from PG had no detectable activity, even at maximum tested concentration (1500 µg/mL) (**Table 10).** The extract which has better activity, i.e., lower EC_{50}, was ODL50 (EC_{50}=84±03 µg/mL), while DN extract has a weaker activity (EC_{50}=464±28 µg/mL). Referring to the compounds, the best biological activity was displayed by alkaloids from NC (EC_{50}=100±11 µg/mL). The weakest activity is presented by DS1226 compounds (EC_{50}=863±12 µg/mL). Following the categorizing system of Kumaran *et al.* ODL50, ODLBu and alkaloid extract of NC have moderate activity against NO radicals (25< EC_{50}<200 µg/mL), while the DN, ODL30, DS mixture , PPD and PPT have low activity (EC_{50}>200 µg/mL) [100].

Table 10. Effectiveness values (EC_{50}) obtained on NO·scavenging assay of the extracts and compounds/mixture of compounds, compared with standard ascorbic acid

		EC_{50} (µg/mL)
Extracts	DN	464±28
	ODL30	234±20
	ODL50	84±03
	ODLBu	159±24
Compounds	Alkaloids from NC	100±11
	DS1227	253±12
	DS1226	863±12
	PPT	503±20
	PPD	648±26
	RG1	N.D.
	RB1	N.D.

N.D.-non detectable even at maximum tested concentration (1500 µg/mL)

EC_{50} (ascorbic acid):2±1 µg/mL

The results are expressed as mean± SD (n=9)

3.2.2.1. *Hemerocallis citrine* and *Dendrobium nobile* extracts

Regarding to the ODL extracts, ODL50 reveals a better NO scavenging effect due to its lower EC_{50} (84±03 µg/mL), but higher EC_{50} than the standard ascorbic acid (2±1 µg/mL). ODLBu displays a weaker effect (EC_{50} =159±24 µg/mL), followed by ODL30 (EC_{50} = 234 ±20 µg/mL) (**Figure 21)**. These results may be, once again, according to their content

in TP and TF which is higher in ODL50(51,957±0,898 GAE/g and 47,615±0,982 QE/g, respectively) thus contributing to a stronger effect in NO scavenging. The effect of the other extracts is weaker since its content in these compounds is significantly lower than ODL50. Previous studies have shown that aqueous extracts from *Hemerocallis fulva* displayed NO-scavenging activity of 55 % at concentrations of 200 µg/mL [160]. ODL30 (at 250 µg/mL) has 52% of activity (results not shown), therefore being weaker on scavenge NO radicals. On its turn, ODL Bu and ODL50 have 60% and 74% of activity, respectively, so both are stronger than *Hemerocallis fulva* aqueous extract.

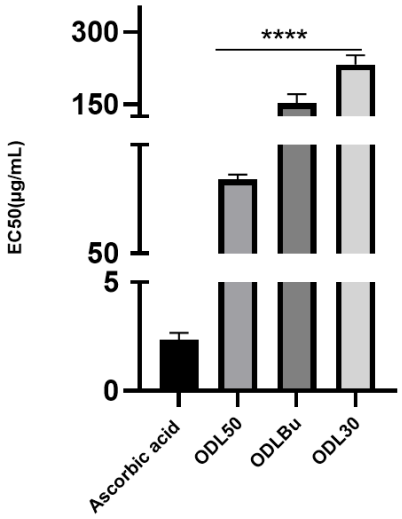

Figure 21. EC_{50} values for NO assay of *Hemerocallis citrina* (ODL)extracts, compared with standard ascorbic acid. Each bar represents the mean ± SD considering the results obtained at least three independent experiments. All the values are statistically different ($p \leq 0.0001$) vs positive control, ascorbic acid.

Regarding to DN extract, the pseudobulb stem plant material of *Flickingeria nodosa*, another specie of orchid, was extracted with Soxhlet and petroleum ether. It was found that has an EC_{50} of 456 µg/mL [161], value similar to DN extract (464±28 µg/mL). Comparing with ODL extracts, DN extracts possess weaker activity.

According to Yenes *et al.* the reactivity of phenols with NO· depended upon the nature, and most importantly, of substituents position with respect to the hydroxy phenol group. Thus, the more activated the phenol, the higher the rate of nitration or nitrosation. Also, reactions of nitrosation occurs mostly on phenol substrates bearing a free para- position with respect to the OH group [162].

3.2.2.2. *Panax ginseng* compounds

Regarding to PG compounds, their scavenging activity on NO radicals seems to be stronger than those observed for DPPH radicals. However, RB1 and RG1 demonstrated once again non-detectable activity even at the maximum tested concentration (1500 µg/mL). Furthermore, the scavenging power among them is according to the same order. It is observed that, at the concentration of 1500 µg/mL, DS1227 presented the strongest activity (79,29%), immediately followed by PPT, PPD (77,69% and 75,97%, respectively) and DS1226(45,66%). Then, RG1 (28,64%) and RB1 (28,99%) displays the weakest activity (**Figure 22)**. Hitherto, our results show that, compared with their precursor ginsenosides (RG1 and RB1), sapogenins or aglycones (PPT and PPD, respectively) display better biological activity, which complements the assumption previously reported, i.e., the bioactivity of *Panax* compounds are dependent from aglycone-structure. Therefore, the non-sugar part of saponins can have a direct

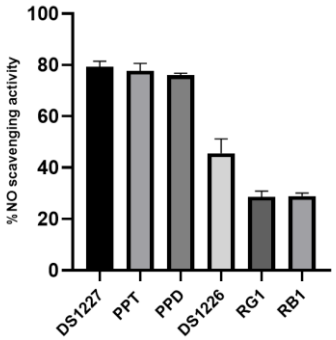

Figure 22. NO· scavenging- activity (%) of *Panax ginseng* compounds at concentrations of 1500 µg/mL.Values represented in mean ±SD.

antioxidant activity which may contribute to the free radical scavenging capacity[50,51]. Concerning to DS mixture, despite the fact of DS1226 contain a higher content in PPT and PPD, DS1227 presented the highest activity.

Ginseng extracts had previously demonstrated as do not possess NO· scavenging activity [163]. Kang *et* al had also showed that ginsenosides RG1 and RB1 do not scavenge ·NO [164]. Therefore, our results confirmed these reports. Regarding to PPT and PPD, there are no reports of direct NO· radical scavenging activity but of indirect effects, namely inhibition of iNOS expression and decreasing NO levels[63].

3.2.2.3. *Nelumbo nucifera* alkaloids

Concerning to nitric oxide scavenging of *Nelumbo nucifera,* it was previously demonstrated that 50% hydroalcholic extract of seeds had an EC_{50} of 85±4 µg/mL [165,166], lower than alkaloid extract of leaves (100±11 µg/mL) . The major secondary metabolites present in the seeds are alkaloids such as dauricine, lotusine, nuciferine, pronuciferine and liensinine. It also contains saponins, carbohydrates and polysaccharides[167]. Therefore, the higher activity of seed extract than our alkaloidal mixture can be explained by the presence of these last compounds that contribute with their chemical groups to scavenge NO· radicals.

3.3. AChE activity

Acetylcholinesterase (AchE) is a key enzyme involved in the termination of impulse transmission at cholinergic synapses by rapid hydrolysis of the neurotransmitter acetylcholine (Ach), producing choline and acetate[168,169]. Ach is a neurotransmitter which mediates an array of functions, including cognition [170]. The enzyme inactivation, induced by various inhibitors, leads to the preservation of Ach levels, thus improving the cholinergic function. AchE inhibitors, interacting with the enzyme as their primary target, are applied as relevant drugs and toxins for the relieving of the symptoms of AD [168,171,172].

The various oligomeric forms of AChE of the electric eel, *Electrophorus electricus,* are structurally similar to those in vertebrate nerve and muscle [169,173] and therefore it was a good approach in this study to evaluate anti-AChE activity. Using Ellman's colorimetric assay, DN and ODL extracts, as well as compounds of PG and NC were evaluated for its activity against AchE, being compared with a commercial drug, physostigmine (EC_{50}=142x10^{-9}±513x10^{-10} µg/mL). It was demonstrated for the extracts under study EC_{50} values from 445 to 1203 µg/mL (**Table 10)** while for the compounds the values ranged to 237 from 647 µg/mL. Santos *et al.* have categorized plant extracts and fractions, according to the EC_{50} values: high potency, EC_{50}< 20 µg/mL; moderate potency, 20< EC_{50}< 200 µg/mL and low potency EC_{50}>200 µg/mL. These cutoffs were set according to the average EC_{50} value described for galantamine in the literature (575x10^{-3} µg/mL) [174]. Therefore, for DN and ODL extracts as well as for DS mixture and total alkaloid extract, since all comprises values EC_{50}>200 µg/mL, its anti-AchE activity can be considered of low potency. By the other hand, the pure compounds ranges comprised, for high potency EC_{50}<15µM; moderate potency, 15 < EC_{50} < 50µM; and low potency,50 < EC_{50} < 1,000µM [175]. Converting in µM units, the compound RG1 has an EC_{50} of

295.88 µM, RB1 583.25µM, PPT 787.6 µM and PPD 603.39 µM. Therefore, all these compounds have low potency on inhibit AchE activity.

Table 11. Effectiveness values (EC_{50}) obtained on AchE assay of the extracts and compounds/mixture of compounds, compared with standard physostigmine

		EC_{50} (µg/mL)
Extracts	DN	740±28
	ODL30	1203±16
	ODL50	445±12
	ODLBu	518±07
Compounds	Alkaloids from NC	366±94
	DS1227	265±11
	DS1226	589 ±03
	PPT	375±40
	PPD	278±21
	RG1	237±26
	RB1	647±56

EC_{50} (physostigmine): $142x10^{-9}$±$513x10^{-10}$ µg/mL
The results are expressed as mean±SD (n=6).

The active site of AChE contains two main subsites, the esteratic (ES) and anionic (AS) subsites, corresponding to the catalytic machinery and the choline-binding pocket, respectively. In the ES the catalytic triad is constituted by the residues of histidine, glutamate and serine, whereas in AS a tryptophan residue is able to bind quaternary ligands, which may act as competitive inhibitors [169,175,176]. Also, there are peripheral anionic site (PAS) [175,176](**Figure 23).**

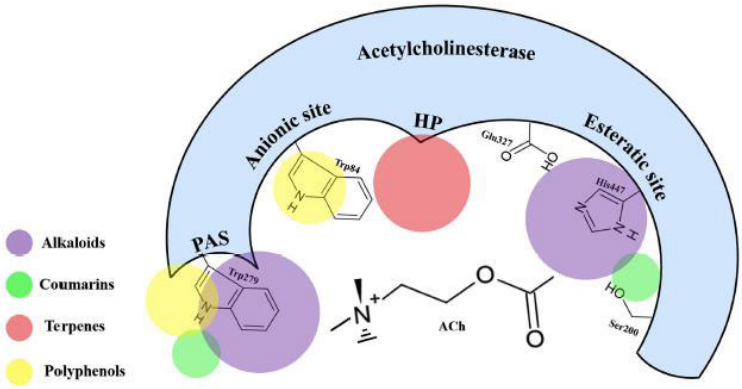

Figure 23. Schematic representation of AchE binding site and the neurotransmitter Ach (from Santos *et al*)[173]. Enzyme pocket is typical composed by esteratic site(ES), anionic site(AS), peripheral anionic site (PAS), as well as hydrophobic pocket (HP). Colored circles represent the main binding sites for different class of compounds.

In silico methods (images obtained by *PyMol* software) also demonstrates the 3D structure of AchE from *Electrophorus eletricus* (**Figure 23**). The enzyme contains 59,42 KDa and is composed by alpha helixes. Its subunits present the capacity to form heteromeric quaternary associations, forming a dihedral symmetrical protein[177]. The active site is inserted in the deep gorge between the dimers[178].

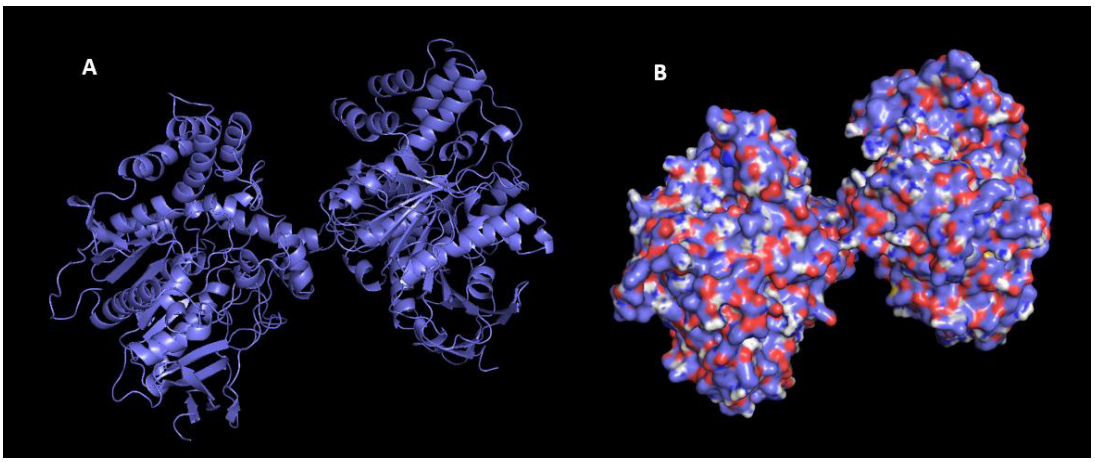

Figure 23. *In silico* image of AChE from *Eletrophorus eletricus* (PDB ID: 1C2B) represented in **a)** cartoon and **b)** surface. Represented structures were obtained by *PyMol* software

3.3.1. *Hemerocallis citrina* and *Dendrobium nobile* extracts

Several non-alkaloidal and potent AChE inhibitors have been obtained from natural sources, including terpenoids and flavonoids[170,172,179]. As reported, some of the structural features and nature of the substitutions in the rings may determine the antioxidant activity of flavonoids. The degree of hydroxylation and the positions of the hydroxyl groups on ring B, in particular, the catechol group, can increase its bioactivities [180]. These compounds seem to act as non-competitive inhibitors which bind to PAS of the enzyme[175].

Concerning to ODL extracts, all the extracts exerted anti-AchE activity (**Figure 24)**, however with low potency(p>0,0001 comparing with positive control, physostigmine) with ODL50 possessing the best activity among them (EC_{50}=445±12 μg/mL), three times stronger than ODL30(EC_{50}=1203±16 μg/mL). This feature follows the previous trend regarding the content of TP/TF of the extracts, much higher in ODL50.

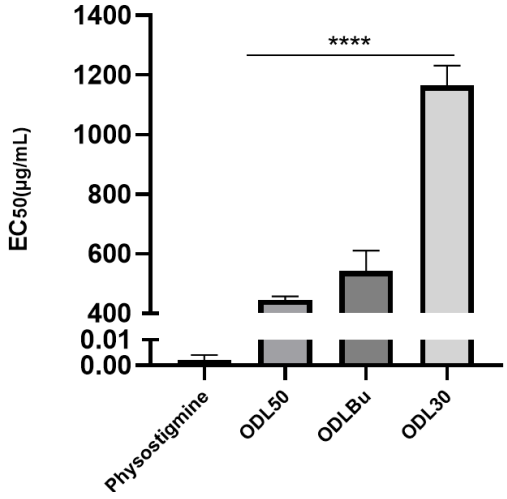

Figure 24. EC_{50} values for AchE assay of *Hemerocallis citrina* (ODL) extracts, compared with standard physostigmine. Each bar represents the mean ± SD considering the results obtained at least three independent experiments. All the values are statistically different (p ≤ 0.0001) vs positive control, physostigmine.

As far as we know, there are no reports regarding AchE activity from *Hemerocallis* and even other species of lilium. Besides that, concerning to ODL effect on neurotransmitter levels *in vivo*, it was only known that the antidepressant-like effect of ODL is dependent on the serotonergic, noradrenergic and dopaminergic systems[181].

DN extract, on its turn, with a similar TF/TP content of ODL30 extracts presented an EC_{50}= 740±28 µg/mL, displaying a higher capacity in inhibit AchE than the other ODL30 (EC50=1203±16 µg/mL). This might be due to the main presence of alkaloids which bind with better affinity to the enzyme by ES or PAS sites [175], as dendrobine, dendromine and nobiline[28,182]. Ethanolic extracts of stems of *Anselia Africana* and *Eulopholia pettersi*, african orchids, have been reported with an EC_{50} of 950±40 µg/mL and 1200±190 µg/mL[183], both values poorer than DN stem extract.

3.3.2. *Panax ginseng* compounds

Ginsenosides and terpenoids obtained from PG also have beneficial and neuroprotective effects, binding mostly to AchE by HP [175,180]. RG1 showed the highest anti-AchE activity(EC_{50}=237±26 µg/mL), while RG1 exhibited the lowest activity(EC_{50}=647±56 µg/mL) (**Figure 25)**.All the compounds presents low potency comparing to physostigmine control(EC_{50}=142x10^{-6}±513x10^{-7} µg/mL).

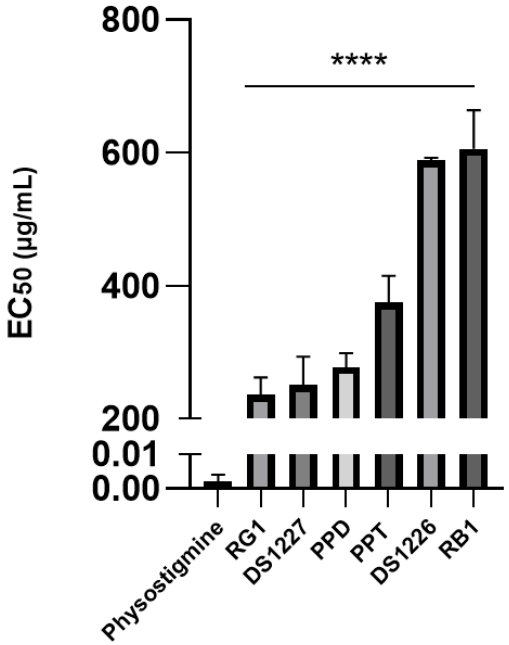

Figure 25. EC_{50} values for AchE assay of *Panax ginseng* compounds, compared with standard physostigmine. Each bar represents the mean ± SD considering the results obtained at least three independent experiments. All the values are statistically different ($p \leq 0.0001$) vs positive control, physostigmine.

DS1226 treatment on mice affected by scopolamine could significantly inhibit the abnormal changes in Ach levels, as showed by Wu *et al.*[68]. As far as reviewed, there is no studies regarding to comparisons within DS1227 and DS1226. As showing in this study, DS 1227 with a composition of around 27% of sapogenins (PPD ,7.02% and PPT,20.51%) and 73% of ginsenosides has an anti-AchE activity with EC_{50} =265± 11mg/m µg/mL. Conversely, DS1226 with around 59% of sapogenins (PPD,16% and PPT,33%) showed a weaker activity (EC_{50} =589 ±03 µg/mL).

Our results show that ginsenosides compounds, with its sugar groups can elicit a better inhibition activity on AChE enzyme, by opposition of general studies that showed that sugar groups are not relevant for biological and pharmaceutical activity[50,51].

In vivo studies performed by Luo *et al* showed that aglycone 20-(S)-PPT and 20-(S)-PPD treatment could reverse scopolamine- decrease of Ach in the hippocampus[62,184]. They found that both sapogenins, at 40 μmol/kg concentration, significantly ($p<0.05$) increase Ach levels. At 20 μmol/kg concentration, PPT is more effective ($p<0.01$), but not PPD. However, our results showed that PPD is stronger on inhibit AChE activity (EC_{50}=278±21 μg/mL) than PPT (EC_{50}=375±40 μg/mL). However, this difference is not significant as shown in molecular docking.

RG1 displayed stronger activity than RB1 (EC_{50}=237±26 μg/mL and EC_{50}=647±56 μg/mL, respectively). Wang *et al* also studied AchE activity in mice with dementia induced by scopolamine posteriorly treated with RG1 and RB1 at concentrations of 6 and 12 mg/kg concentrations. They also found that RG1 is stronger than RB1 in AChE inhibition on mice hippocamp, being the effect of RB1 lower[53,185]. The stronger effect of RG1 than RB1 was also observed by Choi *et al.* in oocytes expressing nicotinic acetylcholine receptors[186].

3.3.2.1 Molecular docking of *Panax ginseng* compounds

The binding affinities and the main interactions between AchE binding site from *Electrophorus electrics* (PDB:1C2B) and PG compounds were obtained using AutoDock Vina[106]. Physostigmine was used as positive control, as standard for comparison. As observed in the **Table 12.**, the calculated binding free energy of PG compounds in the molecular docking study was found to correlate well with its inhibition activity [187]. Thus, RG1 with a $\Delta G_{binding}$ of -10.1 kcal/mol presents the best activity among the four compounds, while RB1 showed a weaker activity with an energy of -7.8 kcal/mol. This follows the tendency observed in AchE assay which predicted RB1<PPT<PPD<RG1 as order of anti-AchE activity.

Table 12. $\Delta G_{binding}$ (kcal/mol) of PG compounds to AchE from *Electrophorus electricus* (EE) and *Homo sapiens* (HS) obtained by AutoVina

	Energy to AchE EE (kcal/mol)	Energy to AchE HS (kcal/mol)
RG1	-10.1	-8.3
PPD	-9.8	-7.2
PPT	-9.5	-7.2
RB1	-7.6	-8.5
Physostigmine	-7.4	-7.4

The positive control, physostigmine, had a $\Delta G_{binding}$ of -7.4 kcal/mol to EE AchE, following the values predicted in the literature[188]. This led us to claim that PG compounds are more effective than the control. However, this is not visualized *in vitro*, as well in literature reports of its anti-AchE activity. Demirezer *et al.* have also shown that rosmarinic acid is more effective than physostigmine, while by Ellman method it inhibited AChE moderately (47.3% at doses of 1000 µg/mL concentration). This discrepancy may be due to the static conformations obtained in PyMOl that do not describe realistically the key-lock binding model of ligands to the enzyme.

As showed in **Figure 26**, the polar contacts between ligands and the receptor are mainly stabilized by hydrogen bonds involving OH and CO groups. RG1 formed 4 polar contacts mainly by residues of Ser293, Tyr72, Gln291 and Gln322. The sapogenins PPD and PPT only formed one polar

contact by the residue of Asp74 and Tyr124, respectively. Finally, RB1 formed 3 polar interactions with Gln421, Gln322 and Thr75.

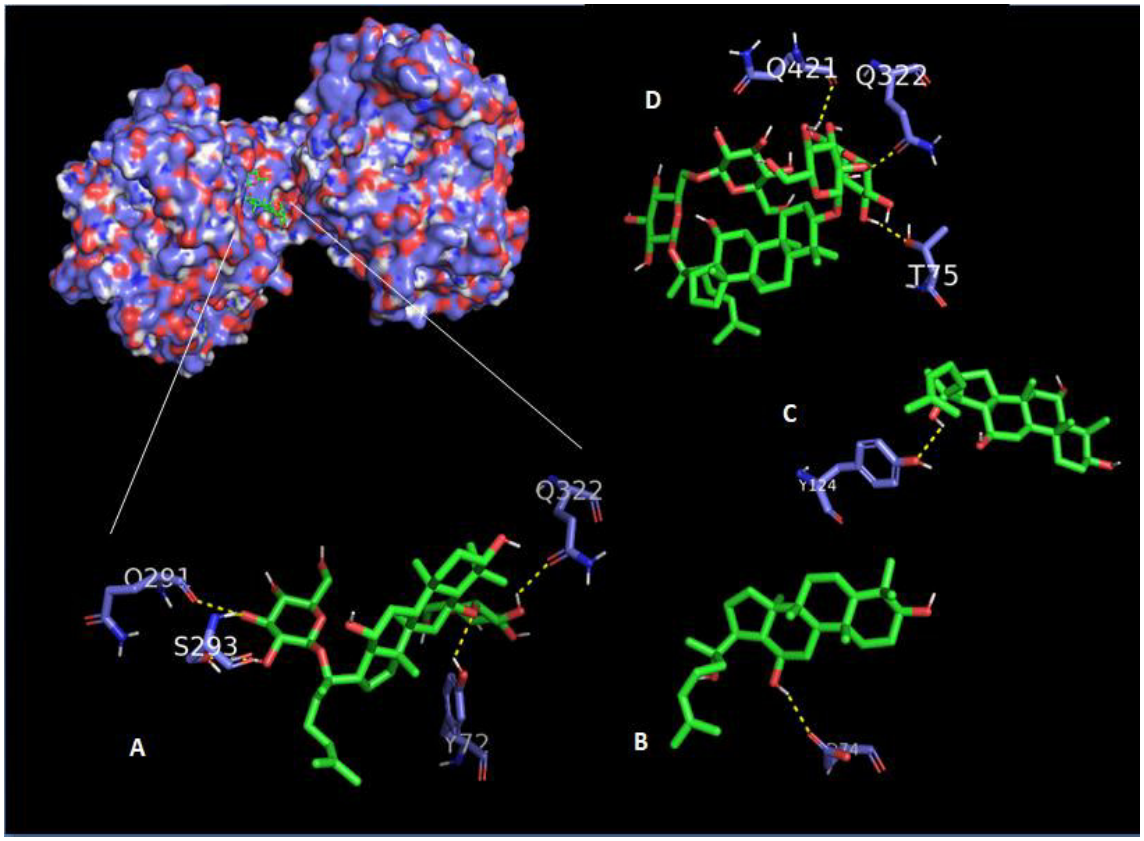

Figure 26. Docking mode of AChE from *Eletrophorus eletricus* (PDB ID: 1C2B) (represented by blue sticks) with **a)** RG1, **b)**PPD **c)**PPT and **d)**RB1(represented by green sticks) obtained by *PyMol* software

As far as we know, studies of molecular docking have only performed on PG ginsenosides. Yu *et al*. demonstrated that RG1 formed 11 hydrogen bonds in the binding site of AChE, while RB1 only 5 [189]. They observed that RB1 possessed better binding fit (68,2%) than RG1(11,8%). They postulated that RB1 interacts to the enzyme mostly by the residues of Asp74, Trp286, Tyr337, Tyr72, Tyr124 and His287. However, the results in our study are not in accordance to Yu *et al.*, since both docking and Elman reaction show that RG1 is more effective than RB1, as well as other reported articles [53,186,190].

Regarding to the compounds itself and structure-activity relationships, as visualized in the **Figure 26** and **Figure 27**, the sapogenins PPT and PPD form one polar contact by -OH group at C12 position. Therefore, the -OH group at R2 on PPT compound does not elicit an additional interaction, which might explain the similar $\Delta G_{binding}$ in PPD and PPT compounds (-9.8 and -9.5 kcal/mol with AchE from EE, respectively). The presence of sugar groups at ginsenosides compounds elicit a higher number of polar contacts (4 with RG1 and 3 with RB1). Despite of the fact of RB1 is a bigger molecule and form several interactions, its $\Delta G_{binding}$ is the poorest of PG compounds (-7.6 kcal/moL with AchE from EE). This might be to the complexity of enzyme and RB1 instability on insert in AchE pocket. In the case of AchE from HS, the BE energy of both ginsenosides are similar and stronger than its sapogenins. Therefore, it may conclude that sugar groups, in this case, are relevant for biological activity.

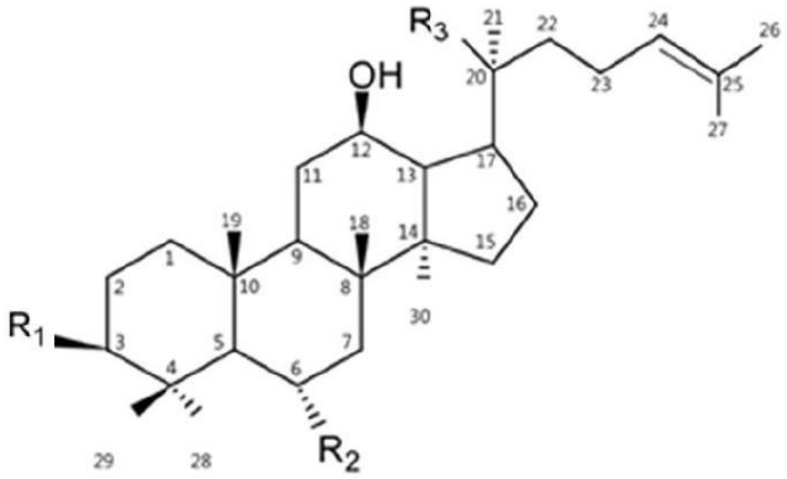

Figure 27. General structure of *Panax ginseng* compounds. Chemical structures of **a)** RG1 (R1=OH, R2-O-Glc, R3-O-Glc), **b)** PPD(R1=OH, R2-H, R3-OH), **c)** PPT(R1=OH, R2-OH, R3-OH) and **d)** RB1 R1= -O-Glc$^{2-1}$Glc, R2-H, R3- O-Glc$^{6-1}$Glc). Adapted from Tawab *et al.*[53]

3.3.3. *Nelumbo nucifera* alkaloids

Most of natural AChEi reported in the literature belong to the alkaloid group, including indole, isoquinoline, quinolizidine, piperidine and steroidal alkaloids [172,175,179]. Anti-AChE activity of alkaloids is ascribed to their complex nitrogen structures, which once positively charged bind to the AS on AChE active site[175]. Physostigmine, the positive control used in this study, is an alkaloid extracted from the seeds of *Physostigma venenosum* and reversibly inhibits the enzyme activity due to this tertiary ammonium compound[191]. In this study, alkaloids from NC displays an EC_{50} value of 366±94 µg/mL. Methanolic and aqueous extracts of NC leaves showed an EC_{50} of 185 µg/mL and 120 µg/mL [175,192], being both extracts more effective in inhibit AchE activity. Since these reported extracts were not exclusively constituted by alkaloids, this may speculate that anti-AchE is not due only to these compounds.

3.3.3.1.Molecular docking of *Nelumbo nucifera* alkaloids

The calculated binding free energy of NC alkaloids(**Figure 28)** in the molecular docking study is presented in **Table 13.** As visualized, NF presents the weakest $\Delta G_{binding}$ (-8.9 kcal/moL for EE AchE of EE and -6.8

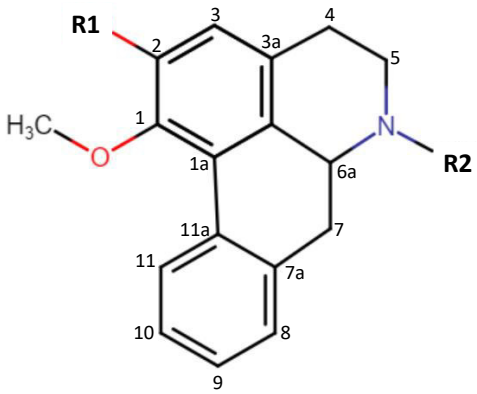

Figure 28. Chemical structures of N-methylasimilobine (R1=OH, R2-CH_3) and 2-hydroxy 1-methoxyaporphine (R1-OH, R2=H). Chemical structure was drawn in *ChemSpace.*

kcal/mol for HS AchE), while N-NF, N-methylasimilobine and HMA display a little stronger effect, being that non-significant among them.

Table 13. $\Delta G_{binding}$ (kcal/mol) of NC alkaloids to AchE from *Electrophorus electricus* (EE) and *Homo sapiens* (HS) obtained by AutoVina

	Energy to AchE EE (kcal/mol)	Energy to AchE HS (kcal/mol)
Nuciferine	-8.9	-6.8
N-nornuciferine	-9.2	-7.0
N-methylasimilobine	-9.3	-7.2
2-hydroxy 1-methoxyaporphine	-9.2	-7.5
Physostigmine	-7.4	-7.4

Analysis of the structure–activity relationship by Yang *et al.* suggested that the alkoxyl of the C1, hydroxyl at the C2 position and the alkyl substituent on the N-atom are the basic pharmacophore for maintaining the AChE inhibition[193].The **Figure 29** shows the optimal complexes formed between each one of NC alkaloids and the correspondent polar contacts to the binding site of EE AChE. Firstly, OH group at C2 in NF and N-NF allows the formation of a hydrogen bond to Tyr72, while hydroxy-metylasimiboline and hydroxy 1-methoxyaporphine, with a $-OCH_3$ do not form a polar contact at this position. Interestingly, compounds N-NF, hydroxy-metylasimiboline and HMA, with a H as substituent on the N-atom binds to Ser293 residue of the enzyme, while NF, with a $-OCH_3$ at this position, does not bind, by opposition of Yang *et al .* predictions. This is similar to the physostigmine which forms polar contact with AchE by its nitrogen and Ser293 from the enzyme (not shown). By these results, it might infer that H substituent at N

and -OH group at C2 positions are specific requirements to maintain compounds activity regarding to AchE inhibition.

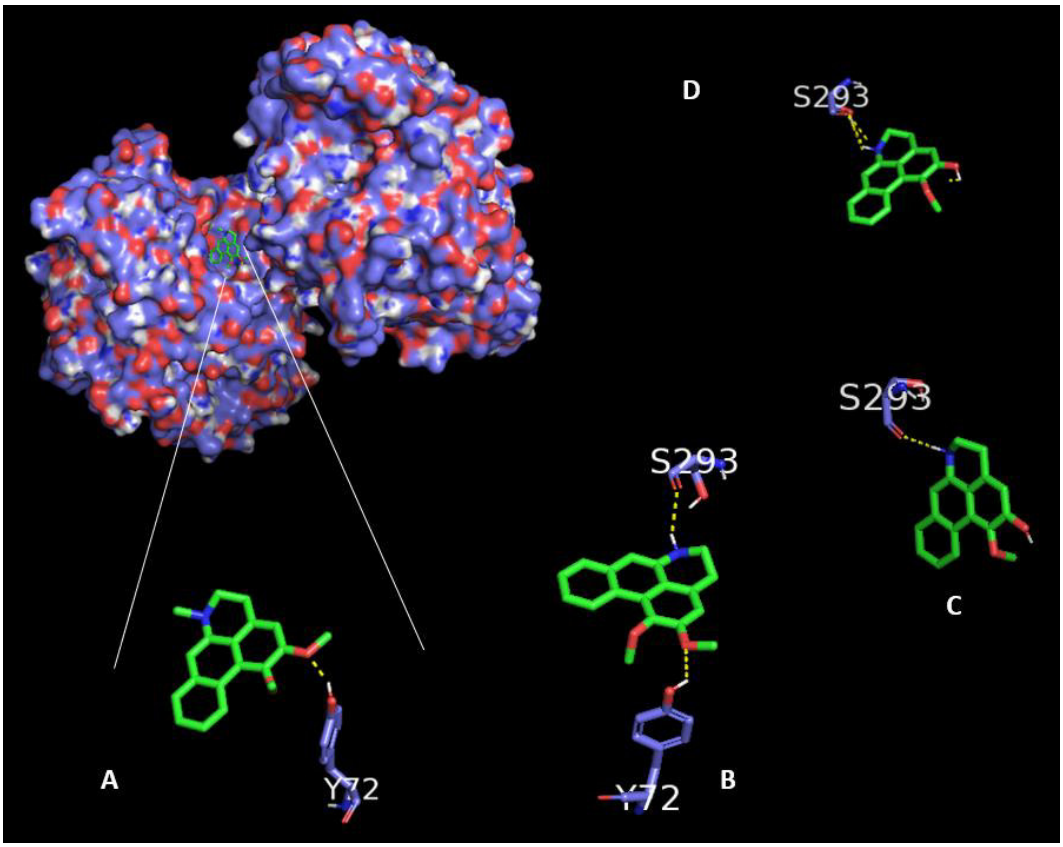

Figure 29. Docking mode of AChE from *Eletrophorus eletricus* (PDB ID: 1C2B) (represented by blue sticks) with **a)** nuciferine, **b)**N-nornuciferine **c)** Hydroxy-metylasimiboline and **d)** 2-hydroxy 1-methoxyaporphine (represented by green sticks) obtained by *PyMol* software.

Zhond-duo yang *et al.* found, using *Glide* (version5.5) docking program for NC alkaloids, that the presence of -OH at C2 position allow the formation of a hydrogen bond, which confirms these results[194]. The presence of $-OCH_3$ instead of -OH substituent at C2 position might create different angles of torsion which do not allow the formation of a polar contact with Tyr72 [195].

3.4. Cytoxicity/cytoprotection effects of extracts and compounds on BV2 cell line

LPS stimulation of BV2 microglia cells leads to production of several bioactive molecules, such as NO, PGE2, ROS and pro-inflammatory cytokines[196]. Since this excess production can promote neuronal injury, intervention in a microglial stimulation stage could be a promising approach that can be used for the prevention of neurodegenerative conditions[196]. The BV2 cell line is an immortalized murine microglial cell line that reproduces primary microglia with high fidelity and is frequently employed as the *in vitro* model for screening and evaluation of anti-neuroinflammatory agents [196]. In addition, the DN and ODL extracts, as well as PG and NC alkaloids compounds were studied regarding to their cytotoxicity and cytoprotecting effects against oxidative insults(t-BHP, commonly used as a model compound for evaluation of mechanisms resulting from oxidative stress in cells and tissues[197]).

3.4.1. *Hemerocallis citrina* and *Dendrobium nobile* extracts

The cytotoxic effect of ODL extracts of 50, 100 and 250 μg/mL concentrations was investigated by MTT cell viability assay, which relies on mitochondrial metabolic capacity of viable cells [115]. Cell viability results after 24 h of incubation with ODL are shown on **Figure 30**. As observed, ODL did not decrease the viability of the BV2 microglial cells when they were incubated at the concentrations of 50 and 100μg/mL, therefore not elicit a toxic effect on microglia cells. At 250 μg/mL concentration, ODL30, ODLBu and ODL50 reduced cell viability by ≥10%, eliciting a little toxic effect. Based on these results, 50 and 100 μg/mL concentrations of ODL extracts were chosen for treating cells in further experiments.

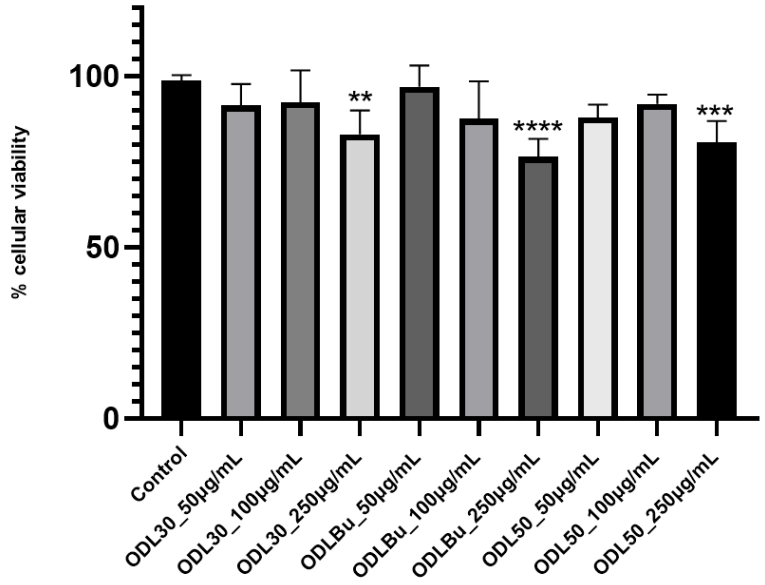

Figure 30 . Effect of ODL treatment on BV2 cell lines. Values represent mean± standard deviation (SD) of three independent experiments. Statistical differences are presented **p<0,01, ***p<0,001, **** p < 0.0001 vs. control (cells subject to medium without treatment).

To evaluate the cytoprotective effect against t-BHP oxidative insult (0,5 mM, 2hours and 30 minutes), BV2 cells were pre-incubated with the extracts for 3h (assessing a direct cytoprotective effect) and for 20 h (assessing an indirect one). Previously, an ethyl acetate fraction of ODL70, at 100, 200 and 300 µg/mL concentrations, has showed decreased t-BHP induced oxidative stress in BRL-3A cells[42]. This study also shown that this effect is mediated by an increase in the activity of antioxidant enzymes as SOD and CAT, increase of GSH levels, as well as decrease of caspase-3 and caspase-9 activity. Therefore, the studied fraction has shown to confer protection against t-BHP via antioxidant and antiapoptotic pathways [42] .

As shown in **Figure 31**, the positive control treated with t-BHP decreased cell viability (±11%) and cells pre-incubated for 3 hours with non-toxic concentrations of ODL does not significantly inhibit t-BHP toxicity(a).On the other hand, after 20 hours of pre-incubation, ODL significantly inhibited t-BHP toxicity in a dose dependent manner(b), being the cytoprotective that effect is stronger with ODL50 treatment and weaker with ODL30 incubation, in accordance with the previously results. Since the

relieving of t-BHP-induced cell impairment by ODL extracts is notorious after 20 hours of pre-incubation and not 3 hours, it might be inferred that the extracts have no direct (scavenging) effect following t-BHP insult, but a clear indirect effect[198] (e.g. likely through increased activity of antioxidant enzymes).

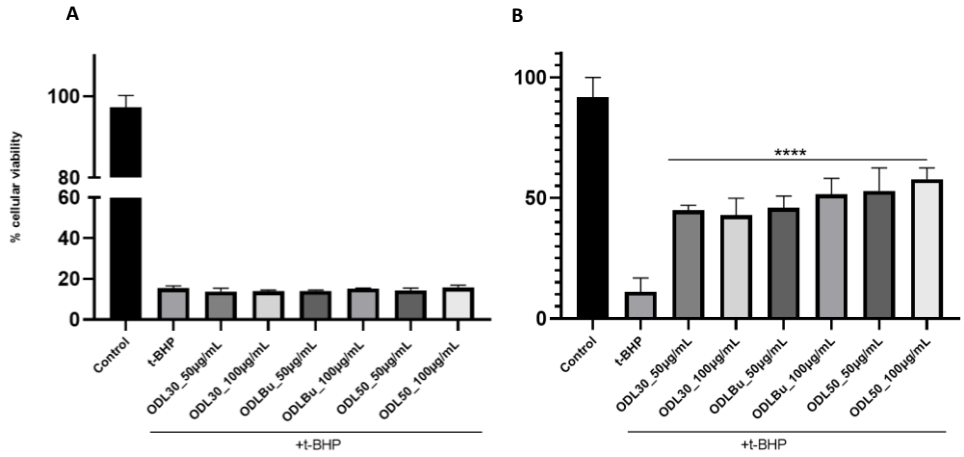

Figure 31 . Effect of ODL extracts at 50 and 100 µg/mL against t-BHP insult. BV2 cells were treated with extracts for **a)** 3 h and **b)** 20 h, then were co-incubated with t-BHP for 2h30 min. Then, supernatant was removed and cells were incubated for 1 h with MTT, to evaluate cell viability. Data are represented as means ± SD (n = 9) with one-way ANOVA. Statistical differences are presented **** $p < 0.0001$ vs. control (cells subject with t-BHP treatment).

Concerning to DN extract, cell viability results after 24 h of incubation showed a significantly decrease in cell viability (by ≥50%), at concentrations of 1,5 and 5 µg/mL concentrations (**Figure 32)**. Therefore, DN extract was not evaluated in further experiments.

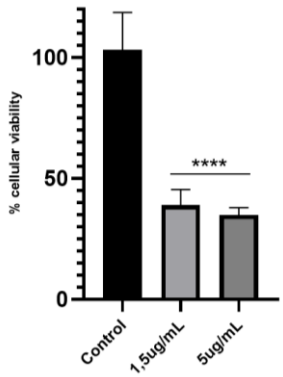

Figure 32. Effect of DN treatment on BV2 cell lines. Values represent mean ±SD of three independent experiments. Statistical differences are presented **** $p < 0.0001$ vs. control (cells subject to medium without treatment).

3.4.2. *Panax ginseng* compounds

PG compounds generally exhibited a cell viability higher than 90% at the referred tested concentrations (**Figure 33)**. The exceptions were observed for the compounds PPT, at concentrations of 1 and 1,5 µg/mL (**Figure 33b)** as well as for the mixture of compounds DS1227 at concentrations of 2 µg/mL, which reveal a significant toxic effect (p<0,001) (**Figure 33c).**In order to perform a comparison among sapogenins, saponins and its mixtures, 0,5 µg/mL was the chosen concentration of for further experiments since it does not exert toxicity in any compound.

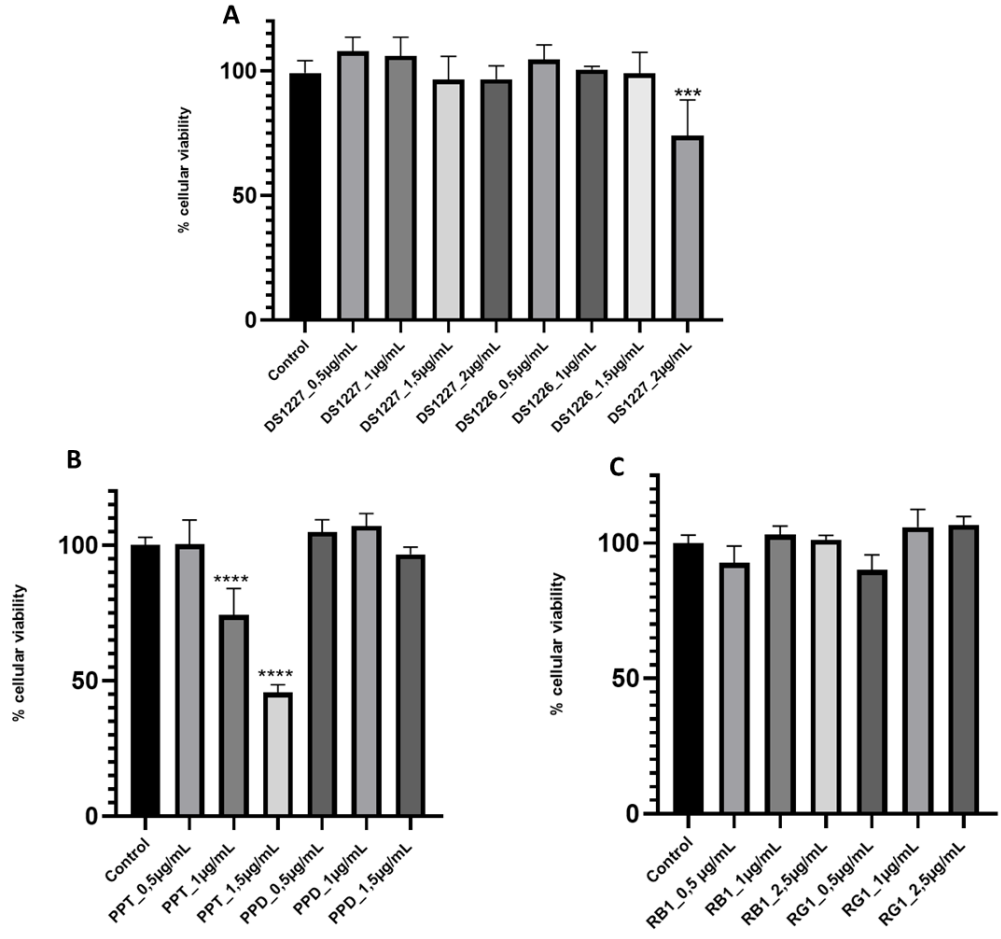

Figure 33. Effect of PG compounds treatment on BV2 cell lines a)mixture of compounds DS1227 and 1226 at concentrations of 0.5,1, 1.5 and 2 µg/mL , **b)** sapogenins PPT and PPD at 0.5,1 and 1.5 µg/mL and **c)** ginsenosides RB1 and RG1 at 0.5,1 and 2.5 µg/mL Values represent mean ±SD of three independent experiments. Statistical differences are presented ***p<0.001,**** p < 0.0001 vs. control (cells subject with medium without treatment).

saponins and its mixtures, 0,5 µg/mL was the chosen concentration of for further experiments since it does not exert toxicity in any compound.

PG compounds were also assayed for cytoprotective effect against an oxidative insult (t-BHP 0, 5Mm, 2hours and 30minutes), either directly (3h pre-incubation) or indirectly (20 hours re-incubation) in BV2 cells. As showed in **Figure 34**, positive control treated with t-BHP decreased cell viability (±15%) and cells pre-incubated with non-toxic concentrations of PG compounds did not significantly inhibit t-BHP toxicity after 3 and 20hours of pre-incubation (a and b), except for the ginsenosides compounds RG1 and RB1. These compounds exhibited a 2,8X fold protection against t-BHP toxicity after 20 hours of pre-incubation.

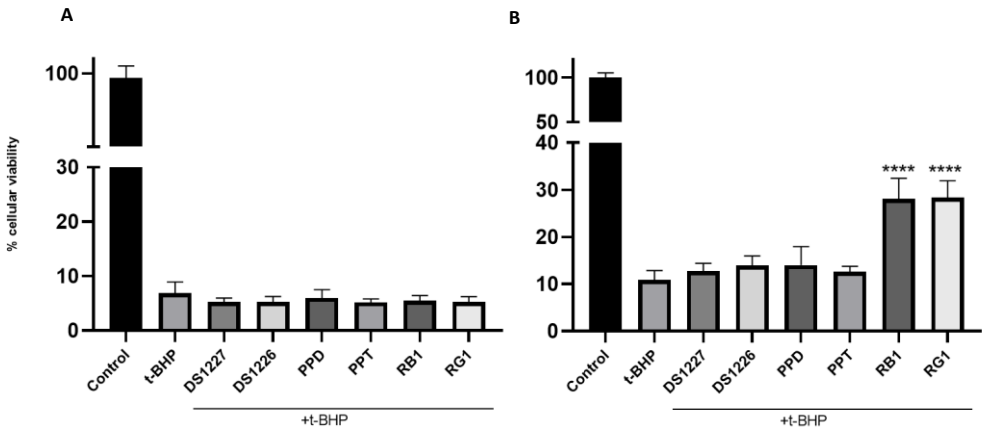

Figure 34. Effect of PG compounds at 0,5 µg/mL against t-BHP insult. BV2 cells were treated with extracts for **a)** 3 h and **b)** 20 h, then were co-incubated with t-BHP for 2h30 min. Then, supernatant was removed and cells were incubated for 1 h with MTT, to evaluate cell viability. Data are represented as means ± SD (n = 9) with one-way ANOVA. Statistical differences are presented **** $p < 0.0001$ vs. control (cells subject with t-BHP treatment).

Treatment with Rb1 and its metabolite compound K was performed in HepG2 cell line by Lee *et al.* [199]. RB1 did not induce cellular cytoxicity in the tested concentrations (0.01-10µM or 0,00801-8,01µg/mL), while its metabolite is toxic at concentrations higher than 10 µM [199]. RG1 was previously studied in BV2 cells line by Lu *et al.* [197]being found that RG1 did not exhibit any toxic effects on BV2 cells, at 10, 30 and 50 µM (40,5 µg/mL)

concentrations. The viability of cells that were treated with 10 mM t-BHP for 24 h in the co-presence of 50 mM RG1 effectively reversed t-BHP induced cytotoxicity in BV2 cells[197].

3.4.3. *Nelumbo nucifera* alkaloids

NC alkaloids decrease significantly (p<0,0001) in a dose dependent manner the cell viability by >75% after 24 h of incubation (**Figure 35)**. NC alkaloids were not evaluated in further experiments not due to its toxicity but also because of scarcity of the material provided by Chinese collaborator.

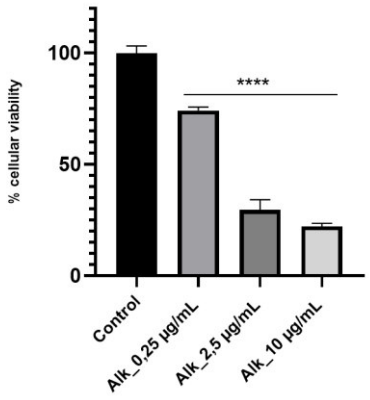

Figure 35. Effect of NC alkaloids treatment on BV2 cell lines at concentrations of 0.25, 2.5 and 10 µg/mL. Values represent mean±SD of three independent experiments. Statistical differences are presented **** $p < 0.0001$ vs. control (cells subject to medium without treatment).

Chang *et al.* proceed to a separation of alkaloids isolated from NC stems and evaluated its cytotoxic activities against HL-60 carcinoma cell line[200,201,202]. Among fifteen compounds, it was demonstrated that the compounds NF, N-NF and N-methylasimilobine , commonly present in the alkaloid extract of leaves , showed significant cytotoxic activities with inhibitory ratios of 59.09%, 52.51% and 51.43% at concentration of 10 µM [200,201,202].

3.5. Anti-inflammatory potential on BV2 cells

ROS play a critical role in enhancing neuroinflammation through the activation of redox-sensitive transcriptional factors such as NF-kB and increased expression of several proinflammatory genes such as COX-2 and iNOS. The increased expression of iNOS can produce excessive level of NO which in turn exacerbates the pathologic process in inflammatory CNS diseases[203,204]. Thus, blocking the microglial over-activation could be a reasonable strategy to inhibit toxic pro-inflammatory cytokines-mediated neurodegenerative damage [204]. In order to clarify whether extracts and compounds of study inhibit NO production from LPS-stimulated BV2 microglial cells, NO concentrations in the culture media were measured by Griess assay [205]. LPS, a major component of the cell walls of many Gram-negative bacteria, was used in order to induce inflammation[206,207].

3.5.1. *Hemerocallis citrina* extracts

Data from the **Figure 36** showed that LPS at 2µg/mL elicited a dramatic increase in NO production compared to that in control cells[205,208] and that ODL treatment attenuated the LPS-induced NO production in a dose-responsive manner. The inhibition on NO production by ODL was significant ($p < 0.001$), except for ODL30, at 25 µg/mL concentration where it does not display significant effect respecting to the positive control (cells incubated with LPS). Specifically, 60%, 56.2% and 54.6% decreases in NO production have been obtained with ODL50, ODLBu and ODL30, at concentrations of 50 µg /mL, according with the pattern observed in antioxidant assays, AchE activity and cytoprotection against t-BHP.

As previously mentioned, ODL75 showed a significant reversion of the reduction of sucrose preference in mice treated with LPS[38]. This

pretreatment has also normalized the activation of NF-kB, iNOS and COX-2 by LPS in prefrontal cortex of mice[38]. Moreover, ODL75 displayed an inhibition of IL-1β, IL-6 and TNF-α expression on CUMS models[41]. Therefore, the anti-inflammatory effect of ODL reported in our work is according with the literature.

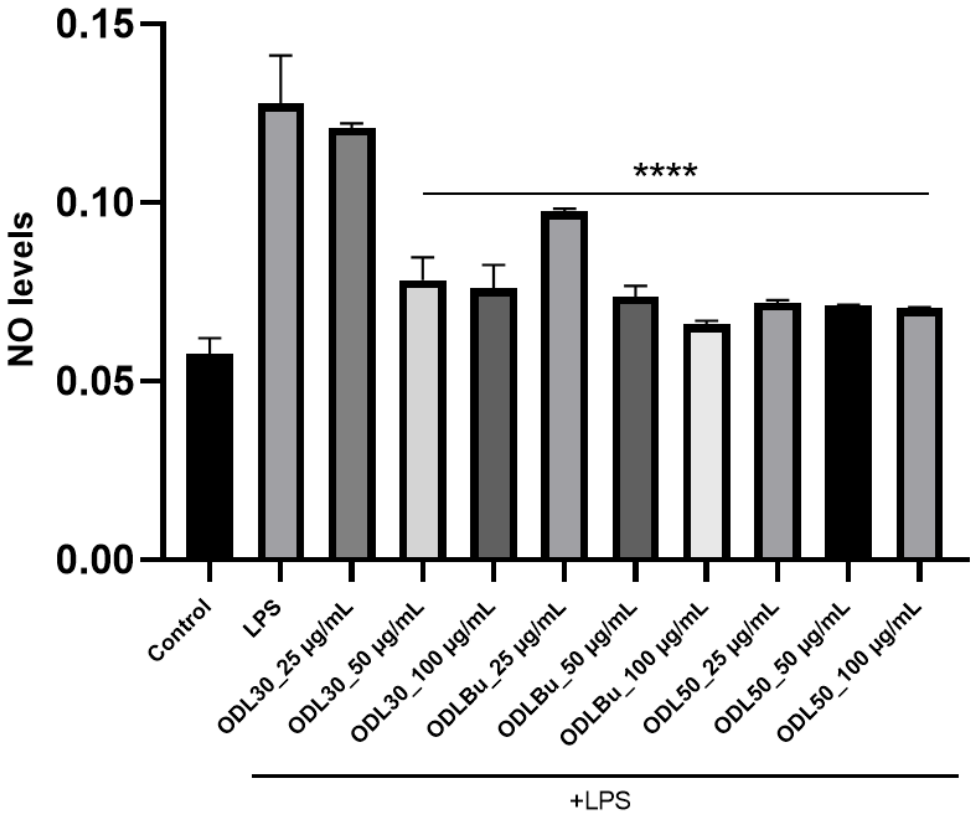

Figure 36. Effects of ODL extracts on NO production induced by LPS in BV2 cells. Microglia were pretreated with ODL50, ODLBu and ODL30 extracts at concentrations of 25,50 and 100 µg/mL, followed by stimulation with LPS (2µg/ml) for 3 hr. Cell-conditioned supernatants were collected, and the production of NO was measured by the presence of nitrite in the supernatants using Griess reaction. Values represent mean ±SD of three independent experiments. Statistical differences are presented **** $p < 0.001$ vs. control (LPS 2µg/mL).

3.5.2. *Panax ginseng* compounds

Regarding to the effect of the mixture of compounds DS1226 and DS1227 on NO production (LPS-induced), DS1227 treatment elicited a little significant effect, at both concentrations of 0,5 and 1,5µg/mL, but not DS1226 (**Figure 37**).

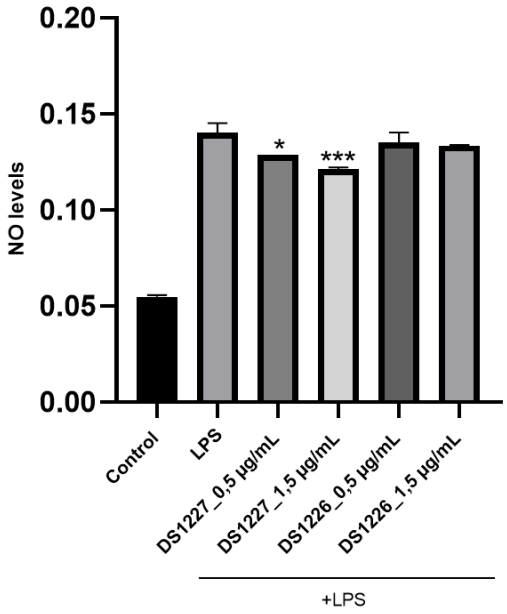

Figure 37. Effects of dammarane sapogenins compounds on NO production induced by LPS in BV2 cells. Microglia were pretreated with DS1227 and 1226 at concentrations of 0.5 and 1.5 µg/mL, followed by stimulation with LPS (2µg/ml) for 3 hr. Cell-conditioned supernatants were collected, and the production of NO was measured by the presence of nitrite in the supernatants using Griess reaction. Values represent mean±SD of three independent experiments. Statistical differences are presented **** $p < 0.001$ vs. control (LPS 2µg/mL).

As far as we know, for this mixture of compounds there are no reports regarding inhibition of NO production. Concerning these results and the obtained activity on NO biochemistry assay, showing a better activity for DS1227 (EC_{50}=265±11µg/mL) than DS1226 (EC_{50}=589±03 µg/mL), it may be inferred that DS compounds regulate their activity on direct scavenging of NO radicals, not through regulation of the genetic machinery. Besides that, this effect is stronger on DS1227.

Concerning to the compounds RG1 and RB1 and its aglycones, PPT and PPD, a significant effect in inhibit NO production ($p < 0.001$) compared with control treated only with LPS 2μg/mL was obtained (**Figure 38).**

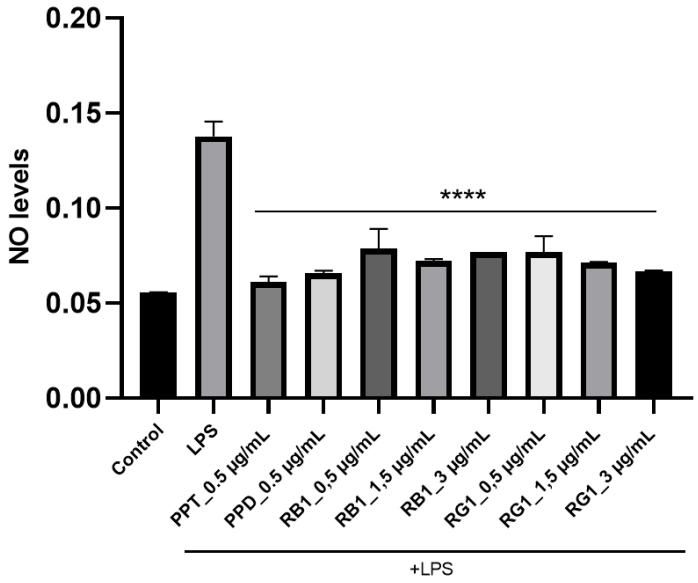

Figure 38. Effects of ginsenosides and its aglycones on NO production induced by LPS in BV2 cells. Microglia were pretreated with RB1 and RG1 at concentrations of 0.5,1.5 and 3 μg/mL, followed by stimulation with LPS (2μg/ml) for 3 hr. Cell-conditioned supernatants were collected, and the production of NO was measured by the presence of nitrite in the supernatants using Griess reaction. Values represent mean ±SD of three independent experiments. Statistical differences are presented **** $p < 0.001$ vs. control (LPS 2μg/mL).

20-(S)-PPT had previously showed to inhibit LPS-induced iNOS and COX-2 expressions through inactivation of NF-kB in RAW-264.7 cells [63]. The anti-inflammatory activity of 20(S)-PPD has been also evaluated. Lee *et al*.(2005) found that 20(S)-PPD inhibited degradation of inhibitory factor IF-kBα, inactivated NF-kB and eventually suppressed the expression of iNOS which were induced by LPS [209].

Lee *et al.* (2013) studied the effect of RB1 administration on mice subjected with LPS and observed that this compound reduced the upregulation of TNF-α, IL-1β, IL-6 and COX-2, thus playing a modulatory role in microglia activation and neuroinflammation [210]. RG1 has been previously tested in BV2 LPS-activated microglial cells[211], as well as in mice

models and RAW-264.7 cells [52,54]. In the cellular models, it has been demonstrated that RG1 treatment at 10, 20, and 40 μM has an inhibitory effect on phospholipase C-Y1, an enzyme that hydrolyze phospholipids, generating two second messengers, inositol 1,4,5-trisphosphate (IP3) and diacylglycerol (DAG), both mediating several cellular functions including the inflammatory response[211]. Moreover, RG1 treatment reduced the phosphorylation of IkB-α, CREB, ERK1/2, JNK and p38 MAPK, therefore exerting anti-inflammatory effects [211].

Results of biochemical NO assays and the cellular anti-inflammatory assays are quite different, regarding RG1 and RB1 treatment. On the one hand, RG1 and RB1 have a non-detectable activity on scavenging NO radicals; on the other, both ginsenosides decreased NO levels after LPS-induced stimulation. Therefore, it might be inferred that the effect of ginsenoside compounds is regulated in terms of genetic machinery instead of direct scavenging of NO· radicals[46,164].

Besides that, its aglycones, PPT and PPD, at 0.5μg/mL concentrations, showed a higher decrease in NO levels than their precursor ginsenosides. As showed *in vitro* on NO biochemical assay, PPT presented, among the four compounds, a lower EC_{50} than PPD, which on turn are far lower than RG1 and RB1(non-detectable activity). It be may inferred that, beside of an effect on genetic machinery, as confirmed in literature, the direct NO-scavenging effects are likely to be one of the mechanisms of these sapogenins to decrease the NO level in culture supernatant fluids of LPS-activated microglial cells. Once again, it might indicate that the sugar groups are not specific requirements for its biological activity [50,51].

3.6. RT-PCR

Given the overall results obtained from biochemical and cellular assays and the recent information for ODL effect on inflammation[38,41], RT-PCR was performed for *Hemerocallis citrina* extracts, assessing the expression of a number of pro-inflammatory genes in BV2 cells pre-treated or not with ODL50 and ODLBu extracts at 50 µg/mL for 3 hours followed by inflammation induction with LPS for 16 hours. The cells were then collected, and its total RNA was extracted using a kit. The RNA purity and concentration were assessed in *NanoDrop* ND100, and its integrity was verified in 1% agarose gel (**Figure 39).** Then, the use of kit Xpert cDNA Synthesis Mastermix (Grisp) enabled the preparation of samples´ cDNAs, which were used in RT-PCR.

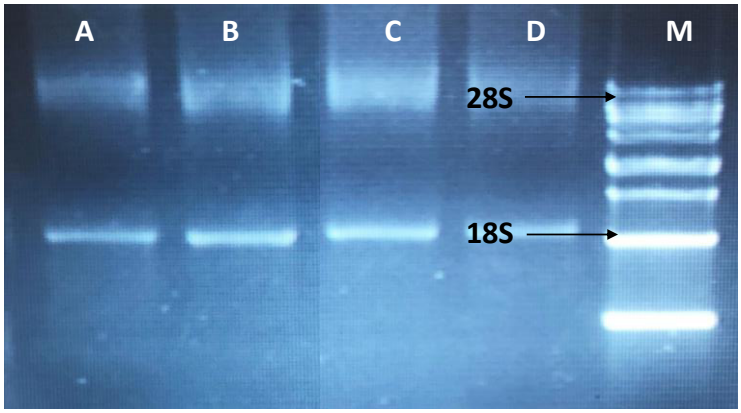

Figure 39. Analyzes of RNA integrity by denaturing agarose gel electrophoresis 1% (w/v). RNA extracted from samples **a)** negative control; **b**) positive control; **c)** ODL50; **d)** ODLBu; **(M)** molecular marker. 2 bands, corresponding to 28S and 18S RNA, were visualized, proving the RNA integrity of the samples.

RT-PCR is a technique that provides a high sensitivity for the detection and quantification of the expression of a higher number of genes[212,213]. Its detection is based on the measurement of the fluorescence emitted by probes incorporated in the newly formed PCR product. The probe SYBR Green molecule has a higher affinity for double-strand DNA,

being largely used in several studies [212,214]. Thus, SYBR Green RT quantitative PCR has been used for estimating the amount of genes related with inflammation on ODL-treated cells co-supplemented with LPS insult. LPS, which is a cell wall component of *E. coli*, activate TLR4, phosphorylating MAPK and translocating NF-kB into the PI3K/Akt pathway [215,216]. Microglia activated by LPS is a 'M1'' form of microglial ''classically activated'' [217]. This via plays a vital role in the defense against insults by production of proinflammatory cytokines, such as IL-1β, TNF-α, IL-6, and free radicals such as ROS[217]. Inflammation also induces the increase of the expression of prostaglandin H2 (PGH2) synthase (also known as cyclooxygenase, or COX-2), an enzyme that plays a central role in the inflammatory cascade by converting arachidonic acid into bioactive prostanoids[218].On the other hand, the M2 anti-inflammatory phenotype promotes tissue remodeling/ repair and angiogenesis through release of high levels of anti-inflammatory cytokines such as IL-10, IL-4, IL-13, and TGF-β, and low levels of pro-inflammatory cytokines[217].

Thus, as seen in the **Figure 40**, in the LPS-stimulated microglia the mRNA levels of IL-6, iNOS, TNF-α and COX-2 were dramatically increased [215]. ODL extracts treatment significantly reduced this mRNA expression. Also, it is verified a stronger effect of ODL50 than ODLBu on IL-6, iNOS and

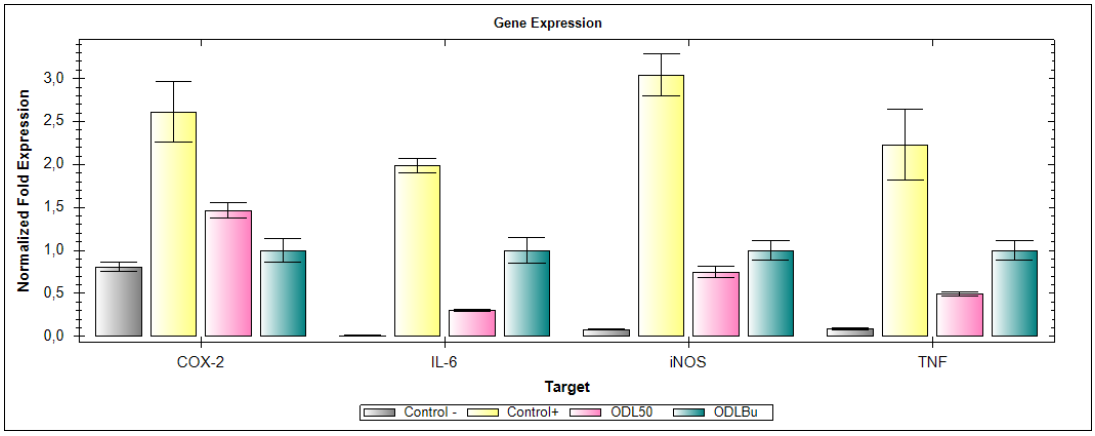

Figure 40. Gene expression of 4 selected genes (COX-2, IL-6, iNOS and TNF) obtained by RT-PCR. Results are expressed as mean±SD. Experiments were analyzed with the software Bio-Rad CFX Manager, using GAPDH as internal control.

TNF expression, in accordance with the previous results. Interestingly, COX-2 expression decreased more on ODLBu than ODL50. It might infer that ODL50 is stronger on inhibit the enzyme related with NO production (iNOS), as confirmed in Griess reaction, and in decrease pro-inflammatory cytokines (IL-6, TNF-α). By the other hand, ODLBu, probably for the presence of specific compounds present in this mother fraction, is stronger in decrease COX-2 mRNA expression levels.

In sum, the results indicate a regulation by ODL extracts in the genes encoding pro-inflammatory mediators in LPS-stimulated BV2 cells. Therefore, these extracts show potential in anti-inflammatory activity.

4.CONCLUSIONS

Given their therapeutic activity, natural products have been used in traditional medicines throughout the centuries. The growing interest of the scientific community in phytopharmaceuticals has resulted in a significant number of research efforts towards understanding their effect in the potential treatment of ND. An approach to develop new ways of treatment concerns to face the context of neuroinflammation/oxidative stress on ND. Thus, by reverting and/or attenuating this state, natural products can prevent and treat NDs through modulation of microglia, inhibiting or reducing its inflammatory toxicity, as well as oxidative stress.

The compounds of *Panax ginseng* demonstrated, at first level, a non-detectable activity in scavenge DPPH radicals. On the other hand, it was detected NO-scavenging activity, except for ginsenosides RG1 and RB1.It was shown a better activity of aglycones regarding to its precursor ginsenosides, following the tendency that sugar groups may not be relevant for biological activity. However, for anti-AchE activity the sugar groups of RG1 demonstrated to be important to inhibit AchE activity. BV2 cellular assays did not show direct effect on revert t-BHP insult, instead an indirect effect was observed for RB1/RG1 (cytoprotection following 20 h incubation). Finally, it was observed an anti-inflammatory effect from PG compounds that might be due to regulation of genetic machinery, as reported in the literature.

The alkaloids from *Nelumbo nucifera* showed a scavenging activity at both DPPH and NO radicals, also showing an anti-AchE effect. SARs studies demonstrated that -H substituent at N and -OH group at C2 positions are specific requirements to maintain compounds activity regarding to AchE inhibition. However, its potential antioxidant and anti-inflammatory effect was not evaluated on BV2 cells due to its high toxicity and material scarcity.

Concerning to plant extracts, *Dendrobium nobile* has demonstrated to have a similar content in phenolic acids and flavonoids to ODL30,

presenting the weakest activity among the 4 extracts in the biochemical assays (DPPH, NO). However, in anti-AchE activity, it displayed a better activity than ODL30. Its major composition in alkaloids as dendrobine and dendromine might explain its neuroprotective effect. Also, this alkaloidal composition could explain this displayed toxicity on BV2, which did not enable the execution of further assays.

All the assays were performed for *Hemerocallis citrina* extracts. ODL showed anti-DPPH, anti-NO and anti-AchE activity. It was also observed indirect effect in revert t-BHP insult (cytoprotection following 20h incubation), as well in attenuating the increase of NO levels caused by LPS insult. This anti-inflammatory effect has been also detected by RT-PCR in the decrease of IL-6, iNOS, TNF-α and COX-2 mRNA levels. Finally, these activities follow the tendency ODL30<ODLBu<ODL50, according to their content in phenols and flavonoids, especially caffeoylquinic acids, quercetin derivatives and apigenin derivatives. Thus, the results presented in this work demonstrated the potentiality of ODL extracts in reverting neuroinflammation/oxidative stress. The ODL50 extract, which elicits the best activity could be used to a therapeutic effect *in vivo.*

The objectives proposed for this work were generally achieved. For future approaches, it is proposed: i)to perform more *in vitro* assays as iron-chelating activity and thiobarbituric acid reactive substances, following the possible effect on chelate metals and in revert lipid peroxidation ; ii)to evaluate the effect of these compounds/plant extracts on HepG2 hepatocellular cells, also studying its action on reverting t-BHP insult effect ; iii) to develop more sensitive techniques to characterize and compare the plant extracts, as HPLC-MS, providing structural identity of the individual components with high molecular specificity and detection; iv) to evaluate the activity of enzymes as SOD, CAT and GSH to elucidate its antioxidant activity. ; v) to study the expression of genes related with NF-kB, lipoxygenase and other anti-inflammatory cytokines as IL-10 and TGF-β, in

order to better understand and confirm the effect of these plants and vi) to evaluate the expression of the proteins coded by the studied inflammatory genes through Western Blot.

5.REFERENCES

1. Jin, X. *et al.* Natural products as a potential modulator of microglial polarization in neurodegenerative diseases. *Pharmacol. Res.* **145**, (2019).
2. Pal, R. *et al*. *The potential of proteomics in understanding neurodegeneration*. *International Review of Neurobiology* vol. 121 (Elsevier Inc., 2015).
3. Kempuraj, D. *et al.* Neuroinflammation Induces Neurodegeneration. *J. Neurol. Neurosurg. spine* **1**, 1–15 (2016).
4. Ganash, M. A. Proteomics Analysis for Therapeutic Options of Neurodegeneration: A Review. *J. Proteomics Bioinform.* **10**, 135–143 (2017).
5. Dwivedi, N. & Al., E. Nanoneuromedicine for management of neurodegenerative disorder. *J. Drug Deliv. Sci. Technol.* **49**, 477–490 (2019).
6. Soares, T. B. *et al.* Lipid nanocarriers loaded with natural compounds: Potential new therapies for age related neurodegenerative diseases? *Prog. Neurobiol.* **168**, 21–41 (2018).
7. Fischer, R. & Maier, O. Interrelation of oxidative stress and inflammation in neurodegenerative disease: Role of TNF. *Oxid. Med. Cell. Longev.* 1–18 (2015).
8. Hayward, J. H. & Lee, S. J. A Decade of Research on TLR2 Discovering Its Pivotal Role in Glial Activation and Neuroinflammation in Neurodegenerative Diseases. *Exp. Neurobiol.* **23**, 138–147 (2014).
9. Glass, C. K. *et al*. Mechanisms Underlying Inflammation in Neurodegeneration. *Cell* **140**, 918–934 (2010).
10. Lawrence, T. The Nuclear Factor NF-kB Pathway in Inflammation. *Cold Spring Harb. Perspect. Biol.* 1–10 (2009).
11. Khansari, N., Shakiba, Y. & Mahmoudi, M. Chronic Inflammation and Oxidative Stress as a Major Cause of Age- Related Diseases and Cancer. *Recent Pat. Inflamm. Allergy Drug Discov.* **3**, 73–80 (2009).
12. Biswas, S. K. Does the Interdependence between Oxidative Stress and Inflammation Explain the Antioxidant Paradox? *Oxid. Med. Cell.*

Longev. **2016**, 17–19 (2016).

13. Reuter S., Gupta S., Chaturvedi M., A. B. Oxidative stress, inflammation, and cancer. *Free Radic. Biol. Med.* **49**, 1603–1616 (2011).
14. Morató, L. *et al.* Mitochondrial dysfunction in central nervous system white matter disorders. *Glia* **62**, 1878–1894 (2014).
15. Morgan, M. J. & Liu, Z. G. Crosstalk of reactive oxygen species and NF-κB signaling. *Cell Res.* **21**, 103–115 (2011).
16. Emerit, J., Edeas, M. & Bricaire, F. Neurodegenerative diseases and oxidative stress. *Biomed. Pharmacother.* **58**, 39–46 (2004).
17. Valacchi, G. *et al.* OxInflammation: From subclinical condition to pathological biomarker. *Front. Physiol.* **9**, 1–15 (2018).
18. Silva, A. *et al*. Comprehensive review on the interaction between natural compounds and brain receptors: Benefits and toxicity. *Eur. J. Med. Chem.* **174**, 87–115 (2019).
19. Chen, W. *et al.* Natural Products for the Prevention of Oxidative Stress-Related Diseases: Mechanisms and Strategies. *Oxid. Med. Cell. Longev.* (2016).
20. Luo, A. & Fan, Y. In vitro antioxidant of a water-soluble polysaccharide from Dendrobium fimhriatum Hook.var.oculatum Hook. *Int. J. Mol. Sci.* **12**, 4068–4079 (2011).
21. Hwang, J. S. *et al.* Phenanthrenes from Dendrobium nobile and their inhibition of the LPS-induced production of nitric oxide in macrophage RAW 264.7 cells. *Bioorganic Med. Chem. Lett.* **20**, 3785–3787 (2010).
22. Wang, Q. *et al.* Neuroprotective effects of Dendrobium alkaloids on rat cortical neurons injured by oxygen-glucose deprivation and reperfusion. *Phytomedicine* **17**, 108–115 (2010).
23. Zhang, Y. *et al.* Structural characterization and conformational properties of a polysaccharide isolated from Dendrobium nobile Lindl. *Food Hydrocoll.* **98**, (2020).
24. Li, Y. *et al*. Inhibitory effects of dendrobium alkaloids on memory impairment induced by lipopolysaccharide in rats. *Planta Med.* **77**,

117–121 (2011).

25. Li, X. L. & Hong, M. Aqueous extract of Dendrobium officinale confers neuroprotection against hypoxic-ischemic brain damage in neonatal rats. *Kaohsiung J. Med. Sci.* **36**, 43–53 (2020).
26. Huang, S. *et al.* Alkaloids of dendrobium nobile lindl. Altered hepatic lipid homeostasis via regulation of bile acids. *J. Ethnopharmacol.* **241**, 111976 (2019).
27. Xu, Y. Y. *et al.* Dendrobium nobile Lindl. alkaloids regulate metabolism gene expression in livers of mice. *J. Pharm. Pharmacol.* **69**, 1409–1417 (2017).
28. Li, S. *et al.* Induction of Nrf2 pathway by Dendrobium nobile Lindl. alkaloids protects against carbon tetrachloride induced acute liver injury. *Biomed. Pharmacother.* **117**, (2019).
29. Nie, J. *et al.* Dendrobium alkaloids prevent aß25-35-induced neuronal and synaptic loss via promoting neurotrophic factors expression in mice. *PeerJ* **2016**, 1–16 (2016).
30. Yang, S. *et al.* Alkaloids enriched extract from Dendrobium nobile Lindl. attenuates tau protein hyperphosphorylation and apoptosis induced by lipopolysaccharide in rat brain. *Phytomedicine* **21**, 712–716 (2014).
31. Xing, X. *et al.* A review of isolation process, structural characteristics, and bioactivities of water-soluble polysaccharides from Dendrobium plants. *Bioact. Carbohydrates Diet. Fibre* **1**, 131–147 (2013).
32. Luo, A. X. *et al.* In vitro antioxidant activities of a water-soluble polysaccharide derived from Dendrobium nobile Lindl. extracts. *Int. J. Biol. Macromol.* **45**, 359–363 (2009).
33. Luo, A. X. *et al.* Purification, composition analysis and antioxidant activity of the polysaccharides from Dendrobium nobile Lindl. *Carbohydr. Polym.* **79**, 1014–1019 (2010).
34. Fan, Y. *et al.* Effects of non-thermal plasma treatment on the polysaccharide from Dendrobium nobile Lindl. And its immune activities in vitro. *Int. J. Biol. Macromol.* **153**, 942–950 (2020).

35. Zhang, X. *et al.* Bioactive bibenzyl derivatives and fluorenones from Dendrobium nobile. *J. Nat. Prod.* **70**, 24–28 (2007).
36. Lin, T. H. et al. Two phenanthraquinones from Dendrobium moniliforme. *J. Nat. Prod.* **64**, 1084–1086 (2001).
37. Ma, C. *et al.* New sesquiterpenoids from the stems of Dendrobium nobile and their neuroprotective activities. *Fitoterapia* **138**, 104351 (2019).
38. Li, C. F. *et al.* Evaluation of the toxicological properties and anti-inflammatory mechanism of Hemerocallis citrina in LPS-induced depressive-like mice. *Biomed. Pharmacother.* **91**, 167–173 (2017).
39. Du, B. *et al.* Antidepressant-like effects of the hydroalcoholic extracts of Hemerocallis Citrina and its potential active components. *BMC Complement. Altern. Med.* **14**, 1–11 (2014).
40. Gu, L. *et al.* Role for monoaminergic systems in the antidepressant-like effect of ethanol extracts from Hemerocallis citrina. *J. Ethnopharmacol.* **139**, 780–787 (2012).
41. Liu, X. L. *et al.* Ethanol extracts from Hemerocallis citrina attenuate the upregulation of proinflammatory cytokines and indoleamine 2,3-dioxygenase in rats. *J. Ethnopharmacol.* **153**, 484–490 (2014).
42. Wang, J. *et al.* Ethyl acetate fraction of hemerocallis citrina baroni decreases tert-butyl hydroperoxide-induced oxidative stress damage in BRL-3A Cells. *Oxid. Med. Cell. Longev.* **2018**, (2018).
43. Nijveldt, R. J. *et al.* Flavonoids: A review of probable mechanisms of action and potential applications. *Am. J. Clin. Nutr.* **74**, 418–425 (2001).
44. Tian, H. *et al.* Effects of phenolic constituents of daylily flowers on corticosterone- and glutamate-treated PC12 cells. *BMC Complement. Altern. Med.* **17**, 1–12 (2017).
45. Xu, T. *et al.* Urinary metabolomics analysis of the anti-depressive effects of Hemerocallis citrina extracts in a simulated microgravity-induced rat model of depression. *J. Chinese Pharm. Sci.* 176–191 (2020).

46. Chen, X. J. *et al.* Anticancer Activities of Protopanaxadiol- and Protopanaxatriol-Type Ginsenosides and Their Metabolites. *Evidence-based Complement. Altern. Med.* **2016**, (2016).
47. Tawab, M. A. *et al.* Degradation of ginsenosides in humans after oral administration. *Drug Metab. Dispos.* **31**, 1065–1071 (2003).
48. Kong, L. T. *et al.* Different pharmacokinetics of the two structurally similar dammarane sapogenins, protopanaxatriol and protopanaxadiol, in rats. *Fitoterapia* **86**, 48–53 (2013).
49. Jiang, N. *et al.* Dammarane sapogenins alleviates depression-like behaviours induced by chronic social defeat stress in mice through the promotion of the BDNF signalling pathway and neurogenesis in the hippocampus. *Brain Res. Bull.* **153**, 239–249 (2019).
50. Zhao, J. M. *et al.* Novel dammarane-type sapogenins from Panax ginseng berry and their biological activities. *Bioorganic Med. Chem. Lett.* **21**, 1027–1031 (2011).
51. Jiang, N. *et al.* Antidepressant effects of dammarane sapogenins in chronic unpredictable mild stress-induced depressive mice. *Phyther. Res.* **32**, 1023–1029 (2018).
52. Kim, J. H., Yi, Y. S., Kim, M. Y. & Cho, J. Y. Role of ginsenosides, the main active components of Panax ginseng, in inflammatory responses and diseases. *J. Ginseng Res.* **41**, 435–443 (2017).
53. Ahmed, T. *et al.* Ginsenoside Rb1 as a neuroprotective agent: A review. *Brain Res. Bull.* **125**, 30–43 (2016).
54. Ahn, S. *et al.* Anti-inflammatory activity of ginsenosides in LPS-stimulated RAW 264.7 cells. *Sci. Bull.* **60**, 773–784 (2015).
55. Ni, N. *et al.* Ginsenoside Rb1 protects rat neural progenitor cells against oxidative injury. *Molecules* **19**, 3012–3024 (2014).
56. Mohanan, P. *et al*. Molecular signaling of ginsenosides Rb1, Rg1, and Rg3 and their mode of actions. *J. Ginseng Res.* **42**, 123–132 (2018).
57. Liu, Q. *et al*. Ginsenoside Rg1 protects against hydrogen peroxide-induced cell death in PC12 cells via inhibiting NF- k B activation. *Neurochem. Int.* **58**, 119–125 (2011).

58. Bak, D. H. *et al.* Neuroprotective effects of 20(S)-protopanaxadiol against glutamate-induced mitochondrial dysfunction in PC12 cells. *Int. J. Mol. Med.* **37**, 378–386 (2016).
59. Jian-Ming, L. *et al.* Ginseng Compounds: An Update on Their Molecular Mechanisms and Medical Applications. *Curr Vasc Pharmacol* 293–302 (2009).
60. Xue, J. F. *et al.* Ginsenoside Rb1 promotes neurotransmitter release by modulating phosphorylation of synapsins through a cAMP-dependent protein kinase pathway. *Brain Res.* **1106**, 91–98 (2006).
61. Wang, M. *et al.* Dammarane-type leads panaxadiol and protopanaxadiol for drug discovery: Biological activity and structural modification. *Eur. J. Med. Chem.* **189**, (2020).
62. Lu, C. *et al.* Neuroprotective effects of 20(S)-protopanaxatriol (PPT) on scopolamine-induced cognitive deficits in mice. *Phyther. Res.* **32**, 1056–1063 (2018).
63. Oh, G. S. *et al.* 20(S)-Protopanaxatriol, one of ginsenoside metabolites, inhibits inducible nitric oxide synthase and cyclooxygenase-2 expressions through inactivation of nuclear factor-κB in RAW 264.7 macrophages stimulated with lipopolysaccharide. *Cancer Lett.* **205**, 23–29 (2004).
64. Zhang, B. B. *et al.* Neuroprotective Effects of Dammarane-Type Saponins from Panax notoginseng on Glutamate-Induced Cell Damage in PC12 Cells. *Planta Med.* **85**, E2 (2019).
65. Hsu, M. F. *et al.* Hormetic property of ginseng steroids on anti-oxidant status against exercise challenge in rat skeletal muscle. *Antioxidants* **6**, (2017).
66. Jiang, J. *et al.* Ginsenoside metabolite 20(S)-protopanaxatriol from Panax ginseng attenuates inflammation-mediated NLRP3 inflammasome activation. *J. Ethnopharmacol.* **251**, 112564 (2020).
67. Hong-wei, W. *et al*. Improving effect of the ginsenoside hydrolysis product DS-1227 on scopolamine-induced learning and memory impairment in mice. *Chinese J. Comp. Med.* 27–32 (2015).

68. Wu, X. *et al.* Dammarane sapogenins Ameliorates Neurocognitive Functional Impairment induced by simulated long-duration spaceflight. *Front. Pharmacol.* **8**, 1–16 (2017).
69. Pohlman, R. L. Effects of Moderate Swim Exercise on Adiposity and Metabolic Function in Mice. *Med. Exerc. Sport. Exerc.* **44**, 593–594 (2012).
70. Park, E. *et al.* Anti-inflammatory effects of Nelumbo leaf extracts and identification of their metabolites. *Nutr. Res. Pract.* **11**, 265–274 (2017).
71. Kim, E. S. *et al.* Cognitive enhancing and neuroprotective effect of the embryo of the nelumbo nucifera seed. *Evidence-based Complement. Altern. Med.* **2014**, (2014).
72. Sung, J., Sung, J. S. & Shin, H. S. Cytoprotective effects of lotus (Nelumbo nucifera Gaertner) seed extracts on oxidative damaged mouse embryonic fibroblast cell. *Food Sci. Biotechnol.* **20**, 1533–1537 (2011).
73. Yang, W. M. *et al.* Novel effects of Nelumbo nucifera rhizome extract on memory and neurogenesis in the dentate gyrus of the rat hippocampus. *Neurosci. Lett.* **443**, 104–107 (2008).
74. Yoo, D. Y. *et al.* Effects of luteolin on spatial memory, cell proliferation, and neuroblast differentiation in the hippocampal dentate gyrus in a scopolamine-induced amnesia model. *Neurol. Res.* **35**, 813–820 (2013).
75. Oh, J. H. *et al.* Nelumbo nucifera semen extract improves memory in rats with scopolamine-induced amnesia through the induction of choline acetyltransferase expression. *Neurosci. Lett.* **461**, 41–44 (2009).
76. Jang, M. H. *et al.* Inhibition of cholinesterase and amyloid-&bgr; aggregation by resveratrol oligomers from Vitis amurensis. *Phyther. Res.* **22**, 544–549 (2008).
77. Kumaran, A., Ho, C. C. & Hwang, L. S. Protective effect of Nelumbo nucifera extracts on beta amyloid protein induced apoptosis in PC12

cells, in vitro model of Alzheimer's disease. *J. Food Drug Anal.* **26**, 172–181 (2018).

78. Ye, L. H. *et al.* Pharmacokinetics of nuciferine and N-nornuciferine, two major alkaloids from Nelumbo nucifera leaves, in rat plasma and the brain. *Front. Pharmacol.* **9**, 1–7 (2018).
79. Paudel, K. R. & Panth, N. Phytochemical profile and biological activity of Nelumbo nucifera. *Evidence-based Complement. Altern. Med.* **2015**, (2015).
80. Yan, M. Z. *et al.* Lotus Leaf Alkaloid Extract Displays Sedative-Hypnotic and Anxiolytic Effects through GABAA Receptor. *J. Agric. Food Chem.* **63**, 9277–9285 (2015).
81. Ma, C. *et al.* Purification and characterization of aporphine alkaloids from leaves of nelumbo nucifera gaertn and their effects on glucose consumption in 3T3-L1 adipocytes. *Int. J. Mol. Sci.* **15**, 3481–3494 (2014).
82. Ye, L. H. *et al.* Identification and characterization of potent CYP2D6 inhibitors in lotus leaves. *J. Ethnopharmacol.* **153**, 190–196 (2014).
83. Meng, X. L. *et al.* Inhibitory effects of three bisbenzylisoquinoline alkaloids on lipopolysaccharide-induced microglial activation. *RSC Adv.* **7**, 18347–18357 (2017).
84. Jiang, X. L. *et al.* Flavonoid glycosides and alkaloids from the embryos of Nelumbo nucifera seeds and their antioxidant activity. *Fitoterapia* **125**, 184–190 (2018).
85. Zhao, F. K. *et al. T*he extraction and the improvement of determination method for total alkaloids in Dendrobium nobile Lindl. *J. Zunyi Med. Univ.* **38**, 532–535 (2015).
86. Singleton, V. L., Orthofer, R. & Lamuela-Raventós, R. M. B. T.-M. in E. [14] Analysis of total phenols and other oxidation substrates and antioxidants by means of folin-ciocalteu reagent. in *Oxidants and Antioxidants Part A* vol. 299 152–178 (Academic Press, 1999).
87. BiQuoChem. Folin Ciocalteau Phenolic Content Quantification Assay Kit 400 tests (96 well plate).

88. Magalhães, L. M., Santos, F., Segundo, M. A., Reis, S. & Lima, J. L. F. C. Talanta Rapid microplate high-throughput methodology for assessment of Folin-Ciocalteu reducing capacity. **83**, 441–447 (2010).
89. Hatami, T. *et al.* Total Phenolic Contents and Antioxidant Activities of Different Extracts and Fractions from the Aerial Parts of Artemisia biennis Willd. **13**, 551–558 (2014).
90. Chilian, A., Bancuta, I., Ion, R. & Setnescu, R. Improvement of spectrophotometric method for determination of phenolic compounds by statistical investigations. (2016).
91. Chavan, J. J., Gaikwad, N. B., Kshirsagar, P. R. & Dixit, G. B. South African Journal of Botany Total phenolics , fl avonoids and antioxidant properties of three Ceropegia species from Western Ghats of India. *South African J. Bot.* **88**, 273–277 (2013).
92. Chang, C. *et al.* Estimation of Total Flavonoid Content in Propolis by Two Complementary Colorimetric Methods. **10**, 178–182 (2002).
93. Amorim, E. L. *et al.* A Simple and Accurate Procedure for the Determination of Tannin and Flavonoid Levels and Some Applications in Ethnobotany and Ethnopharmacology. (2008).
94. W.Brand-Williams, Cuvelier, M. E. & Berset, C. Use of a Free Radical Method to Evaluate Antioxidant Activity. **30**, 25–30 (1995).
95. Alam, N. & Bristi, N. J. Review on in vivo and in vitro methods evaluation of antioxidant activity. 143–152 (2013).
96. Bryan, N. S. & Grisham, M. B. Methods to Detect Nitric Oxide and its Metabolites in Biological Samples. *Free Radic. Biol. Med.* **43**, 645–657 (2008).
97. Promega. Griess Reagent System. 1–7 (2009).
98. Sylvie, D. D. *et al.* Comparison of in vitro antioxidant properties of extracts from three plants used for medical purpose in Cameroon: Acalypha racemosa, Garcinia lucida and Hymenocardia lyrata. *Asian Pac. J. Trop. Biomed.* **4**, S625–S632 (2014).
99. Awah, F. M. & Verla, A. W. Antioxidant activity, nitric oxide scavenging

activity and phenolic contents of Ocimum gratissimum leaf extract. *J. Med. Plants Res.* **4**, 2479–2487 (2010).

100. Kumaran, A. & Joel Karunakaran, R. Antioxidant and free radical scavenging activity of an aqueous extract of Coleus aromaticus. *Food Chem.* **97**, 109–114 (2006).
101. Mathew, M. & Subramanian, S. In Vitro Screening for Anti-Cholinesterase and Antioxidant Activity of Methanolic Extracts of Ayurvedic Medicinal Plants Used for Cognitive Disorders. **9**, 1–7 (2014).
102. Worek, F. & Thiermann, H. Determination of acetylcholinesterase activity by the Ellman assay : A versatile tool for in vitro research on medical countermeasures against organophosphate poisoning. 282–291 (2012).
103. J.Olson, O. T. and A. AutoDock Vina: improving the speed and accuracy of docking with a new scoring function, efficient optimization and multithreading. *J Comput Chem* **31**, 455–461 (2010).
104. Nnyigide, O. S., Lee, S. & Hyun, K. In Silico Characterization of the Binding Modes of Surfactants with Bovine Serum Albumin. 1–16 (2019).
105. Malde, A. K. *et al.* An Automated Force Field Topology Builder (ATB) and Repository : Version 1 . 0. 4026–4037 (2011).
106. Seeliger, D., Groot, B. L. De & Pymol, V. Ligand docking and binding site analysis with PyMOL and Autodock / Vina. 417–422 (2010).
107. Anja Henn, S. *et al.* The Suitability of BV2 Cells as Alternative Model System for Primary Microglia Cultures or for Animal Experiments Examining Brain Inflammation. *ALTEX* 83–94 (2009).
108. Vries, G. H. De & Boullerne, A. I. Glial Cell Lines : An Overview. *Neurochem Res* 1978–2000 (2010).
109. Macedo, Fernando, L. Effects of Salvia officinalis in the liver: Relevance of glutathione levels. (2006).
110. Abcam. Sample preparation for western blot.
111. Lima, C. F. *et al.* Water and methanolic extracts of Salvia officinalis

protect HepG2 cells from t -BHP induced oxidative damage. **167**, 107–115 (2007).

112. Lima, C. F., Fernandes-ferreira, M. & Pereira-Wilson, C. Phenolic compounds protect HepG2 cells from oxidative damage : Relevance of glutathione levels. *Life Sci.* **79**, 2056–2068 (2006).
113. Sun, G. Y., Chen, Z., Jasmer, K. J. & Chuang, D. Y. Quercetin Attenuates Inflammatory Responses in BV-2 Microglial Cells : Role of MAPKs on the Nrf2 Pathway and Induction of Heme Oxygenase-1. *PLoS One* 1–20 (2015).
114. Aslantürk, Ö. S. In Vitro Cytotoxicity and Cell Viability Assays: Principles, Advantages, and Disadvantages. in *Genotoxicity - A Predictable Risk to Our Actual World Advantages:* 1–16 (2018).
115. Kuete, V., Karaosmanog, O. & Sivas, H. Anticancer Activities of African Medicinal Spices and Vegetables. in *Medicinal Species and Vegetables from Africa* (2017).
116. Mosmann, T. Rapid Colorimetric Assay for Cellular Growth and Survival : Application to Proliferation and Cytotoxicity Assays. **65**, 55–63 (1983).
117. Grisp. GRS Total RNA Kit-Blood & Cultured Cells. 615–619 (2016).
118. Grisp. Xpert cDNA Synthesis Mastermix. **0100**, 2–3 (2018).
119. Barber, R. D. *et al.* GAPDH as a housekeeping gene : analysis of GAPDH mRNA expression in a panel of 72 human tissues. *Physological Genomics* 389–395 (2005).
120. Maisuthisakul, P., Suttajit, M. & Pongsawatmanit, R. Assessment of phenolic content and free radical-scavenging capacity of some Thai indigenous plants. *Food Chem.* **100**, 1409–1418 (2007).
121. Wong, S. P., Leong, L. P., Hoe, J. & Koh, W. Food Chemistry Antioxidant activities of aqueous extracts of selected plants. **99**, 775–783 (2006).
122. Meda, A., Euloge, C., Romito, M., Millogo, J. & Germaine, O. Food Chemistry Determination of the total phenolic , flavonoid and proline contents in Burkina Fasan honey , as well as their radical scavenging

activity. **91**, 571–577 (2005).

123. Shahidi, F. & Zhong, Y. Measurement of antioxidant activity. *J. Funct. Foods* **18**, 757–781 (2015).
124. Bucić-Kojić, A. *et al.* Effect of extraction conditions on the extractability of phenolic compounds from lyophilised fig fruits (ficus carica l.). *Polish J. Food Nutr. Sci.* **61**, 195–199 (2011).
125. Bhattacharyya, P., Kumaria, S., Diengdoh, R. & Tandon, P. Genetic stability and phytochemical analysis of the in vitro regenerated plants of Dendrobium nobile Lindl., an endangered medicinal orchid. *Meta Gene* **2**, 489–504 (2014).
126. Mammen, D. & Daniel, M. A critical evaluation on the reliability of two aluminum chloride chelation methods for quantification of flavonoids. *Food Chem.* **135**, 1365–1368 (2012).
127. Locatelli, M. *et al.* Recent HPLC strategies to improve sensitivity and selectivity for the analysis of complex matrices. *Instrum. Sci. Technol.* **40**, 112–137 (2012).
128. Lin, L. *et al.* Macroporous resin purification behavior of phenolics and rosmarinic acid from Rabdosia serra (MAXIM.) HARA leaf. *Food Chem.* **130**, 417–424 (2012).
129. Wang, M. *et al.* A review on flavonoid apigenin: Dietary intake, ADME, antimicrobial effects, and interactions with human gut microbiota. *Biomed Res. Int.* **2019**, (2019).
130. Lin, Y. *et al*. Antioxidative Caffeoylquinic Acids and Flavonoids from Hemerocallis fulva Flowers. *J. Agric. Food Chem.* 8789–8795 (2011).
131. Janovik, V. *et al.* HPLC/DAD Analysis, Determination of Total Phenolic and Flavonoid Contents and Antioxidant Activity from the Leaves of Cariniana domestica (Mart)Miers. *Res. J. Phytochem.* **5**, 209–215 (2011).
132. Sun, J. *et al.* The analysis of phenolic compounds in daylily using UHPLC-HRMSn and evaluation of drying processing method by fingerprinting and metabolomic approaches. *J. Food Process. Preserv.* **42**, (2018).

133. Nie, X., Chen, Y., Li, W. & Lu, Y. Anti-aging properties of Dendrobium nobile Lindl.: From molecular mechanisms to potential treatments. *J. Ethnopharmacol.* **257**, 112839 (2020).
134. R. Verpoorte, A. B. S. General Aspects of HPLC of Alkaloids. *J. Chromatogr. A* **23**, 223–233 (1984).
135. Song, T. H. *et al.* Dendrobine targeting JNK stress signaling to sensitize chemotoxicity of cisplatin against non-small cell lung cancer cells in vitro and in vivo. *Phytomedicine* **53**, 18–27 (2019).
136. Gandıa-Herrera, F., Escribano, J. & Garcı, F. The Role of Phenolic Hydroxy Groups in the Free Radical Scavenging Activity of Betalains. *J Nat. Prod.* 1142–1146 (2009).
137. Kuete, V. & Efferth, T. Cameroonian medicinal plants : pharmacology and derived natural products. *Pharmacology* **1**, 1–19 (2010).
138. Hilmi, Y. *et al.* A study of antioxidant activity , enzymatic inhibition and in vitro toxicity of selected traditional sudanese plants with anti-diabetic potential. *BMC Complement. Altern. Med.* **14**, 1–5 (2014).
139. Chao, P. Y. *et al.* Antioxidant Activity in Extracts of 27 Indigenous Taiwanese Vegetables. *Nutrients* **6**, 2115–2130 (2014).
140. Chimsook, T. Phytochemical screening, total phenolic content, antioxidant activities and cytotoxicity of Dendrobium signatum leaves. *MATEC Web Conf.* **62**, 1–6 (2016).
141. Paudel, M. R. *et al.* Assessment of antioxidant and cytotoxic activities of extracts of Dendrobium crepidatum. *Biomolecules* **9**, 1–13 (2019).
142. Fahmideh, L. *et al*. Total Phenol / Flavonoid Content , Antibacterial and DPPH Free Radical Scavenging Activities of Medicinal Plants. *J. Agr. Sci. Tech.* **21**, 1459–1471 (2019).
143. Yin, J., Kwon, G. & Wang, M. The antioxidant and cytotoxic activities of Sonchus oleraceus L . extracts *. **1**, 189–194 (2007).
144. Foti, M. C. Chemistry and Biology of Antioxidants Antioxidant properties of phenols. **2007**, 1673–1685 (2007).
145. Foti, M. C. *et al.* Reaction of Phenols with the 2 , 2-Diphenyl-1-picrylhydrazyl Radical . Kinetics and DFT Calculations Applied To

Determine ArO-H Bond Dissociation Enthalpies and Reaction Mechanism. (2008).

146. Banjarnahor, S. D. S. & Artanti, N. Antioxidant properties of flavonoids. **23**, 239–244 (2014).
147. Foti, M. C. & Daquino, C. Kinetic and thermodynamic parameters for the equilibrium reactions of phenols with the dpph ? radical. *Chem Comm* 3252–3254 (2006).
148. Schaich, K. M., Tian, X. & Xie, J. Hurdles and pitfalls in measuring antioxidant efficacy: A critical evaluation of ABTS, DPPH, and ORAC assays. *J. Funct. Foods* **14**, 111–125 (2015).
149. Kang, K. S. *et al*. ESR study on the structure and hydroxyl radical-scavenging activity relationships of ginsenosides isolated from Panax ginseng C. A. MEYER. *Biol. Pharm. Bull.* **30**, 917–921 (2007).
150. Chae, S., Kang, K. A., Youn, U., Park, J. S. & Hyun, J. W. A comparative study of the potential antioxidant activities of ginsenosides. *J. Food Biochem.* **34**, 31–43 (2010).
151. Xie, J. T. *et al.* Antioxidant effects of ginsenoside Re in cardiomyocytes. *Eur. J. Pharmacol.* **532**, 201–207 (2006).
152. Hussain, G. *et al.* Role of plant derived alkaloids and their mechanism in neurodegenerative disorders. *Int. J. Biol. Sci.* **14**, 341–357 (2018).
153. Milián, L. *et al.* Reactive oxygen species (ROS) generation inhibited by aporphine and phenanthrene alkaloids semi-synthesized from natural boldine. *Chem. Pharm. Bull.* **52**, 696–699 (2004).
154. Liu, C. M. *et al.* Antioxidant and anticancer aporphine alkaloids from the leaves of Nelumbo nucifera Gaertn. cv. Rosa-plena. *Molecules* **19**, 17829–17838 (2014).
155. Zhao, Q., Zhao, Y. & Wang, K. Antinociceptive and free radical scavenging activities of alkaloids isolated from Lindera angustifolia Chen. *J. Ethnopharmacol.* **106**, 408–413 (2006).
156. O'Brien, P., Carrasco-Pozo, C. & Speisky, H. Boldine and its antioxidant or health-promoting properties. *Chem. Biol. Interact.* **159**, 1–17 (2006).

157. Habu, J. B. & Ibeh, B. O. In vitro antioxidant capacity and free radical scavenging evaluation of active metabolite constituents of Newbouldia laevis ethanolic leaf extract. *Biol. Res.* **43**, 1–10 (2015).
158. Venkatesan, K., Joshi, I. & Merish, S. In-vitro antioxidant activity of a herb medicine Karisalai Chooranam. *J. Res. Biomed. Sci. A* **1**, (2019).
159. Junmarkho, K. & Hansakul, P. Thai pigmented rice bran extracts inhibit production of superoxide , nitric oxide radicals and inducible nitric oxide synthase in cellular models. *Asian Pac. J. Trop. Biomed.* **9**, 291–298 (2019).
160. Chen, H. Y. & Yen, G. C. Effect of sulfite-treated daylily (Hemerocallis fulva L.) flower on the production of nitric oxide and DNA damage in macrophages. *J. Food Drug Anal.* **15**, 63–70 (2007).
161. Nagananda, G. S. & Rajath, S. Phytochemical Evaluation and in vitro Free Radical Scavenging Activity of Cold and Hot Successive Pseudobulb Extracts of Medicinally Important Orchid Flickingeria nodosa (Dalz.) Seidenf. *J.Med. Sci* 401–409 (2013).
162. Yenes, S. & Messeguer, A. A Study of the Reaction of Different Phenol Substrates with Nitric Oxide and Peroxynitrite HO. *Tetrahedron* **55**, 14111–14122 (1999).
163. Kim, Y. K., Guo, Q. & Packer, L. Free radical scavenging activity of red ginseng aqueous extracts. *Toxicology* **172**, 149–156 (2002).
164. Ki, S. K., Yokozawa, T., Hyun, Y. K. & Jeong, H. P. Study on the nitric oxide scavenging effects of ginseng and its compounds. *J. Agric. Food Chem.* **54**, 2558–2562 (2006).
165. Rai, S. *et al*. Antioxidant activity of Nelumbo nucifera (sacred lotus) seeds. *J. Ethnopharmacol.* **104**, 322–327 (2006).
166. Mehta, N. R. *et al.* Nelumbo Nucifera (Lotus): A Review on Ethanobotany, Phytochemistry and Pharmacology. *Indian J. Pharm. Biol. Res.* **1**, 15r2–167 (2013).
167. Dey, A. & Mukherjee, A. Plant-Derived Alkaloids: A Promising Window for Neuroprotective Drug Discovery. in *Discovery and Development of Neuroprotective Agents from Natural Products: Natural Product Drug*

Discovery 237–320 (Elsevier Inc., 2017).

168. Neagu, E. *et al*. Antioxidant activity , acetylcholinesterase and tyrosinase inhibitory potential of Pulmonaria officinalis and Centarium umbellatum extracts. *Saudi J. Biol. Sci.* **25**, 578–585 (2018).
169. Dvir, H. *ei al.* Acetylcholinesterase: From 3D Strucuture to Function. *Chem Biol Interact* **187**, 10–22 (2011).
170. Khan, H., Amin, S., Amjad, M. & Patel, S. Biomedicine & Pharmacotherapy Flavonoids as acetylcholinesterase inhibitors : Current therapeutic standing and future prospects. *Biomed. Pharmacother.* **101**, 860–870 (2018).
171. Dong, L. *et al.* Radioprotective effects of dammarane sapogenins against 60Co-induced myelosuppression in mice. *Phyther. Res.* **32**, 741–749 (2018).
172. Ranjan, N. & Kumari, M. Acetylcholinesterase inhibition by medicinal plants : A Review. **6**, 1640–1644 (2017).
173. Sigma-Aldrich. Acetylcholinesterase from Electrophorus electricus. 1–2 (2018).
174. Pires, T. C. S. P. *et al.* Phenolic compounds profile, nutritional compounds and bioactive properties of Lycium barbarum L.: A comparative study with stems and fruits. *Ind. Crops Prod.* **122**, 574–581 (2018).
175. Santos, T. *et al.* Naturally Occurring Acetylcholinesterase Inhibitors and Their Potential Use for Alzheimer ' s Disease Therapy. *Front. Pharmacol.* **9**, 1–14 (2018).
176. Colovic, M. B. *et al.* Acetylcholinesterase Inhibitors : Pharmacology and Toxicology. *Curr. Neuropharmacol.* 315–335 (2013).
177. Bourne, Y. *et al.* Conformational flexibility of the acetylcholinesterase tetramer suggested by x-ray crystallography. *J. Biol. Chem.* **274**, 30370–30376 (1999).
178. Boublik, Y. *et al.* Acetylcholinesterase engineering for detection of insecticide residues. *Protein Eng.* **15**, 43–50 (2002).

179. Kurgat, E. & Ghareeb, D. Bioactive Compounds and Essential Oils as Acetylcholinesterase Inhibitors. **7**, 155–158 (2019).
180. Granja, F. *et al.* Medicinal Plants with Acetylcholinesterase Inhibitory Activity : Therapeutic Potential of Brazilian Plants for the Treatment of Alzheimer ' s Disease. *Pharmacol. Res.* **13**, 45–49 (2019).
181. Gu, L. *et al.* Role for monoaminergic systems in the antidepressant-like effect of ethanol extracts from Hemerocallis citrina. *J. Ethnopharmacol.* **139**, 780–787 (2012).
182. Wiart, C. Alkaloids. in *Lead Compounds from Medicinal Plants for the Treatment of Neurodegenerative Diseases* (ed. Wiart, C. B. T.-L. C. from M. P. for the T. of N. D.) 1–188 (Academic Press, 2014).
183. Chinsamy, M., Finnie, J. F. & Staden, J. Van. South African Journal of Botany mutagenicity of South African medicinal orchids. *South African J. Bot.* **91**, 88–98 (2014).
184. Lu, C. *et al.* 20(S)-protopanaxadiol (PPD) alleviates scopolamine-induced memory impairment via regulation of cholinergic and antioxidant systems, and expression of Egr-1, c-Fos and c-Jun in mice. *Chem. Biol. Interact.* **279**, 64–72 (2018).
185. Wang, Q. *et al.* Comparison of Ginsenosides Rg1 and Rb1 for Their Effects on Improving Scopolamine- induced Learning and Memory Impairment in Mice. **1754**, 1748–1754 (2010).
186. Choi, S. *et al.* Effects of ginsenosides, active components of ginseng, on nicotinic acetylcholine receptors expressed in Xenopus oocytes. *Eur. J. Pharmacol.* **442**, 37–45 (2002).
187. Zhang, H. C. *et al.* Development of molecular docking-based binding energy to predict the joint effect of BPA and its analogs. *Hum. Exp. Toxicol.* **30**, 318–327 (2011).
188. Demirezer, L. Ö. *et al.* Molecular docking and ex vivo and in vitro anticholinesterase activity studies of Salvia sp . and highlighted rosmarinic acid. *Turkish J. Med. Sci.* 1141–1148 (2015).
189. Yu, L. *et al.* Target Molecular-Based Neuroactivity Screening and Analysis of Panax ginseng by Affinity Ultrafiltration, UPLC-QTOF-MS

and Molecular Docking. *Am. J. Chin. Med.* **47**, 1345–1363 (2019).

190. Xie, X. l. *et al.* Ginsenoside Rb1 protects PC12 cells against β ·amyloid·induced cell injury. 635–639 (2010).
191. Batiha, G. E. & Beshbishy, A. M. Physostigmine : A Plant Alkaloid Isolated from Physostigma venenosum : A Review on Pharmacokinetics , Pharmacological and Toxicological Activities. *J. Drug Deliv. Sci. Technol.* 187–190 (2020).
192. Jung, H. A. *et al.* BACE1 and cholinesterase inhibitory activities of Nelumbo nucifera embryos. *Arch. Pharm. Res.* **38**, 1178–1187 (2015).
193. Yang, Z. *et al.* Synthesis and structure·Activity relationship of nuciferine derivatives as potential acetylcholinesterase inhibitors. *Med. Chem. Res.* **23**, 3178–3186 (2014).
194. Yang, Z. D. *et al.* An aporphine alkaloid from Nelumbo nucifera as an acetylcholinesterase inhibitor and the primary investigation for structure·activity correlations. *Nat. Prod. Res.* **26**, 387–392 (2012).
195. Qu, F. *et al.* Sterically demanding methoxy and methyl groups in ruthenium complexes lead to enhanced quantum yields for blue light triggered photodissociation. *Dalt. Trans.* **47**, 15685–15693 (2018).
196. Kim, D. *et al.* Anti·neuroinflammatory activities of indole alkaloids from kanjang (Korean fermented soy source) in lipopolysaccharide·induced BV2 microglial cells. *Food Chem.* **213**, 69–75 (2016).
197. Lu, D. *et al.* Ginsenoside Rg1 relieves tert·butyl hydroperoxide·induced cell impairment in mouse microglial BV2 cells. *J. Asian Nat. Prod. Res.* **17**, 930–945 (2015).
198. Hamed, A. *et al.* Antioxidant and Cytoprotective Properties of Three Egyptian Cyperus Species Using Cell·free and Cell·based Assays. *Pharm. Crop.* **3**, 88–93 (2012).
199. Lee, H. U. *et al.* Hepatoprotective effect of ginsenoside Rb1 and compound K on tert·butyl hydroperoxide·induced liver injury. *Liver Int.* **25**, 1069–1073 (2005).
200. Duan, X.·H., Pei, L. & Jiang, J.·Q. Cytotoxic alkaloids from stems of Nelumbo nucifera. *Zhongguo Zhong Yao Za Zhi* **38**, 4104–4108 (2013).

201. Chaichompoo, W. *et al.* Cytotoxic alkaloids against human colon adenocarcinoma cell line (HT-29) from the seed embryos of Nelumbo nucifera. *Med. Chem. Res.* **27**, 939–943 (2018).
202. Manogaran, P. *et al.* The Cytoprotective and Anti-cancer Potential of Bisbenzylisoquinoline Alkaloids from Nelumbo nucifera. *Current Topics in Medicinal Chemistry* vol. 19 2940–2957 (2019).
203. Cho, N. *et al.* Neuroprotective and anti-inflammatory effects of flavonoids isolated from Rhus verniciflua in neuronal HT22 and microglial BV2 cell lines. *Food Chem. Toxicol.* **50**, 1940–1945 (2012).
204. Eun, C. *et al*. The protective effect of fermented Curcuma longa L . on memory dysfunction in oxidative stress-induced C6 gliomal cells , cells , and scopolamine-induced amnesia model in mice. 1–12 (2017).
205. Won, H. *et al.* Hexane fraction of Zingiberis Rhizoma Crudus extract inhibits the production of nitric oxide and proinflammatory cytokines in LPS-stimulated BV2 microglial cells via the NF-kappaB pathway. *Food Chem. Toxicol.* **47**, 1190–1197 (2009).
206. Dai, X. *et al.* Activation of BV2 microglia by lipopolysaccharide triggers an inflammatory reaction in PC12 cell apoptosis through a toll-like receptor 4-dependent pathway. *Cell Stress Chaperones* 321–331 (2015).
207. Lin, C. *et al.* Lipopolysaccharide-Induced Nitric Oxide , Prostaglandin E2 , and Cytokine Production of Mouse and Human Macrophages Are Suppressed by Pheophytin-b. *Int. J. Mol. Sci.*
208. Lau, F. C. *et al.* Inhibitory Effects of Blueberry Extract on the Production of Inflammatory Mediators in Lipopolysaccharide-Activated BV2 Microglia. *J. Neurosci. Res.* **1017**, 1010–1017 (2007).
209. Lee, S. H. *et al.* Anti-Inflammatory Activity of 20 (S) - Protopanaxadiol : Enhanced Heme Oxygenase 1 Expression in RAW 264.7 Cells. *Planta Med.* **20**, 3–6 (2005).
210. Lee, J., Song, J., Sohn, N. & Shin, J. Inhibitory Effects of Ginsenoside Rb1 on Neuroin fl ammation Following Systemic Lipopolysaccharide Treatment in Mice. **1276**, 1270–1276 (2013).

211. Zong, Y. & Al., E. Ginsenoside Rg1 Attenuates Lipopolysaccharide-Induced Inflammatory Responses Via the Phospholipase C- 1 Signaling Pathway in Murine BV-2 Microglial Cells. *Curr. Med. Chem.* **1**, 770–779 (2012).
212. Gachon, C. Real-time PCR: what relevance to plant studies? *J. Exp. Bot.* **55**, 1445–1454 (2004).
213. Nygard, A. *et al.* Selection of reference genes for gene expression studies in pig tissues using SYBR green qPCR. *BMC Mol. Biol.* **6**, 1–6 (2007).
214. Bulcke, M. V. D. *et al.* A theoretical introduction to " Combinatory SYBR ® Green qPCR Screening " , a matrix-based approach for the detection of materials derived from genetically modified plants. *Anal Bioanal Chem* 2113–2123 (2010).
215. Park, B. *et al.* Antineuroinflammatory and Neuroprotective Effects of Gyejibokryeong-Hwan in Lipopolysaccharide-Stimulated BV2 Microglia. *Evidence-based Complement. Altern. Med.* 1–19 (2019).
216. Lively, S., Schlichter, L. C. & Symes, A. J. Microglia Responses to Pro-inflammatory Stimuli (LPS , IFN γ + TNF α) and Reprogramming by Resolving Cytokines (IL-4, IL-10). *Front. Cell. Neurosci.* **12**, 1–19 (2018).
217. Wang, W., Tan, M., Yu, J. & Tan, L. Role of pro-inflammatory cytokines released from microglia in Alzheimer ' s disease. *Ann Transl Med* **3**, 1–15 (2015).
218. Jayasooriya, R. G. P. T. *et al.* Inhibition of nitric oxide and prostaglandin E2 expression by methanol extract of polyopes affinis in lipopolysaccharide-stimulated BV2 microglial cells through suppression of akt-dependent NF-κB activity and MAPK pathway. *Trop. J. Pharm. Res.* **12**, 63–70 (2013).